OUKA
The University of Osaka
Institutional Knowledge Archive

Title	A Study on Integrated Forecasting and Optimization Framework for Behind-the-Meter Energy Management
Author(s)	岩渕, 厚樹
Citation	大阪大学, 2026, 博士論文
Version Type	VoR
URL	https://doi.org/10.18910/105499
rights	
Note	

The University of Osaka Institutional Knowledge Archive : OUKA

https://ir.library.osaka-u.ac.jp/

The University of Osaka

A Study on Integrated Forecasting and Optimization Framework for Behind-the-Meter Energy Management

Submitted to
Graduate School of Information Science and Technology
The University of Osaka

January 2026

Koki IWABUCHI

Publications

Journal Article (Refereed)

[J1] Koki Iwabuchi, Daichi Watari, Dafang Zhao, Ittetsu Taniguchi, Francky Catthoor, and Takao Onoye, "Enhancing grid stability in PV systems: A novel ramp rate control method utilizing PV cooling technology," *Applied Energy*, vol. 378, p. 124737, 2025.

[J2] Koki Iwabuchi, Kenshiro Kato, Daichi Watari, Ittetsu Taniguchi, Francky Catthoor, Elham Shirazi, and Takao Onoye, "Flexible electricity price forecasting by switching mother wavelets based on wavelet transform and Long Short-Term Memory," *Energy and AI*, vol. 10, p. 100192, 2022.

International Conference Papers (Refereed)

[I1] Koki Iwabuchi, "Integrated Forecasting and Cooling-Based Ramp Rate Control for Energy Systems," in *Proceedings of the 12th ACM International Conference on Systems for Energy-Efficient Buildings, Cities, and Transportation (BuildSys)*, pp. 353–354, 2025.

[I2] Koki Iwabuchi, Dafang Zhao, Ittetsu Taniguchi, Francky Catthoor, and Takao Onoye, "Ramp Rate Control for PV Systems Using Solar Irradiance Forecasting with Wavelet Transform and LSTM," in *Proceedings of the 16th ACM International Conference on Future and Sustainable Energy Systems (e-Energy)*, pp. 987–988, 2025.

[I3] Koki Iwabuchi, Daichi Watari, Dafang Zhao, Ittetsu Taniguchi, and Takao Onoye, "Flexible Electricity Demand Forecasting Based on mRMR Feature Selection and WT-LSTM," in *Proceedings of the 40th European Photovoltaic Solar Energy Conference and Exhibition (EUPVSEC)*, 5CO.6.1, pp. 020491-001–020491-004, 2023.

[I4] Kenshiro Kato, Koki Iwabuchi, Daichi Watari, Dafang Zhao, Hiroki Nishikawa, Ittetsu Taniguchi, and Takao Onoye, "Exploring Models of Electricity Price Forecasting: Case Study on A FCAS Market," in *Proceedings of the 14th ACM International Conference on Future and Sustainable Energy Systems (e-Energy)*,

pp. 115–119, 2023.

[I5] Naoya Kaneko, Koki Iwabuchi, Kenshiro Kato, Daichi Watari, Dafang Zhao, Ittetsu Taniguchi, Hiroki Nishikawa, and Takao Onoye, "An Evaluation of Electricity Demand Forecasting Models for Smart Energy Management Systems," in *Proceedings of the 19th International SoC Design Conference (ISOCC)*, pp. 195–196, 2022.

[I6] Koki Iwabuchi, Kenshiro Kato, Daichi Watari, Ittetsu Taniguchi, Francky Catthoor, Elham Shirazi, and Takao Onoye, "Demand-Aware Electricity Price Prediction Based on LSTM and Wavelet Transform," in *Proceedings of the 38th European Photovoltaic Solar Energy Conference and Exhibition (EUPVSEC)*, 7DV.1.4, pp. 1668–1670, 2021.

Summary

The accelerating deployment of photovoltaic (PV) generation plays a critical role in the global transition toward environmentally sustainable power systems. PV systems offer carbon-neutral energy production with low operating cost, which makes them highly attractive for both residential and commercial adoption. Their installation continues to expand rapidly due to decreasing manufacturing costs, policy support, and improved power conversion technologies. However, PV generation is strongly affected by weather conditions, solar irradiance variability, and rapid cloud movements, leading to unstable and unpredictable power output. Such variability causes significant fluctuations in PV power generation, including steep ramp rates that pose severe challenges for maintaining stable grid operation.

In conventional grid architectures, these fluctuations are typically mitigated by large-scale storage or dispatchable power plants. In practice, grid operators rely heavily on quickly dispatchable backup units, especially diesel engines and, more recently, gas turbines, to compensate for rapid PV variability and maintain system stability. Yet, these solutions remain costly, resource-intensive, and environmentally burdensome. Behind-the-meter (BTM) systems present an alternative approach by enabling localized energy management performed directly by end users equipped with distributed energy resources. BTM systems allow users to monitor, forecast, and regulate their own energy generation and consumption. This transforms traditional consumers into "prosumers" capable of both producing and controlling local power in coordination with the wider grid.

The emergence of BTM energy management systems (EMS) creates new opportunities for efficient PV utilization. An EMS can schedule battery operation, manage flexible loads, and regulate PV output while reflecting user objectives and system constraints. A central motivation for BTM energy management is to minimize the amount of renewable energy that would otherwise be curtailed or wasted during periods when PV generation exceeds instantaneous local demand. By coordinating storage, controllable loads, and conversion efficiency, the EMS enables surplus energy to be absorbed, shifted, or delivered more effectively. Nevertheless, BTM energy management remains challenging due to several key factors. These include the non-stationarity of energy-related time series, limitations of forecasting accuracy, steep ramp rates in PV output, and operational constraints associated with batteries and power electronics. These issues

highlight the need for EMS approaches that couple accurate forecasting with proactive control strategies, ensuring that renewable resources are utilized as efficiently as possible while maintaining stable operation.

This dissertation addresses these challenges by presenting an integrated forecasting and optimization framework for BTM PV systems. The research is structured around three key questions concerning forecasting, ramp rate control, and forecast-informed system integration. The first question focuses on how accurate forecasting of critical time series can be achieved for EMS decision-making. The second question examines how PV ramp rates can be mitigated without requiring large battery capacity. The third question investigates how forecasting and optimization can be integrated to enable proactive BTM operation.

To address the first question, this dissertation develops a wavelet transform–long short-term memory forecasting framework tailored to non-stationary time series in BTM environments. Conventional statistical approaches rely on linear assumptions that fail to capture nonlinear and complex variations in solar irradiance, electricity demand, and electricity prices. Existing wavelet–machine learning approaches improve accuracy, but they often depend on fixed decomposition, ad hoc feature selection, and limited use of explanatory variables. To overcome these limitations, the proposed method introduces a systematic feature screening process and an adaptive mother wavelet selection technique. These innovations jointly improve decomposition quality and predictive performance across multiple forecasting tasks. As a result, the proposed method provides a reliable forecasting foundation for EMS planning and real-time control.

Building upon forecasting capabilities, this dissertation addresses the second research question by introducing a novel control knob that directly influences the amount of PV energy supplied to the local grid, implemented through a cooling-based PV ramp rate control strategy. Unlike battery-only solutions, the method regulates PV output by adjusting panel temperature to modulate conversion efficiency. This approach leverages the thermal properties of PV cells to suppress steep power fluctuations. By selectively activating cooling during rapid irradiance transitions, the method reduces ramp rate violations without excessive storage use. Simulation studies based on real-world irradiance measurements demonstrate reductions of 43.5% in mean ramp rates and 76.2% in maximum ramp rates. Moreover, these improvements are achieved using a cooling device with a coefficient of performance below 10 and only 20 kWh of storage capacity. These results reveal a cost-effective method that minimizes dependence on large batteries while increasing PV usability.

To address the third research question, the forecasting and cooling-based control strategies are integrated into an iterative hierarchically organized forecast-informed EMS framework. The framework anticipates power fluctuations using short-term predictions and preemptively optimizes output prior to ramp rate violations. Forecasts with a horizon of 30–60 seconds reduce ramp rate violations by up to 20% relative to a no-control baseline.

Overall, this dissertation provides a unified perspective on forecasting and control for BTM PV systems. It demonstrates that accurate forecasting, thermal regulation, and sequential optimization enable stable, cost-effective, and lightweight BTM system design. The results show that proactive control strategies can reduce ramp rate violations, minimize unnecessary battery cycling without costly infrastructure expansion. Future research will explore uncertainty-aware forecasting, online learning for adaptive model updates, improved cooling system modeling, and hardware-in-the-loop validation for field deployment. Together, these directions aim to further increase the practicality and robustness of forecast-informed PV control in BTM environments.

Acknowledgments

First and foremost, I would like to express my deepest gratitude and special appreciation to my supervisor, Associate Professor Ittetsu Taniguchi, Department of Information Systems Engineering, Graduate School of Information Science and Technology, The University of Osaka. His continuous guidance, insightful advice, and dedicated support have been invaluable throughout the course of my doctoral research. Without his kind support and understanding of my circumstances as a working doctoral student, I would not be who I am today, nor would I be leading the life I currently do. Thanks to his invaluable guidance and encouragement, I was able to achieve refined outcomes in my research.

I am deeply grateful to Professor Takao Onoye, Department of Information Systems Engineering, Graduate School of Information Science and Technology, The University of Osaka, for his thoughtful feedback and valuable comments. His technical insights have always been precise and to the point, and I sincerely appreciate his careful guidance throughout this research.

I am very grateful to Professor Francky Catthoor, National Technical University of Athens (NTUA) and previously IMEC, Belgium. His invaluable ideas and advice have supported me on numerous occasions. He has consistently promoted collaborative research with colleagues at EnergyVille, NTUA/AUTH and IMEC, and facilitated connections with researchers in related fields. It is clear that without his contributions, this dissertation would not have grown to its present scope. Furthermore, during my stay at EnergyVille in Belgium, he truly supported my daily life, for which I am sincerely thankful.

I would like to express my sincere gratitude to Professor Yasushi Sakurai, The Institute of Scientific and Industrial Research, The University of Osaka, for his detailed review and insightful comments, which guided my dissertation toward a better and novel direction.

I am sincerely grateful to Assistant Professor Hiroki Nishikawa, Department of Information Systems Engineering, Graduate School of Information Science and Technology, The University of Osaka, for his valuable suggestions and generous support. I have always learned a great deal from his insightful perspectives on research and his constructive comments. I am also thankful for his kindness in looking after me, including accompanying me on a trip to Spain during my stay in Belgium.

I wish thanks to Specially-appointed Assistant Professor Dafang Zhao, Department of Information Systems Engineering, Graduate School of Information Science and Technology, The University of Osaka, for his valuable comments on my research and for taking care of me in many aspects.

I would like to express my gratitude to Associate Professor Patrizio Manganiello, Department of Industrial Engineering Sciences, Hasselt University. He provided me with valuable advice during meetings and warmly welcomed me each time I visited Europe. I am confident that this research could not have progressed without his support.

I would like to thank Assistant Professor Elham Shirazi, Faculty of Engineering Technology, University of Twente, for her valuable feedback and collaboration on this research. During my visit to the Netherlands, she kindly organized a lab tour, which provided me with an excellent opportunity to deepen my knowledge.

I would like to thank the members of imec EnergyVille, Professor Ivan Gordon, Professor Michael Daenen, Dr. Apostolos Bakovasilis, Mr. Richard de Jong, Ms. Sara Bouguerra, Dr. Santhosh Ramesh, and Mr. Olivier Dupon. Their support not only in research but also in life during my stay in Belgium helped me a lot.

I would also like to express my gratitude to Professor Yoshiyuki Shimoda in the Division of Sustainable Energy and Environmental Engineering, Graduate School of Engineering, The University of Osaka, Associate Professor Toshihiro Suzuki in the Campus Sustainability Office at The University of Osaka, and the employees of DAIKIN Industries, Ltd. Mr. Shinya Harada, Mr. Sumio Shioji, and Mr. Yoshinori Yura provided invaluable insights and extensive cooperation in the research on forecasting.

I would like to thank all members of Onoye Laboratory for the brilliant and wonderful time. Mrs. Yuki Yoshida, the secretary of Onoye Laboratory, supported me in all of my laboratory life. Her kind support allowed me to focus on my research. I am deeply grateful to Dr. Daichi Watari, an alumnus of the Onoye Laboratory. His support extended beyond research assistance and guidance in laboratory life. More importantly, he pioneered the path to the doctoral program and set an example that illuminated the way for juniors like myself. I am also thankful for his kindness and support during my time in Tokyo. I am also deeply grateful to Dr. Kenshiro Kato, an alumnus of the Onoye Laboratory. Since the time of my initial assignment, he has kindly served as a mentor to me. Not only did he support my research, but his presence undoubtedly became one of my sources of mental strength. I also thank members of Group CPS, Mr. Yuki Ozawa, Mr. Kaneko Naoya, Mr. Shunsaku Miyatake, Mr. Kazuki Okazawa, Mr. Ren Sasaki, and Mr. Shuhei Mitsunaga. Their comments and suggestions at meetings always helped me and my research, and the wonderful time I had with them was a pleasure and always motivating for me. I would like to express my special gratitude to my classmates, Mr. Shun Kimura, Mr. Kai Matsuo, Mr. Taiyo Natomi, and Mr. Rikiya Fukushima, with whom I conducted research in the laboratory. I believe that who I am today is largely because I was able to spend my master's program together with them. I am also grateful to Mr. Kento Sakurauchi, Mr. Jo Yoshimoto, and Mr. Motoki Manabe, who have contin-

ued to spend time with me in Tokyo even after graduation. It has been truly wonderful for me to have friends in Tokyo with whom I can share stories and discussions about our laboratory.

I would also like to express my gratitude to my colleagues at Recruit Co., Ltd., who made it possible for me to pursue the path of a working doctoral student, which is still relatively uncommon. In particular, I am grateful to my supervisor, Mr. Ippei Kataoka, who may have been inconvenienced at times, yet always watched over me with warmth and understanding. I also wish to thank Mr. Ryunosuke Ikeda, Mr. Daiki Yamane, Ms. Yurika Ono, Mr. Yuta Matsumoto, and other peers in Data Management & Planning Office. The enjoyable times I shared with them were an important factor that sustained me throughout my journey as a working doctoral student.

I would like to express my heartfelt gratitude to my family members, Mr. Masahiro Iwabuchi, Mrs. Yukiko Iwabuchi, Ms. Yuka Iwabuchi and Ms. Misaki Iwabuchi. Your unwavering love and patience have supported me every single day. Without your support, I could not have completed this journey.

Contents

1 Introduction **1**
- 1.1 Background . . . 1
- 1.2 Behind-the-Meter Energy Systems and Applications . . . 3
  - 1.2.1 Distributed Energy Resources in BTM . . . 4
  - 1.2.2 Energy Management Systems in BTM . . . 6
  - 1.2.3 Ramp Rate Regulations . . . 8
- 1.3 Research Questions and Issues . . . 9
- 1.4 Objective and Organization . . . 12

2 WT-LSTM Based Forecasting for Behind-the-Meter System **17**
- 2.1 Introduction . . . 17
- 2.2 Related Works . . . 18
  - 2.2.1 Statistical Forecasting Methods . . . 18
  - 2.2.2 Machine Learning Forecasting Methods . . . 20
  - 2.2.3 Hybrid Forecasting Methods . . . 20
- 2.3 WT-LSTM Based Forecasting Methodology . . . 22
  - 2.3.1 Wavelet Transform . . . 22
  - 2.3.2 Long Short-Term Memory . . . 23
  - 2.3.3 Forecasting Methodology . . . 25
- 2.4 Electricity Price Forecasting . . . 34
  - 2.4.1 Problem Definition . . . 34
  - 2.4.2 Simulation Setup . . . 37
  - 2.4.3 Simulation Results . . . 38
- 2.5 Electricity Demand Forecasting . . . 46
  - 2.5.1 Problem Definition . . . 46
  - 2.5.2 Simulation Setup . . . 47
  - 2.5.3 Simulation Results . . . 48
- 2.6 Solar Irradiance Forecasting . . . 50
  - 2.6.1 Problem Definition . . . 50
  - 2.6.2 Simulation Setup and Results . . . 51
- 2.7 Summary . . . 53

3 Cooling-Based Optimization for PV Ramp Rate Minimization **55**
3.1 Introduction . . . 56
3.2 Related Works . . . 57
3.2.1 Ramp rate control methods . . . 57
3.2.2 PV cooling methods . . . 60
3.3 Cooling-Based Control Methodology . . . 63
3.3.1 Overview of the proposed ramp rate control method . . . 63
3.3.2 How to utilize PV cooling units . . . 65
3.4 System Model . . . 67
3.4.1 Targeted microgrids . . . 67
3.4.2 PV and PV cooling unit model . . . 67
3.4.3 Battery model . . . 69
3.4.4 Mathematical formulation of PV system operation optimization 70
3.5 Simulation Experiments . . . 70
3.5.1 Simulation Setup . . . 70
3.5.2 Simulation Results . . . 72
3.6 Summary . . . 78

4 Implementation of Forecast-Based Ramp Rate Control **81**
4.1 Introduction . . . 81
4.2 Related Works . . . 82
4.3 Proactive Solar Power Control Through Integrated Forecasting . . . 84
4.3.1 Overview of the Framework . . . 84
4.3.2 Solar Irradiance Prediction and Error Correction . . . 85
4.3.3 Ramp Rate Estimation, Optimization, and System Update . . . 86
4.4 Simulation Experiments . . . 87
4.4.1 Simulation Setup . . . 87
4.4.2 Simulation Results . . . 87
4.5 Summary . . . 89

5 Conclusion and Future Work **91**
5.1 Conclusion . . . 91
5.2 Future Work . . . 94

Bibliography **99**

List of Figures

1.1 Trends in electricity generation by each renewable energy source. . . . 2
1.2 Overview of front-of-the-meter and behind-the-meter energy systems. . 3
1.3 Schematic overview of an energy management system in behind-the-meter environments. 7
1.4 Study scope of this dissertation. 10

2.1 Layered structure of RNN. 24
2.2 Architecture of an LSTM cell with input, forget, and output gates. . . . 25
2.3 Overview of the proposed forecasting method. 25
2.4 Electricity prices and demand in New South Wales, Australia (May 25 - May 31, 2013). 27
2.5 Original electricity price series and its frequency-domain decomposed components. 30
2.6 Original electricity price series and its time-domain decomposed components. 31
2.7 Commonly used mother wavelet functions for time series forecasting. . 32
2.8 Electricity price data from New South Wales, Australia, in 2013 [1]. . . 33
2.9 Example of the JEPX wholesale electricity price transition (January 28, 2021) [2]. 35
2.10 Overview of Electricity Trading in Australia. 36
2.11 Overview of one-step-ahead prediction. 37
2.12 Actual prices, predicted prices of the replicated Chang et al. [3] model, and predicted prices of the proposed electricity demand addition model. 39
2.13 Details of the experimental period. 41
2.14 Actual and predicted electricity prices for July 22–23, along with the corresponding absolute prediction errors for each mother wavelet. . . . 43
2.15 Weekly forecast accuracy (MAPE) and rank of each mother wavelet in forecasting electricity price. 44
2.16 Average rank of accuracy of electricity price forecasts over the entire experimental period. 44
2.17 Standard deviation of the accuracy ranking of electricity price forecasts over the entire experimental period. 45

2.18 Energy management system overview. 47
2.19 Electricity demand change in one building at the Graduate School of Information Science and Technology, the University of Osaka for one year in FY2019. 48
2.20 Accuracy ranking of each mother wavelet by week. 49
2.21 Maximum weekly MAPE of each feature selection. 50

3.1 Schematic of the target microgrid with mathematical notation for each system variable. 64
3.2 Overview of the proposed optimization-based control framework for PV systems incorporating PV cooling units. 65
3.3 PV cooling–based control strategy for regulating power generation. . . . 66
3.4 PV-electrical, PV-thermal, and PV cooling unit model. 68
3.6 Solar irradiance in Oldenburg on July 7, 2015 from 12:30 to 12:45. . . . 71
3.8 Changes in power (a) and temperature (b) over a 200-second interval during summer noon under rapidly changing solar irradiance conditions. 75
3.9 Power delivered to the grid between 430 and 450 seconds, with and without PV cooling. 76
3.10 Mean (a) and maximum (b) ramp rates for each season and time period, normalized to the no-cooling case. 77
3.11 Mean (a) and maximum (b) ramp rates, and accumulated energy (c), for each battery capacity and COP. 77

4.1 Workflow of the proposed framework. 84
4.2 Number of ramp rate violations for baseline (no control), prediction-based control, and ideal prediction-based control at each forecast horizon. 88
4.3 Accumulated energy transmitted to the main grid for baseline (no control), prediction-based control, and ideal prediction-based control at each forecast horizon. 89

List of Tables

2.1 Training, validation, and test data period 39
2.2 The published and reproduced values of the prediction error of the model of Chang et al. [3] and the prediction error of the proposed model 40
2.3 MAPE of each mother wavelet (MW) in electricity price forecast over entire experimental period 42
2.4 MAPE of each mother MW in electricity demand forecast over entire experimental period 48
2.5 RMSE, MAE, MAPE at each forecast horizon. 52

3.1 Pros and cons of typical ramp rate control approaches. 62
3.2 Parameters settings of battery. 71
3.3 Date and time of selected 15 minutes of temperature and solar irradiance data for each season and time of day. 72
3.4 Parameters settings of PV. 72
3.5 Baseline load profile components categorized by season and time of day [kW]. 73
3.6 Mean and maximum ramp rates under summer noon conditions, with and without cooling. 73

Chapter 1

Introduction

1.1 Background

The global transition toward a sustainable energy future has accelerated the deployment of renewable energy sources in recent decades [4] [5]. As illustrated in Fig. 1.1, the worldwide installed capacity of renewable energy has steadily increased, with solar photovoltaics (PV) and wind power experiencing particularly rapid growth [6]. Solar PV, in particular, has become a central component of modern energy systems owing to its low operating cost, modularity, and minimal environmental impact. These advantages have contributed to its widespread installation not only at the utility scale but also in residential, commercial, and industrial facilities.

Despite their environmental benefits, renewable energy sources also introduce substantial operational challenges, particularly concerning system stability and reliability [7]. PV generation is inherently variable and dependent on stochastic environmental conditions such as cloud movement, solar irradiance, and panel temperature. Unlike conventional thermal units—which can ramp up or down in a controlled manner—PV output is uncontrollable and non-dispatchable. Consequently, increasing PV penetration can lead to severe grid stability issues, including frequency deviations, power congestion, and significant ramp rate fluctuations [8]. These challenges become more critical as renewable energy continues to proliferate.

Meanwhile, the increasing availability of distributed energy resources (DERs) and advances in information and communication technology (ICT) are rapidly transforming traditional energy systems into decentralized, flexible, and consumer-centric structures [9]. To clarify this transformation, Fig. 1.2 provides a conceptual overview of front-of-the-meter (FTM) and behind-the-meter (BTM) systems. FTM resources—such as utility-scale generators, substations, and transmission infrastructure—operate on the grid side and are centrally managed by utilities. BTM resources, in contrast, reside on the customer side of the meter and include rooftop PV, residential batteries, electric vehicles (EVs), heating, ventilation, and air-conditioning (HVAC) systems, and other

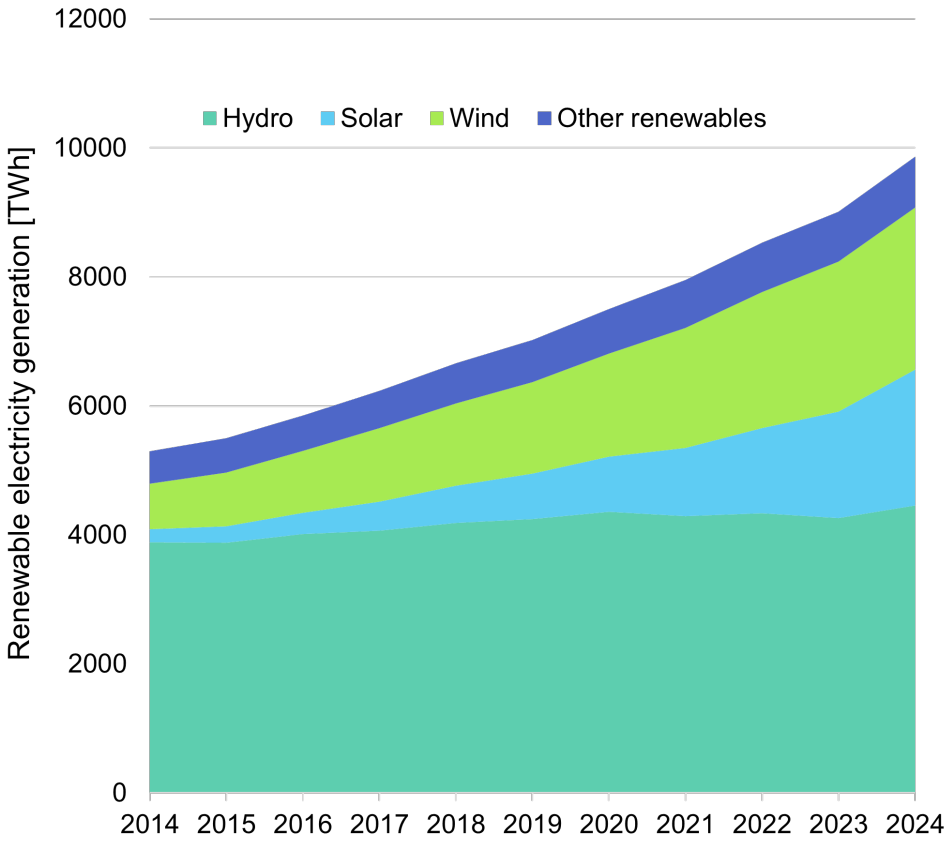


Figure 1.1: Trends in electricity generation by each renewable energy source.

controllable loads. The utility meter defines the operational boundary between the two domains, with FTM assets ensuring bulk system reliability and BTM assets contributing localized, prosumer-driven flexibility. As DER adoption increases, power flows become bidirectional, allowing BTM systems not only to consume but also to export energy back to the grid. In residential and commercial sectors, BTM systems are gaining remarkable attention. Equipped with smart metering and automation technologies, end users can now monitor, manage, and optimize their own energy consumption and generation, effectively shifting from passive consumers to active prosumers.

This evolution has led to a paradigm shift in the relationship between the supply and demand side of the power system. Traditionally, electricity systems relied on unidirectional power flow from centralized power plants to end users, with utilities responsible for balancing supply and demand. However, the increasing diversity of consumption patterns and the proliferation of DERs have made system-level energy balancing significantly more complex. In the emerging next-generation energy system, power flow

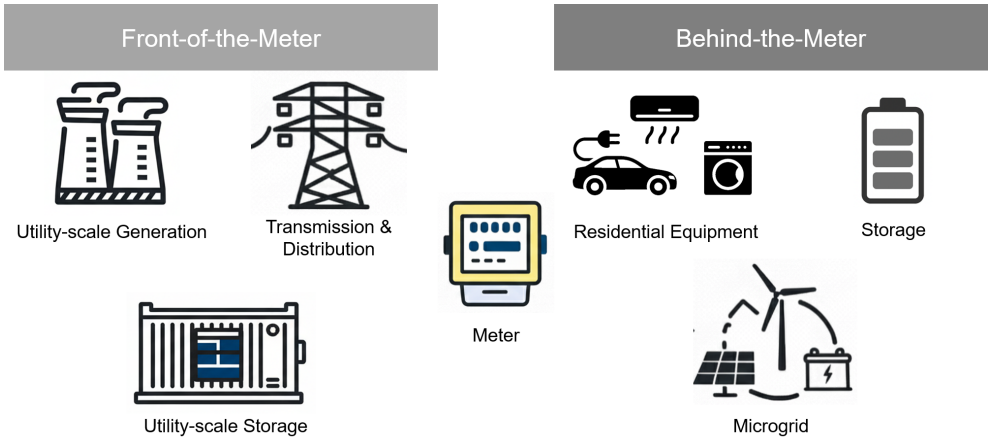


Figure 1.2: Overview of front-of-the-meter and behind-the-meter energy systems.

have become bidirectional, and local energy systems play an increasingly active role in supporting grid operations. BTM systems can mitigate supply–demand mismatches by offering distributed flexibility, reducing peak loads, and alleviating network congestion, while simultaneously suppressing excessive ramp rates that are unacceptable for the main grid and reducing the amount of wasted renewable energy when local production exceeds instantaneous demand.

BTM resources are expected to play a crucial role in future power systems. The International Energy Agency reports rapid growth in DER adoption, including heat pumps, EVs, and residential PV–battery systems [10] [11]. Under the Stated Policies Scenario, demand-side flexibility is projected to provide nearly one-quarter of total system flexibility by 2050 [12]. Unlocking this flexibility requires advanced energy management strategies capable of forecasting local conditions, controlling DER operation, and optimizing system-level interactions.

As BTM systems continue to expand and diversify, their contribution to power system flexibility is expected to become increasingly significant. The coordinated use of DERs—supported by advances in forecasting, control technologies, and energy management systems (EMS) —will open new opportunities for enhancing both local efficiency and global grid stability. By enabling prosumers to participate more actively in energy management and grid support, next-generation BTM solutions hold great promise for unlocking substantial economic and operational value in future power systems.

1.2 Behind-the-Meter Energy Systems and Applications

This section outlines the fundamental components of BTM energy systems and their practical applications. First, the major types of DERs commonly deployed in residen-

tial, commercial, and industrial BTM environments are introduced. Then, the operational roles of EMS and their relevance to local monitoring, control, and optimization are described. In addition, the mechanisms and implications of ramp rate regulations and other grid-support requirements are explained, as they directly affect PV-integrated BTM systems.

1.2.1 Distributed Energy Resources in BTM

In BTM energy systems, various DERs play a central role in enabling local generation, storage, and flexible energy use. In addition to renewable generation such as rooftop PV systems, typical DERs in BTM environments include battery storage systems, controllable household and commercial appliances, HVAC equipment, as well as small-scale wind turbines that serve as another important source of distributed renewable generation.

Photovoltaic Systems

PV systems are one of the most widely adopted renewable energy technologies in BTM environments, providing clean and on-site electricity generation for residential, commercial, and industrial users [13]. The power output of a PV system depends primarily on solar irradiance and panel temperature [14], and rooftop PV installations have become increasingly common due to their modularity, declining installation costs, and compatibility with existing building structures [15].

PV systems play a central role in reducing electricity imports from the grid and lowering operational costs for prosumers. However, their power output is inherently variable and strongly influenced by environmental conditions such as cloud movement, shading, and ambient temperature. These characteristics make PV generation a key contributor to short-term fluctuations in BTM power profiles and can lead to rapid ramping events that affect both local and system-level stability.

With the advancement of ICT, PV systems can now be monitored and managed more precisely [16]. Real-time irradiance measurements, power output monitoring, and forecasting tools enable prosumers and EMS to estimate future PV generation and adjust consumption or storage strategies accordingly. In addition, PV systems equipped with module-level power electronics, such as microinverters or DC optimizers, can enhance controllability by providing granular measurements and enabling partial shading mitigation.

Despite these advancements, PV systems also exhibit operational constraints that must be considered. In particular, panel temperature has a significant impact on power conversion efficiency, and elevated temperatures can lead to noticeable performance degradation. Therefore, effective utilization of PV systems requires not only accurate forecasting and careful coordination with other DERs, but also an understanding of their physical characteristics and environmental dependencies.

Energy Storage Systems

Battery energy storage systems (BESS) are essential components of BTM energy systems and play a critical role in enhancing local flexibility and operational stability [17]. Owing to their rechargeable nature, BESS function as dynamic energy buffers that can reshape demand profiles by storing surplus electricity and discharging it when needed. In particular, they can mitigate sudden changes in local power balance and smooth voltage or power fluctuations caused by variable renewable generation such as rooftop PV. Moreover, BESS can effectively reduce electricity costs for prosumers by shifting energy consumption from high-price periods to off-peak hours.

Various types of batteries exist depending on the underlying material chemistry, including lead-acid, nickel–metal hydride, and lithium-ion batteries [18]. Among these, lithium-ion batteries are most widely adopted in BTM applications and EVs due to their high energy density, long cycle life, and rapid response characteristics [19].

Beyond electrochemical batteries, other forms of energy storage can also be employed in BTM or local energy systems [20]. Mechanical storage technologies—such as flywheels—provide fast-response and high-cycling capability, while gravitational or hydraulic storage (e.g., behind small uphill reservoirs) can store surplus energy at larger scales when local geography permits. Although their applicability to typical residential or small commercial BTM settings is more limited, these technologies illustrate the broader spectrum of storage options that may complement or substitute battery systems depending on context.

Despite their operational usefulness, large-capacity storage systems—particularly electrochemical batteries—pose several practical challenges in BTM environments. The production and disposal of batteries can impose substantial environmental burdens due to the extraction of critical materials and the energy-intensive manufacturing processes involved [21]. Additionally, the installation of high-capacity BESS requires significant initial investment, and their operation involves non-negligible maintenance and replacement costs stemming from performance degradation over time. These economic and environmental considerations can limit the scalability of battery-based solutions, especially when frequent cycling is required to manage rapid fluctuations in PV generation.

Therefore, while storage systems offer valuable capabilities for balancing local supply and demand, relying heavily on large battery capacities may not always be financially or environmentally optimal. Effective BTM management thus requires careful consideration of alternative or complementary strategies—such as operational forecasting and non-battery-based control methods—to achieve stable and cost-effective system performance.

Other Distributed Energy Resources in Behind-the-Meter Systems

Beyond PV systems and BESS, BTM environments may incorporate a variety of other DERs that contribute to local energy management and flexibility. Representative ex-

amples include controllable household and commercial appliances, HVAC equipment, and EVs, as well as small-scale wind turbines that can provide supplemental distributed renewable generation in suitable locations. Although their operational characteristics differ, these DERs can influence local demand patterns and provide additional opportunities for improving energy efficiency or interacting with grid services.

Controllable appliances—such as water heaters, refrigerators, or commercial equipment—can adjust their operating cycles within certain comfort or process constraints, thereby offering modest but useful flexibility during specific periods. HVAC systems, which account for a significant share of building electricity consumption, can also modify their operation through temperature setpoint adjustments or pre-heating/pre-cooling strategies when managed by an EMS. In addition, EVs act as both mobility devices and flexible electrical loads, and their charging behaviors can significantly affect short-term BTM demand profiles. Furthermore, small-scale wind turbines may also appear in BTM settings as an additional form of distributed renewable generation.

While these DERs offer meaningful flexibility in many applications, the present study does not focus on their detailed modeling or control. Instead, they are introduced here to highlight the diversity of resources that may coexist within BTM systems and to provide context for the broader operational environment.

1.2.2 Energy Management Systems in BTM

EMSs play a central role in coordinating DERs within BTM environments [22]. With advances in ICT and the widespread deployment of smart meters and monitoring devices, EMSs support a variety of key functions in both residential and commercial BTM systems. Typical EMS functionalities include the following:

- Real-time monitoring of local energy generation, demand, and storage behavior.
- Operational planning of DERs over mid- to long-term horizons, taking into account expected seasonal and daily variations, supported by forecasting of key variables such as solar irradiance, electricity demand, and electricity price.
- Real-time control and dispatch of resources to compensate for rapid fluctuations in PV generation and local demand.
- Provision of auxiliary services such as data visualization, system diagnostics, and automated control routines.

Fig. 1.3 illustrates the basic structure of an EMS in BTM environments. The EMS receives information on local PV generation, battery status, and electrical load, as well as external signals such as electricity prices and weather forecasts. Based on these inputs, the EMS performs monitoring, operational planning, and real-time control to coordinate DERs within the BTM system. The outputs of the EMS include charge–discharge commands for the battery, operational adjustments for PV or other controllable devices, and system-level metrics used for visualization and decision support. Through these functions, the EMS enables prosumers to operate their BTM resources efficiently while

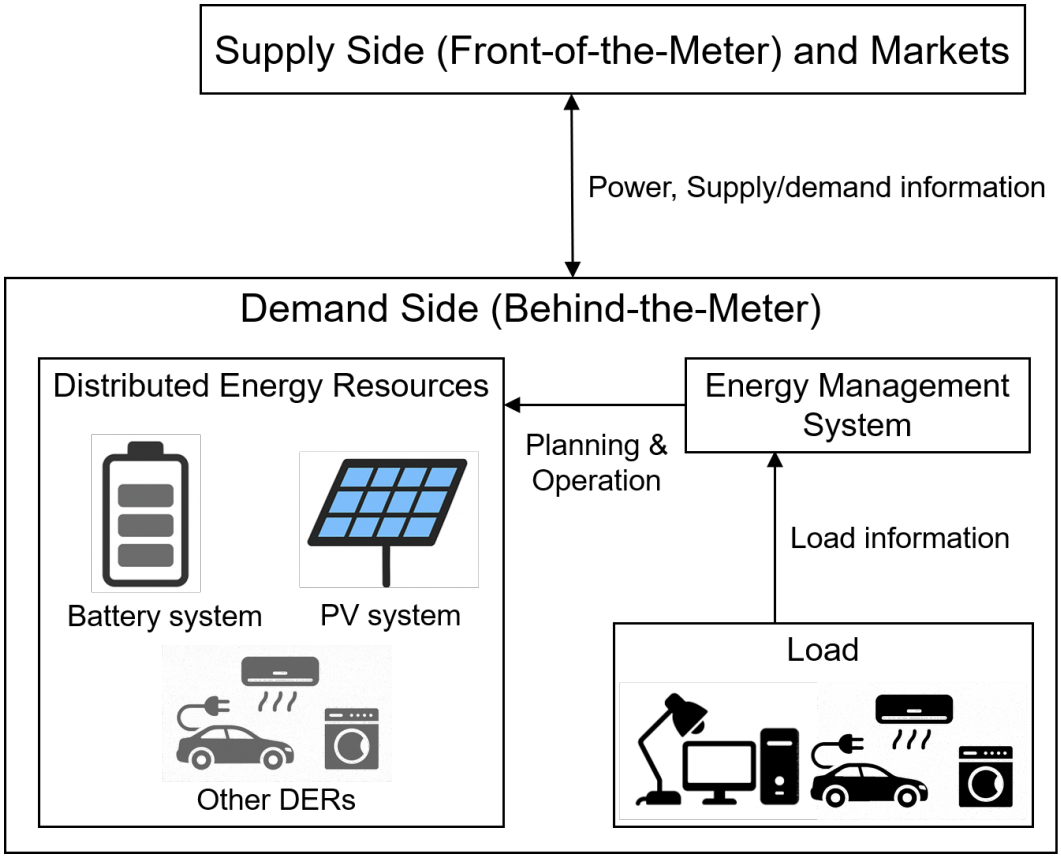


Figure 1.3: Schematic overview of an energy management system in behind-the-meter environments.

maintaining local energy balance and supporting grid stability.

Despite their advanced functionality, EMS operation is particularly challenging in environments with high renewable penetration. Uncertainties arising from the short-term variability of solar irradiance can cause significant mismatches between on-site generation and consumption, potentially leading to energy loss, increased reliance on storage, or local power quality issues. Effective EMS design therefore requires reliable forecasting methods and control strategies that can mitigate such uncertainty. In particular, improving the coordination between PV output, battery operation, and local flexibility is essential for stable and cost-effective BTM energy management, across different time horizons ranging from ultra-short-term (minutes ahead) to day-ahead operational planning.

The scale of systems managed by EMSs ranges from single-family homes to larger commercial facilities and small local energy systems. At the household or building level, EMSs typically aim to minimize electricity costs, maintain system stability, and reduce peak demand by effectively utilizing PV generation and BESS. In multi-user

BTM systems, EMSs additionally coordinate interactions among prosumers, helping mitigate collective peak loads, reduce energy waste by curtailment, balance shared resources, and enhance resilience against external disturbances.

Time scale is another important consideration for EMS performance. Over long time horizons, the EMS must account for changes in PV availability and demand patterns due to seasonal and occupancy variations. In contrast, over short time scales—especially those on the order of seconds—rapid fluctuations in PV output can lead directly to power imbalance. Meeting ramp rate requirements and smoothing short-term power variations are therefore critical aspects of EMS operation in PV-integrated BTM systems. As EMSs must address objectives spanning multiple system scales and time resolutions, their design requires flexible and adaptive approaches tailored to each operational context.

1.2.3 Ramp Rate Regulations

Ramp rate regulations have been introduced in many regions to ensure that rapid fluctuations in renewable generation do not compromise power system stability. Ramp rates define the maximum allowable change in electrical power output over a given time interval, and these requirements typically aim to limit abrupt variations associated with solar PV and wind generation. If the output of a generator exceeds the prescribed ramp rate limit, it may cause frequency deviations, voltage instability, or unexpected stress on network components. Therefore, maintaining compliance with ramp rate regulations is essential for the safe integration of distributed renewable resources into the grid.

In utility-scale systems, ramp rate constraints are often managed through centralized control strategies or by utilizing ancillary services provided by energy storage systems. In BTM systems, however, PV generation is directly affected by local environmental conditions such as cloud movement, shading, and panel temperature, which can cause highly volatile short-term fluctuations. These fluctuations can easily exceed ramp rate limits if not properly mitigated, even when the overall system size is relatively small. As the penetration of rooftop PV increases, the cumulative effect of uncontrolled ramping from many prosumers can pose significant challenges to grid operators.

To satisfy ramp rate requirements, BTM systems commonly rely on BESS to buffer sudden changes in PV output through rapid charging or discharging. While this approach is effective, it often necessitates large battery capacities or frequent cycling, which leads to high installation and maintenance costs. Such economic constraints can make battery-based ramp rate control challenging to adopt widely, particularly in residential or small commercial installations. In addition, exclusive reliance on BESS does not fully exploit the potential of BTM systems to provide flexible, cost-efficient control responses.

Beyond direct ramp-rate compliance, many regions employ curtailment procedures as an additional mechanism to limit renewable generation when rapid output fluctua-

tions or local export violations threaten grid stability. Curtailment—implemented by inverter throttling, disconnection, or export caps—prevents excessive injections that the grid cannot absorb. Although effective from a system protection perspective, curtailment results in the intentional wasting of available renewable energy, especially during high-irradiance periods. In BTM settings, where export limits are commonly imposed, frequent curtailment can significantly reduce the usable PV energy and diminish economic benefits for prosumers. Consequently, reducing curtailment-induced losses has become an important objective for advanced EMS designs.

Another important consideration is the time scale at which ramp rate violations occur. Because PV output can vary within seconds due to fast-moving clouds, ramp rate compliance requires high-resolution monitoring and control actions. Thus, short-term forecasting and rapid decision-making become indispensable for anticipating potential violations and adjusting system operation proactively. These challenges highlight the need for alternative or complementary strategies that can support ramp rate compliance without incurring excessive battery-related costs.

As behind-the-meter PV continues to proliferate, effective ramp rate management will play an increasingly important role in maintaining stable and resilient power systems. For grid operators, improved compliance with ramp rate requirements helps alleviate issues such as frequency deviations, voltage fluctuations, and steep net-load ramps, thereby reducing the need for costly grid-side interventions. For prosumers, enhanced ramp rate control enables greater utilization of rooftop PV without compromising system stability, allowing them to benefit from lower electricity costs and increased energy autonomy. Moreover, the development of cost-effective and flexible ramp rate mitigation techniques—beyond reliance on large-scale batteries—opens new opportunities for innovative control strategies within BTM environments. Thus, advancing ramp rate management represents a mutually beneficial pathway that supports both reliable grid operation and the continued expansion of distributed solar generation.

1.3 Research Questions and Issues

This section presents the remaining research questions that must be addressed to advance effective BTM energy management under high penetration of rooftop PV systems. Fig. 1.4 illustrates the overall scope of this dissertation. This study focuses on three key questions related to forecasting the highly variable conditions in BTM environments as a fundamental enabler for energy management applications, mitigating rapid fluctuations in PV output to satisfy ramp rate requirements, and integrating forecasting and control to achieve proactive and reliable system operation.

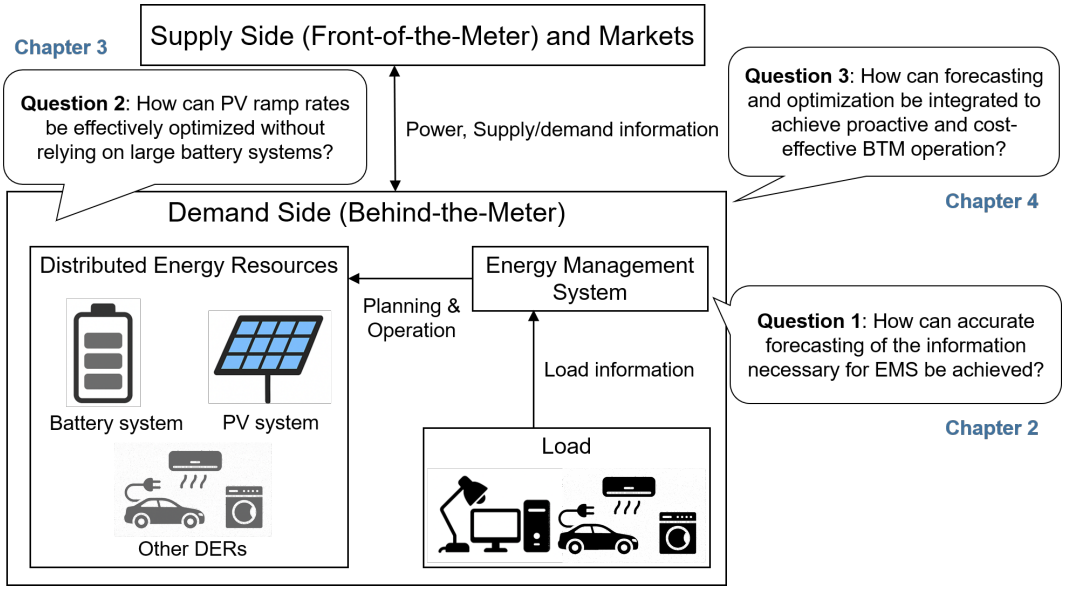


Figure 1.4: Study scope of this dissertation.

Question 1: How can accurate forecasting of the information necessary for EMS be achieved?

In BTM systems, accurate forecasting of key variables is essential for the EMS to evaluate system performance and make proactive control decisions. In particular, forecasting electricity demand, electricity prices, and solar irradiance enables the EMS to anticipate future operating conditions and determine optimal strategies for battery utilization, ramp rate mitigation, and operational planning over various time horizons.

However, accurate forecasting in BTM environments involves several challenges. Demand and electricity prices are affected by user behavior, market conditions, and temporal factors such as time of day and season, while solar irradiance exhibits high variability due to environmental conditions, including cloud movement and climatic changes. These variables are often non-stationary and highly volatile at short time scales, resulting in substantial prediction uncertainty. As a consequence, inaccurate forecasts can directly lead to inefficient EMS decisions, such as unnecessary battery cycling, excessive reliance on storage, or failure to comply with ramp rate requirements.

To address these issues, robust forecasting methodologies are required that account for the stochastic and multi-scale nature of these variables. In particular, forecasting models must be capable of capturing rapid fluctuations while also reflecting broader temporal patterns such as seasonal or daily trends. Accurate forecasting enables the EMS to reduce operational costs, mitigate unnecessary energy losses, and proactively manage DERs within BTM systems.

Question 2: How can PV ramp rates be effectively optimized without relying on large battery systems?

Because PV output fluctuates in real time, mitigating rapid power variations is necessary even within BTM systems to prevent local instability and support grid requirements. Although battery-based buffering methods can smooth PV power fluctuations, frequent and rapid charging–discharging caused by short-term variability leads to challenges in terms of cost and scalability. In particular, relying on large-capacity batteries for ramp rate control is often impractical for residential and small commercial BTM systems due to high installation costs, environmental impacts, and maintenance requirements, and more generally, the use of over-dimensioned storage systems—regardless of the underlying technology—results in unnecessary capital expenditure and inefficient resource utilization. Among these options, electrochemical batteries are especially problematic because their manufacturing, degradation, and replacement processes entail substantial environmental and economic burdens. To address these limitations, alternative control strategies are needed that can regulate PV output without excessive dependence on storage systems.

However, designing such control strategies is challenging because PV behavior is influenced by various environmental and physical factors, including irradiance variability, shading, and module temperature. These dependencies create complex and nonlinear dynamics that make PV output difficult to manage using purely electrical control measures. Thus, an effective approach must be capable of responding to rapid fluctuations, accommodating diverse operating conditions, and minimizing energy losses without requiring oversized storage capacity.

In addition, real-time ramp rate mitigation must operate at a fine temporal resolution to reflect second-level variations in PV output and ensure compliance with grid regulations. The required control framework must process high-resolution data, respond quickly to local conditions, and coordinate available resources in a computationally efficient manner. Therefore, the key challenge is to develop scalable, cost-effective, and adaptive ramp rate control methods that do not rely solely on large battery systems while still supporting stable and reliable PV integration in BTM environments, and to introduce novel production-side control knobs capable of directly modulating PV output. Such control mechanisms have traditionally been absent in PV systems, which typically lack the ability to adjust generation in real time without relying on electrical or storage-based interventions. Establishing a practical and efficient means of directly influencing PV production thus represents a critical missing component in existing BTM ramp-rate mitigation strategies.

Question 3: How can forecasting and optimization be integrated to achieve proactive and cost-effective BTM operation?

While accurate forecasting and effective control methods are each important in BTM energy management, a key challenge remains in how to integrate these functionalities to operate DERs proactively and cost-effectively. Forecasting provides valuable information about future PV generation, demand, and market conditions, whereas control and optimization determine how these resources should be operated at each instant. However, without proper coordination between forecasting and decision-making, BTM systems may fail to utilize prediction results meaningfully, resulting in reactive or inefficient operation. The key challenge is therefore to establish a unified procedure in which forecasting and control are connected in a way that supports proactive and economical BTM operation.

1.4 Objective and Organization

This section summarizes the objectives of the following chapters and outlines how to address the questions described in Chapter 1.3. The objective of this dissertation is to develop a practical BTM energy management framework that enables proactive and cost-effective operation under high penetration of PV systems. To this end, the dissertation investigates forecasting, ramp rate mitigation, and forecast-informed control methodologies to enhance local energy stability and reduce operational dependence on large battery systems. Accordingly, this dissertation addresses three research questions related to accurate forecasting for EMS decision-making, cost-effective ramp rate control, and the integration of forecasting and control, as illustrated in Fig. 1.4. It should be noted that the contributions made in response to each research question are not intended to represent final or complete solutions to the corresponding challenges. Rather, they are positioned as foundational and stepwise contributions toward the broader research theme of forecast-driven energy management and ramp rate control in BTM environments.

Forecasting Method for Non-Stationary Time Series Using WT-LSTM to Address Question 1

For effective energy management in BTM systems, accurate forecasting of key variables such as electricity demand, electricity prices, and solar irradiance must be addressed. This dissertation proposes a forecasting methodology based on a wavelet transform–long short-term memory (WT-LSTM) model to improve prediction accuracy for non-stationary and highly volatile time series frequently observed in BTM environments.

In the proposed method, wavelet transform is used to decompose raw data into multiple sub-patterns, allowing the forecasting model to separately capture long-term trends and short-term fluctuations. These decomposed signals are then modeled by an LSTM predictor, while explanatory variables and systematic feature selection are incorporated to enhance predictive performance under diverse conditions. Furthermore, the forecasting framework supports adaptive wavelet selection, enabling consistent performance across multiple forecasting targets.

The simulation results demonstrate that the proposed WT-LSTM method improves prediction accuracy for electricity prices, electricity demand, and solar irradiance, outperforming conventional and baseline models. Such improvements contribute to more reliable EMS decision-making and reduce inefficiencies caused by reactive or suboptimal operation.

It should be noted that the forecasting methodology in this dissertation is designed to provide accurate point predictions rather than full probabilistic forecasts. While uncertainty modeling is beyond the scope of this research, exploring robust or stochastic forecasting-based control mechanisms remains an important direction for future work.

Cooling-Based PV Ramp Rate Control Strategy to Address Question 2

This dissertation investigates a strategy to mitigate short-term fluctuations in PV output without relying exclusively on large battery systems. The proposed method focuses on real-time regulation of PV generation through cooling-based control, in which the electrical output of PV modules is indirectly adjusted by modulating their operating temperature. This approach leverages the temperature-dependent characteristics of PV efficiency to suppress excessive power ramps and alleviate the need for high-capacity storage resources in BTM environments. Additionally, the strategy can be combined with small-capacity batteries for residual smoothing, offering hybrid operation without requiring large-scale storage investment.

Simulation experiments using real-world irradiance and temperature data demonstrate that the cooling-based control strategy effectively reduces mean and maximum ramp rates, even with modest cooling performance (coefficient of performance below 10) and minimal battery capacity. These results indicate that the method functions not merely as a cooling mechanism but as an innovative production-side control knob: surplus PV generation during high-irradiance periods is intentionally utilized to cool the modules, thereby lowering their temperature and improving conversion efficiency, and the resulting additional production can be exploited at moments when local demand exceeds instantaneous PV output.

It should be noted that the proposed method focuses on regulating PV output through cooling operations rather than optimizing cooling system design or thermal hardware configuration. The integration of more detailed thermodynamic models or advanced cooling technologies remains beyond the scope of this dissertation and offers potential opportunities for future research.

Integrated Forecasting and Optimization Framework to Address Question 3

This dissertation proposes a forecast-informed energy management framework that sequentially integrates forecasting and control to achieve proactive and cost-effective BTM operation. The proposed framework combines short-term forecasting of solar irradiance with a real-time optimization procedure that determines control actions for PV regulation and battery usage. Forecasting results are treated as actionable decision inputs, enabling the system to anticipate upcoming fluctuations and adjust PV output before steep variations occur. While practical EMS implementations operate across multiple temporal layers—from ultra-short-term control to day-ahead planning—the present work focuses explicitly on the short-term horizon. Nevertheless, this framework preserves the conceptual alignment with hierarchical EMS structures by treating short-term forecasting and control as one layer within a broader temporal hierarchy. In this framework, the forecasting and optimization stages are executed sequentially, where the former predicts near-future conditions and the latter determines control responses based on these predictions.

The integrated strategy enables forecast-guided PV ramp mitigation by coordinating cooling-based control and battery usage, resulting in smoother PV output and reduced dependency on large storage systems. Simulation results demonstrate that using forecasts with a 30–60 second horizon enables proactive ramp rate mitigation, reducing the number of violations by up to 20% compared to a no-control baseline.

It should be noted that the proposed framework focuses on sequential integration of forecasting and control and does not consider probabilistic uncertainty modeling or joint optimization of forecast and operation. Extending the framework to incorporate uncertainty-aware decision-making or multi-objective control remains an important topic for future work.

Dissertation Text Organization

The rest of this dissertation is organized as follows. Chapter 2 presents a forecasting methodology for non-stationary time series in BTM energy management. The proposed WT-LSTM-based framework improves prediction accuracy for electricity demand, electricity prices, and solar irradiance by incorporating wavelet decomposition, explanatory variables, and feature selection, providing reliable information for EMS decision-making.

Chapter 3 investigates a cooling-based ramp rate control strategy that regulates PV output by exploiting the temperature dependence of PV efficiency. The control method activates cooling units to suppress steep power changes, reducing ramp rate magnitudes without requiring large battery systems or significant curtailment losses.

Chapter 4 proposes an integrated forecasting–control framework in which short-term predictions are used as decision inputs within a optimization framework. The results show that using forecasts with a 30–60 second horizon enables proactive mitigation of

ramp rate violations and increases power delivery to the grid by enabling preemptive utilization of surplus PV energy. Finally, Chapter 5 summarizes this dissertation and refers to the extensions for future work.

Chapter 2

WT-LSTM Based Forecasting for Behind-the-Meter System

In behind-the-meter systems, accurate forecasting of key variables such as electricity price, electricity demand, and solar irradiance plays a critical role in ensuring economic efficiency and operational stability. These time series are often highly volatile and non-stationary, posing challenges for traditional statistical and machine learning models. This chapter proposes a forecasting methodology based on the integration of wavelet transform (WT) and long short-term memory (LSTM) networks, referred to as WT-LSTM, to address these challenges[1]. The method incorporates explanatory variables, systematic feature selection, and adaptive wavelet selection to enhance predictive performance across different forecasting tasks. Specifically, the proposed WT-LSTM framework is applied to electricity price, demand, and solar irradiance forecasting, enabling a comprehensive evaluation under diverse conditions. The findings demonstrate that the method improves forecasting accuracy across multiple domains, thereby contributing to reliable behind-the-meter management. In principle, the same modeling approach could also be extended to other forms of renewable energy production—such as wind power generation or geothermal output—because these sources similarly exhibit non-stationary and multi-scale temporal characteristics. However, substantiating this broader applicability requires dedicated investigation and validation, and is therefore positioned as future work beyond the scope of this chapter.

2.1 Introduction

Forecasting in behind-the-meter systems plays a crucial role in ensuring efficient and reliable energy management. Accurate forecasting of electricity prices, electricity de-

[1]This chapter refines and extends previously published works: electricity price forecasting is based on [23, 24], electricity demand forecasting is refined from [25], and solar irradiance forecasting builds upon [26].

mand, and solar irradiance enables system operators to optimize scheduling, participate effectively in electricity markets, and maintain grid stability. If these quantities cannot be accurately forecasted, operators may face several issues: electricity price volatility can lead to suboptimal bidding strategies, demand-supply imbalances can threaten the stability of the power system, and unpredictable solar generation can increase the reliance on costly reserves or energy storage. Therefore, reliable forecasting is essential for both economic efficiency and operational security in behind-the-meter environments.

However, forecasting these variables is inherently difficult. Electricity prices exhibit strong non-stationarity due to market fluctuations, electricity demand is influenced by diverse social and environmental factors, and solar irradiance is highly variable under rapidly changing weather conditions. Traditional time series models often struggle to capture such nonlinear and multi-scale dynamics. This motivates the use of hybrid approaches that can both decompose complex signals and learn temporal dependencies effectively.

This chapter develops a unified WT-LSTM based forecasting framework for behind-the-meter applications. The methodology integrates WT for decomposing time series into multiple frequency components with LSTM networks for modeling nonlinear temporal dependencies. By combining these techniques, the framework aims to achieve high forecasting accuracy across different types of energy-related time series.

The main contributions of this chapter are as follows:

- A unified WT-LSTM forecasting methodology is proposed, combining signal decomposition and deep learning for behind-the-meter applications.
- Three novel aspects are introduced into the methodology: (i) incorporating auxiliary features beyond the target variable, (ii) applying a quantitative feature selection method to identify the most relevant inputs, and (iii) dynamically selecting the mother wavelet to improve the decomposition process.
- Simulation results demonstrate that the proposed forecasting framework achieves higher accuracy than conventional approaches across multiple forecasting tasks.

The remainder of this chapter is organized as follows. Section 2.2 reviews related works on forecasting methods. Section 2.3 introduces the WT-LSTM forecasting methodology. Sections 2.4–2.6 present detailed forecasting case studies for electricity price, electricity demand, and solar irradiance, respectively. Finally, Section 2.7 summarizes the chapter and provides concluding remarks.

2.2 Related Works

2.2.1 Statistical Forecasting Methods

Statistical approaches have historically formed the foundation of forecasting research in energy systems. Classical time series models such as auto-regressive integrated mov-

ing average (ARIMA), seasonal ARIMA, and vector auto-regression have been widely applied to electricity price, demand, and renewable generation forecasting. These methods are favored for their simplicity, interpretability, and ability to capture linear temporal dependencies with relatively small datasets. Zhao et al. [27] applied an ARIMA-based approach to model differential electricity price time series, in which prices are expressed as a weighted combination of historical values and stochastic noise. Their study additionally accounted for distinct consumption behaviors observed on weekdays versus holidays. By incorporating a categorical weekday/holiday factor into the model, they achieved improved short-term forecasting performance. Tan et al. [28] proposed a method based on WT combined with ARIMA and generalized auto-regressive conditional heteroscedasticity (GARCH) models. They used Daubechies wavelets of order 4 as mother wavelets (MW) and considered three decomposition levels. Thus, the original price series was decomposed and reconstructed into one approximate series (a3 and A3) and three detailed series (d1, d2, d3, D1, D2, and D3). The approximate series is the low-frequency component of the original price signal and is the trend of the signal. To predict the future values of the approximate series, they applied an ARIMA process with GARCH error components. The detailed series were predicted by the GARCH model, which is able to capture the characteristics of high volatility, as it has been described to be more closely related to the noisy part of the original signal. They demonstrated its effectiveness through verification using data from the Spanish electricity market and other sources. Mohsenian-Rad et al. [29] observed strong correlations between electricity prices and their values one, two, and seven days earlier. Building on this observation, they formulated the forecasted price as a weighted combination of prices from these preceding days. Furthermore, by adjusting the weights according to the day of the week, their approach achieved forecasts with reduced error.

For electricity demand forecasting, Newsham et al. [30] used the ARIMA model to forecast electricity consumption in buildings. They focused on the fact that the presence of people in a building increases electricity consumption, and succeeded in improving accuracy by taking into account the number of people staying in the building in addition to past electricity consumption. Karin [31] predicted electricity demand on a university campus using the auto-regressive with exogenous model, an auto-regressive model with ARIMA and inputs of exogenous disturbances. In addition to past electricity demand data, the number of students staying on campus is used to achieve highly accurate forecasts.

However, these statistical methods express predictions as a linear combination of past values or features. This assumption is not really valid in practical situations because the longer the past time considered or the more features, the more parameters are required. This makes it difficult to handle complex and non-linear time series. Therefore, machine learning is attracting attention due to its outstanding performance in dealing with complex and non-linear problems.

2.2.2 Machine Learning Forecasting Methods

In contrast to traditional statistical models, machine learning forecasting methods provide enhanced flexibility by automatically extracting nonlinear features from observational data. Lu et al. [32] developed an electricity price forecasting model based on artificial neural networks (ANNs). Lago et al. [33] conducted a comparative study between machine learning approaches—such as deep neural networks (DNNs) and LSTM models—and traditional statistical methods including ARIMA, demonstrating that machine learning techniques generally achieve higher prediction accuracy. Xu et al. [34] evaluated several recurrent architectures, including simple recurrent neural networks (RNNs), LSTM, and gated recurrent units (GRUs), and compared their performance with that of feedforward neural networks lacking recurrent structures. They used as inputs the previous day's day-ahead prices, ERCOT's wind and load long-term forecast information, month and day, and time. Their results showed that simple RNN, LSTM, and GRU could predict more accurately because they predict based on past information. Building on the evidence from these studies, machine learning has demonstrated its usefulness in capturing complex forecasting patterns, positioning it as a foundation for advanced frameworks that integrate complementary methods and information sources.

2.2.3 Hybrid Forecasting Methods

In recent years, hybrid approaches that combine machine learning with complementary techniques have attracted significant attention, as they often achieve higher time-series forecasting accuracy than methods relying solely on machine learning models. Peng et al. [35] incorporated a differential evolution (DE) algorithm to determine the parameters of LSTM. The preprocessed time series are predicted by DE-LSTM. Assuming that preprocessing time-series data would better capture its characteristics, an improvement in forecast accuracy has been shown using electricity prices in Australia, Germany, Austria, and other countries. Lago et al. [36] targeted the day-ahead market. In the day-ahead market, wholesalers and buyers bid on day d's power supply before the gates close on day $d-1$, and the 24-hour price for day d is usually set around noon. They demonstrated that a hybrid model combining least absolute shrinkage and selection operator–estimated autoregressive (LEAR) modeling with DNN outperforms approaches using LEAR or DNN alone, and statistically confirmed the improvement in prediction accuracy through formal significance tests. Zhou et al. [37] found that the LSTM model can make full use of the memory characteristic due to the strong regularity of time and to some extent self-correlated in Pennsylvania - New Jersey - Maryland (PJM) electricity prices. The PJM electricity price time series is autocorrelated, which means that past prices are closely related to future prices. Furthermore, they combined LSTM with ensemble empirical mode decomposition to decompose and reconstruct electricity price time series into high- and low-frequency components and fully explore the information contained in the time series, achieving higher accuracy than LSTM alone or stacked

LSTM.

Since it is very effective in forecasting non-stationary time series, research combining machine learning and WT is actively being conducted for various predictions in the energy sector. WT is widely used for decomposing time series into frequency-based components. Su et al. [38] applied a hybrid framework integrating WT, RNN–based deep learning model, and a genetic algorithm to forecast natural gas consumption. In their study, WT reduced forecasting complexity by decomposing the original consumption series into multiple subcomponents, with Daubechies 4 selected as the mother wavelet. Similarly, Liu et al. [39] proposed a WT–LSTM–based method for short-term wind power forecasting, employing Daubechies 7 as the mother wavelet and demonstrating the effectiveness of the approach. In electricity price forecasting, Aggarwal et al. [40] developed a WT-based neural network model to predict price profiles in electricity markets. They compared Daubechies 1 through 4 as candidate mother wavelets and ultimately adopted Daubechies 2, showing that WT-based decomposition improved prediction accuracy. Singh et al. [41] combined WT with generalized neurons, which require fewer training samples, and used Daubechies 4 as the mother wavelet. Their study also evaluated various error functions using electricity price data from New South Wales, Australia. Chang et al. [3] proposed a hybrid WT–LSTM model and evaluated it using datasets from Australia and France. In their approach, the electricity price time series was first decomposed into multiple low-variance components using WT. Each component was then independently modeled using LSTM, and the final price forecast was obtained by aggregating the predicted components. By stabilizing the variance of the time series through WT-based decomposition, the model enabled LSTM to more effectively capture electricity price fluctuations. Their results demonstrated significant accuracy improvements over existing models, including Peng's method [35] and the ARIMA–ANN hybrid proposed by Babu et al. [42]. In the domain of electricity demand forecasting, Ofori-Ntow Jnr et al. [43] introduced a three-level hybrid ensemble framework that combines WT, particle swarm optimization, and a radial basis function neural network for short-term demand prediction. Compared with backpropagation neural network and self adaptive DE - extreme learning machine, they highlighted the superiority of their proposed method. Li et al. [44] proposed a model that combines WT and fuzzy inference system for predicting building electrical demand. In their method, WT was used to obtain diurnal patterns and residual data for forecasting in order to better reflect the actual characteristics of electricity demand. Saoud et al. [45] proposed a method to predict household electricity demand at different resolutions using a machine learning model based on stationary wavelet transform (SWT) and transformers. SWT and its inverse characteristics were used to decompose and reconstruct the actual and predicted household electricity demand data, respectively, while the deep transformer was used to predict the subbands of the SWT.

Although models combining WT and machine learning have demonstrated strong forecasting performance across various domains, existing studies still suffer from three

main limitations: (1) the neglect of potentially relevant variables, (2) the reliance on ad hoc feature selection, and (3) the use of static wavelet decomposition. First, previous studies may not have considered potentially relevant variables. Even Chang et al.'s research [3], which achieved high prediction accuracy using WT-LSTM for electricity price forecasting, has focused solely on past electricity prices. Second, feature selection has often been performed heuristically, which risks introducing biases and may overlook the most informative predictors in a consistent and data-driven manner. Third, wavelet decomposition has typically been applied with fixed MW, failing to adapt to the seasonal variability. A wide variety of MWs exist, each exhibiting different strengths and weaknesses in time-series decomposition depending on the shape and characteristics of the target signal, as discussed by Barzegar et al. [46]. Although real-world time series often exhibit temporal variations in their underlying patterns, the studies reviewed above adopt a fixed MW throughout the entire experimental period. Consequently, even when the shape of the time series changes over time, the decomposition basis remains unchanged, which can lead to period-dependent variations in forecasting accuracy, as reported by Oksuz et al. [47]. To address these limitations, this study introduces an enhanced WT-LSTM forecasting method that incorporates auxiliary features, a quantitative feature selection, and dynamic wavelet selection.

2.3 WT-LSTM Based Forecasting Methodology

First, the basic theories of WT and LSTM are explained. Then, while referring to the proposed method as a whole, the particularly important aspects of auxiliary features, a quantitative feature selection, and dynamic wavelet selection are discussed.

2.3.1 Wavelet Transform

The wavelet transform (WT) is used as an effective time-frequency analysis method. The Fourier transform, which is also a frequency analysis method, replaces all the properties of the signal with frequency information, resulting in the loss of time-related information. However, in WT, the time width to be analyzed is varied according to the frequency. In other words, the analysis time span is lengthened for the lower frequency components and shortened for the higher frequency components. Thus, by making the time width to be analyzed inversely proportional to the frequency, time and frequency can be analyzed simultaneously, so the WT is said to be superior to the Fourier transform in the component analysis of nonstationary signals [48]. Specifically, WT basically represents the input signal by adding small waves (wavelets) by scaling them up or down and translating them. The basic WT is the continuous wavelet transform (CWT), which deals with continuous quantities, but since it is difficult to deal with continuous quantities on a computer, the discrete wavelet transform (DWT) is used. In general, CWT is characterized by its ability to perform more precise analysis than DWT. On the other

hand, DWT is also applied to noise removal [49], image analysis [50], and image compression [51] [52] by processing the transformed information once and inverting it. Let $y(t)$ be the input signal, CWT is defined by the following equation.

$$CWT_y(\alpha,\tau) = \frac{1}{\sqrt{|\alpha|}} \int y(t)\psi^*(\frac{t-\tau}{\alpha})dt, \tag{2.1}$$

where α is the scale parameter, τ is the translation parameter, $\psi^*(x)$ is the complex conjugate function and $\psi(x)$ is MW. DWT is defined by the following equation.

$$DWT_y(m,n) = \alpha_0^{-\frac{m}{2}} \int y(t)\psi^*(\alpha_0^{-m}t - n\tau_0)dt, \tag{2.2}$$

where m,n are both integers.

Various wavelets are used in wavelet analysis, such as Gabor and Mexican hat for CWT, and Spline and Daubechies for DWT. The m in the equation (2.2) is a scaling constant which means the level of resolution; the larger this value is, the finer the signal data representation is, and the smaller the value is, the coarser the signal data representation is. The order of the wavelet is called vanishing moment, and is related to the approximation order and the smoothness of the wavelet. For instance, a wavelet with p vanishing moments is capable of exactly representing polynomials up to order $p-1$. As the number of vanishing moments increases, the associated wavelet can model higher-order polynomial trends, resulting in smoother signal representations.

2.3.2 Long Short-Term Memory

Long short-term memory (LSTM) is a RNN for time series data processing, and has been applied not only to forecasting in the energy sector but also to speech recognition [53] [54] [55], character recognition [53], prediction of precipitation [56], etc. Fig. 2.1 shows a schematic diagram of the RNN layer structure. RNN has an input layer, an intermediate layer, and an output layer, just like a normal neural network. The input layer receives data at each time, and the output layer outputs the result at each time. Unlike normal neural network, RNN have a path to convey the output to the intermediate layer at the next time slot. As shown in Fig. 2.1, this path causes the intermediate layer at time t to receive information from the intermediate layer at the previous time $t-1$, in addition to inputs from the input layer at time t. This information from the previous time makes it possible to take into account the influence between times.

However, the basic RNN has a problem that it cannot capture the long-time dependence of the input data in the learning process due to the gradient vanishing problem. The gradient vanishing problem is a problem in which learning does not progress beyond a certain stage in a multilayered neural network. Learning proceeds by minimizing the error between the predicted value and the actual value, but in a multilayer neural network like RNN, if the gradient of the activation function is close to 0 in even one layer,

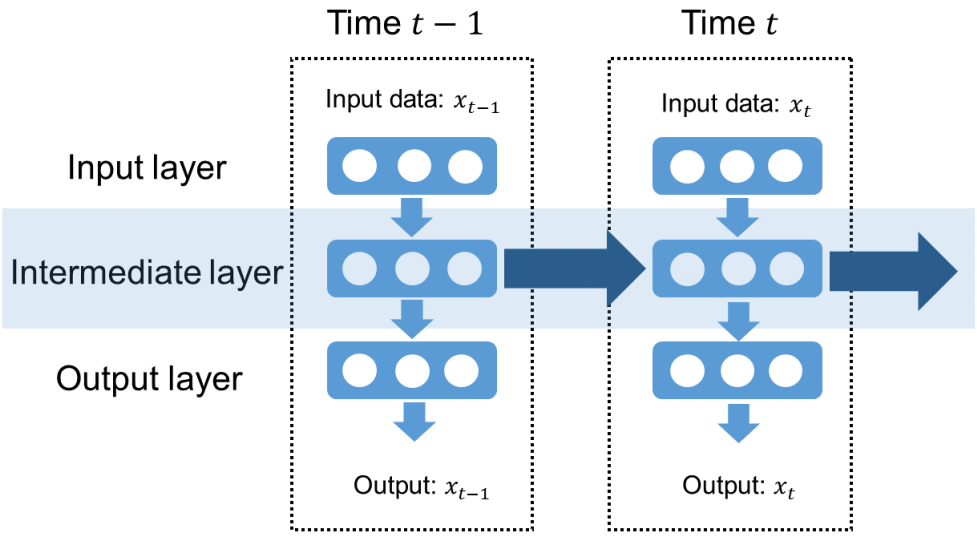


Figure 2.1: Layered structure of RNN.

the gradients of all the layers below it will also be close to 0. When this happens, the weights of the network cannot be modified and the optimal solution cannot be obtained, making learning difficult.

LSTM eliminates this gradient disappearance problem and allows for longer-term dependence. The structure of LSTM is shown in Fig. 2.2. LSTM consists of three gates: an input gate, an output gate, and a forget gate, each of which controls the information it conveys. x_t is the input at time t, h_t is the output at time t, and C_t is a memory cell called constant error carousel (CEC), which stores past data. Each gate is realized by multiplying the output of the sigmoid layer, which outputs a number between 0 and 1, with each component. The forget gate outputs a number between 0 and 1 for the CEC value from h_{t-1} and x_t. For the CEC value, 1 means "keep the value of CEC completely" and 0 means "remove it completely". The input gate creates, through the tanh layer, candidate values for new values to be added to the CEC. The value of CEC is updated by adding the output of the forget gate to this value. Finally, at the output gate, the output value is determined by multiplying the value obtained by applying tanh to the CEC with the output of the sigmoidal layer. In this way, the input gate controls how much of the input value is taken in, the output gate controls how much is transmitted to the next time, and the forget gate controls how much information is retained in the CEC.

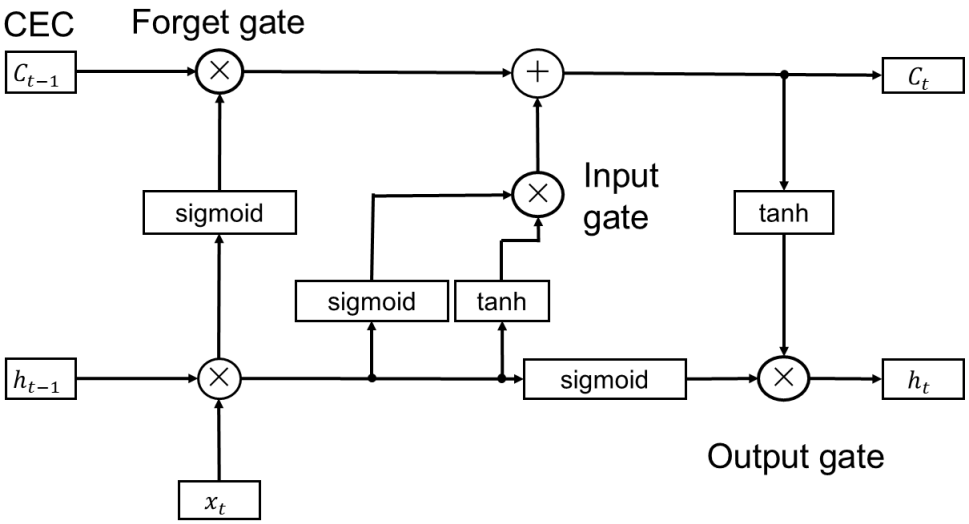


Figure 2.2: Architecture of an LSTM cell with input, forget, and output gates.

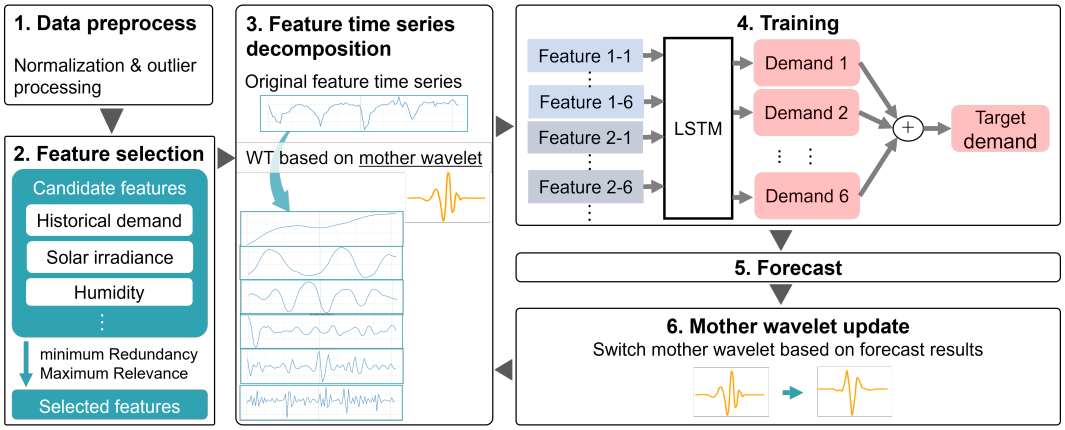


Figure 2.3: Overview of the proposed forecasting method.

2.3.3 Forecasting Methodology

Based on the fundamental techniques introduced in Sections 2.3.1 and 2.3.2, this section describes the proposed forecasting methodology that integrates WT and LSTM to enhance forecasting performance. Fig. 2.3 illustrates the overview of the proposed method using the electricity demand forecasting task as an example, and the following explanation proceeds in accordance with this flowchart. In the following, three particularly important contributions of the procedure—auxiliary features, a quantitative feature selection, and dynamic wavelet selection—will be explained in greater detail. In the first step, outlier handling based on the Pauta criterion and minimum-maximum normaliza-

tion are performed. Pauta criterion is a criterion that sets $\mu - 3\sigma$ and $\mu + 3\sigma$ as threshold values when the standard deviation of the data is σ and the mean is μ. In the outlier process based on Pauta criterion, the standard deviation σ and the mean μ of the data set are first calculated assuming that the data set contains only random errors. Then, errors beyond the range of $(\mu - 3\sigma, \mu + 3\sigma)$ are considered as outliers rather than random errors and are treated as such. Specifically, the following procedures are performed.

1. Calculate the standard deviation σ with the training data as $\chi = (\chi_1, \chi_2, \cdots, \chi_k)$ from the following formula.

$$\sigma = \sqrt{\frac{\sum_{i=1}^{k}(\chi_i - \bar{\chi})^2}{k-1}}, \tag{2.3}$$

   where $\bar{\chi}$ is the mean of the training data and k is the number of data in the training data.
2. For each data in the training data, Pauta criterion is used to determine whether the data is included in the distribution range of $(\mu - 3\sigma, \mu + 3\sigma)$.
   (a) If the data is contained in $(\mu - 3\sigma, \mu + 3\sigma)$, leave the data as is.
   (b) If the data are not included in $(\mu - 3\sigma, \mu + 3\sigma)$, they are considered as outliers and replaced by $\bar{\chi}$.

After outlier processing according to the Pauta criterion, the data are normalized to the range of 0 to 1 by Min-Max normalization. Min-max normalization is a linear transformation of the original data, and the following equation is used for normalization.

$$x' = \frac{x - minA}{maxA - minA}, \tag{2.4}$$

where x is the original value, x' is the normalized value, and $maxA$ and $minA$ are the maximum and minimum values of data set A, respectively.

Next, feature selection is performed in the second step. In this step, a candidate feature set is first created by considering potentially auxiliary features beyond the target variable, one of the contributions of the proposed method. For example, in the case of electricity price forecasting, electricity demand data serve as such auxiliary features. The actual electricity prices and electricity demand in New South Wales, Australia, from May 25 to May 31, 2013 are shown in Fig. 2.4. The horizontal axis represents time, and the left and right vertical axes represent electricity prices and electricity demand, respectively. The green graph shows electricity prices and the red graph shows electricity demand. From Fig. 2.4, it can be seen that fluctuations in electricity prices and electricity demand have a certain correlation with the location of peaks and other factors. Such auxiliary features are incorporated into the candidate feature set to enhance the model's ability to capture relevant dependencies. Subsequently, quantitative feature selection, another contribution of the proposed method, is performed on the created candidate feature set. Quantitative feature selection is achieved by using the minimum redundancy

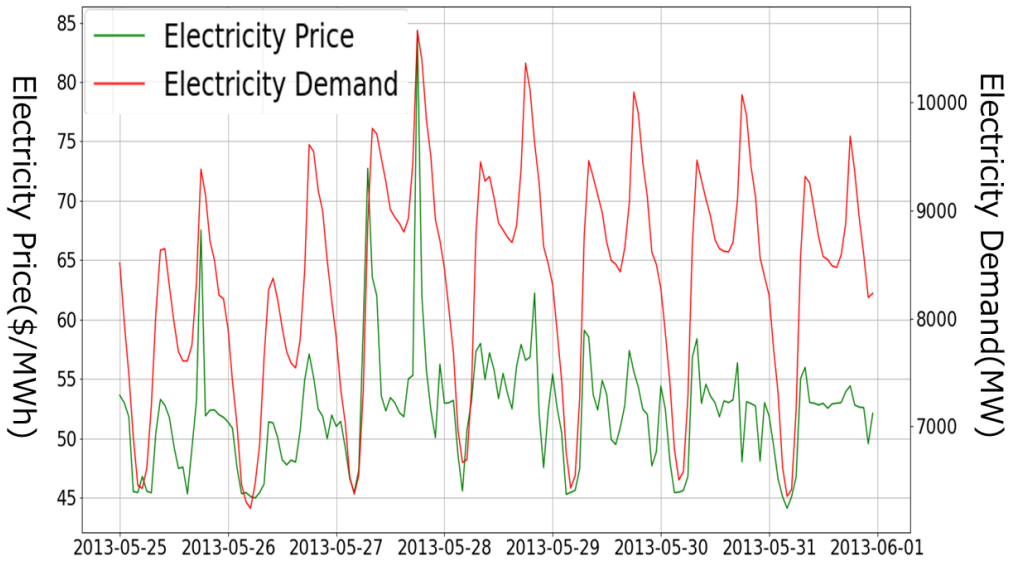


Figure 2.4: Electricity prices and demand in New South Wales, Australia (May 25 - May 31, 2013).

maximum relevance (mRMR), which not only identifies features with high correlation to the target variable (electricity demand in the case of electricity demand forecasting in Fig. 2.3) but also yields a set of features that are non-redundant. This systematic approach prevents the arbitrary selection of input variables and ensures that the selected features contribute complementary information to the forecasting model. Feature selection by mRMR selects the features that maximize the following equation.

$$\max_{x_j \in X - S_{m-1}} \left[I(x_j; c) - \frac{1}{m-1} \sum_{x_i \in S_{m-1}} I(x_j; x_i) \right], \tag{2.5}$$

where x_j is j-th feature candidate, c is objective variable (electricity demand), X is set of feature candidates, $I(\cdot)$ is mutual information, and $S_(m-1)$ is set of selected features of size $m-1$. The first term calculates the mutual information between a feature and the target variable, and the more relevant they are, the more this term contributes to maximizing the overall equation. The second term computes the mutual information between the features, and the smaller their redundancy, the more this term contributes to maximizing the overall equation.

Next, in the third step, the time series is decomposed using WT. This decomposition is applied to all feature time series selected by mRMR in the second step. Fig. 2.5 and 2.6 show the time series decomposition via WT, using the electricity price time series as an example. First, the original price time series is decomposed using WT into multiple component series, as illustrated in Fig. 2.5. The approximation component represents

the low-frequency trend, while the detailed components capture higher-frequency variations, including abrupt changes in the signal. Subsequently, the inverse WT is applied to the approximation and each detailed component to reconstruct their corresponding time-domain series, as shown in Fig. 2.6.

After decomposition, all resulting component series—including both the approximation and all detail components—are used as inputs to the forecasting model. Each component, derived from WT, captures distinct temporal characteristics such as high-frequency fluctuations and long-term trends. By inputting these component series into the corresponding LSTM model, predicted values are generated for each component of the forecast target. The final forecast is then obtained by summing all the predicted component values, effectively reconstructing the overall signal from its learned subcomponents. In the fifth step, the trained model is evaluated by applying the actual test data, allowing assessment of its forecasting performance under real conditions. This evaluation verifies the effectiveness of the proposed methodology in accurately capturing temporal dependencies and reconstructing precise forecasts from decomposed subseries.

In the final sixth step, the dynamic selection of the mother wavelet is performed, which is one of the contributions of the proposed prediction method. Similar to the Fourier transform, where a time series is expressed through scaled and shifted sine and cosine functions, the wavelet transform represents the original signal using scaled and translated basis functions known as mother wavelets (MWs). Because a wide variety of MWs exist, the resulting prediction performance can vary substantially depending on the selected wavelet. Fig. 2.7 illustrates nine MWs that are commonly employed in time-series forecasting, as introduced in Chapter 2.2.3. Here, Daubechies (db) and Symlet (sym) denote the wavelet families, and the accompanying number indicates the corresponding vanishing moments. In general, for time–frequency analysis using WT, it is widely accepted that the MW should be selected based on its similarity to the shape characteristics of the target time series [57]. The actual shape of electricity prices and electricity demand time series, which are frequently the subject of forecasting in the energy sector, varies over time. For example, Fig. 2.8 shows time-series data for electricity prices in Australia over a certain period, with the horizontal axis representing time and the vertical axis representing electricity prices. The price exhibited pronounced volatility between April and August, while fluctuations were comparatively smaller from September to December. Therefore, in the sixth step of the proposed methodology, dynamic MW selection is achieved by periodically switching MW according to the observed variations over days and seasons. During the switching process, the forecast corresponding to MW that achieved the highest prediction accuracy in the previous n weeks—evaluated in Step 5—is adopted as the final forecast. As illustrated in Fig. 2.8, while the time-series shape tends to change within a month, differences over a few consecutive days have minimal impact. Thus, MW is switched on a weekly basis to balance adaptability and stability in forecasting. The optimal value of n was

determined through simulation-based evaluation. In the following sections, the proposed methodology is applied to three forecasting tasks—electricity price forecasting, electricity demand forecasting, and solar irradiance forecasting—to evaluate its effectiveness across different domains.

In this study, LSTM is adopted as the forecasting model because of its capability to explicitly capture nonlinear temporal dependencies and time-varying patterns commonly observed in energy-related time series. These characteristics make LSTM well suited for modeling the complex dynamics of electricity demand, prices, and solar irradiance. However, it is important to emphasize that the primary contribution of this work does not lie in the specific choice of the forecasting model itself, but rather in the overall forecasting framework that integrates wavelet transform, auxiliary features, quantitative feature selection, and dynamic decomposition. From this perspective, the proposed framework is not restricted to LSTM-based predictors. Other machine learning models, such as tree-based methods (e.g., XGBoost) or attention-based architectures (e.g., Transformer models), can be incorporated into the forecasting stage with minimal modification. This flexibility allows practitioners to select appropriate prediction models depending on data characteristics, interpretability requirements, and computational constraints. In this work, LSTM is employed as an initial implementation to demonstrate the effectiveness of the proposed framework, while systematic comparisons with or integration of alternative forecasting models are identified as important directions for future research.

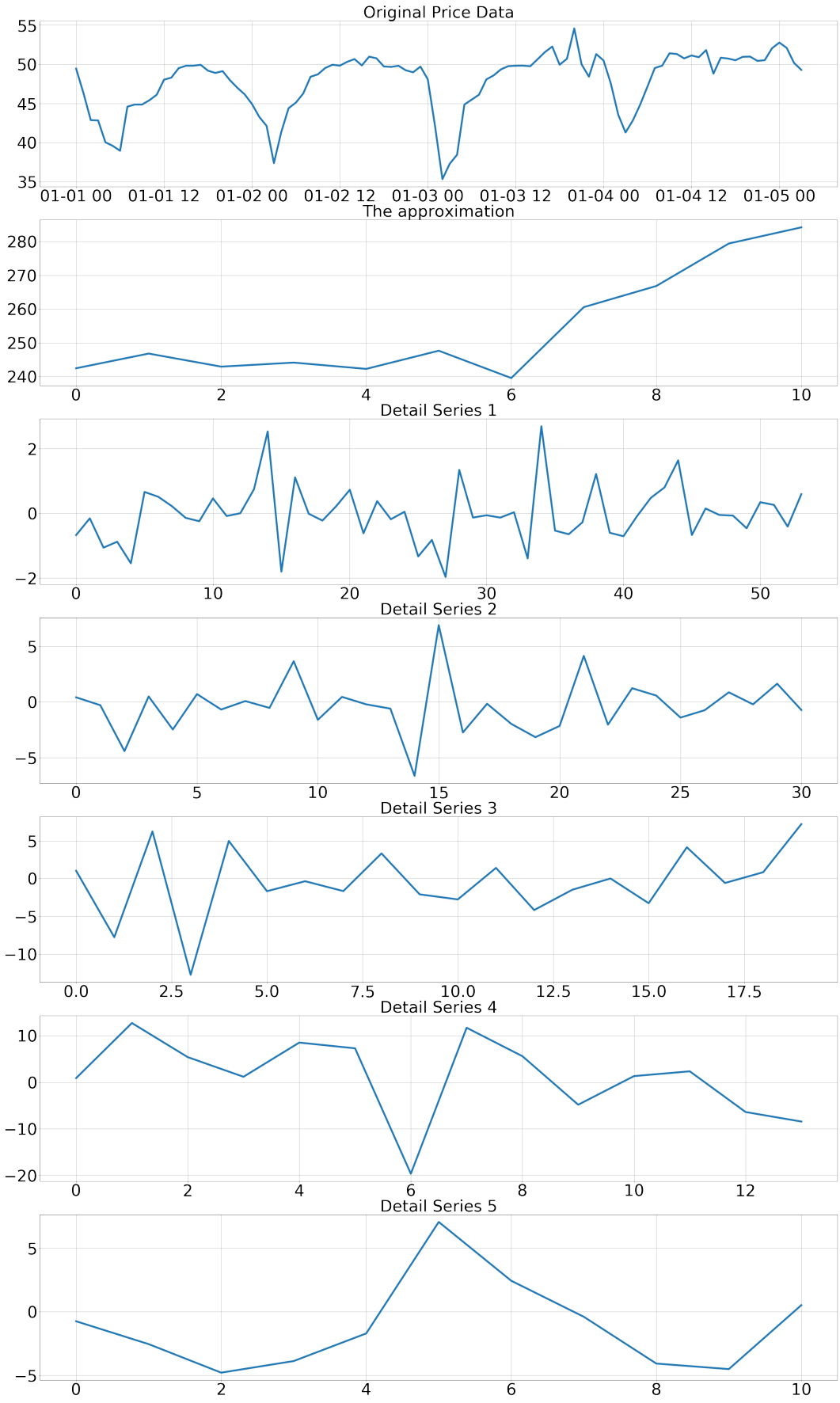


Figure 2.5: Original electricity price series and its frequency-domain decomposed components.



Figure 2.6: Original electricity price series and its time-domain decomposed components.

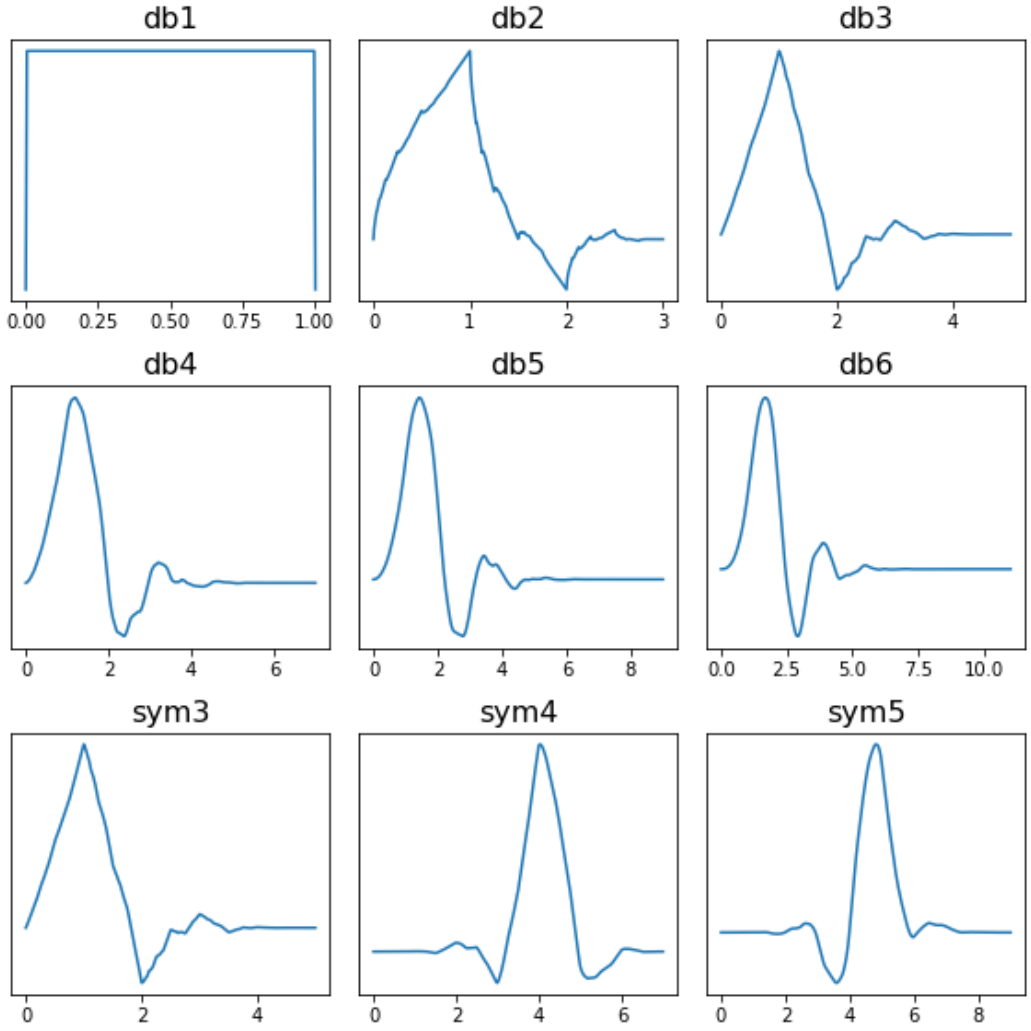


Figure 2.7: Commonly used mother wavelet functions for time series forecasting.

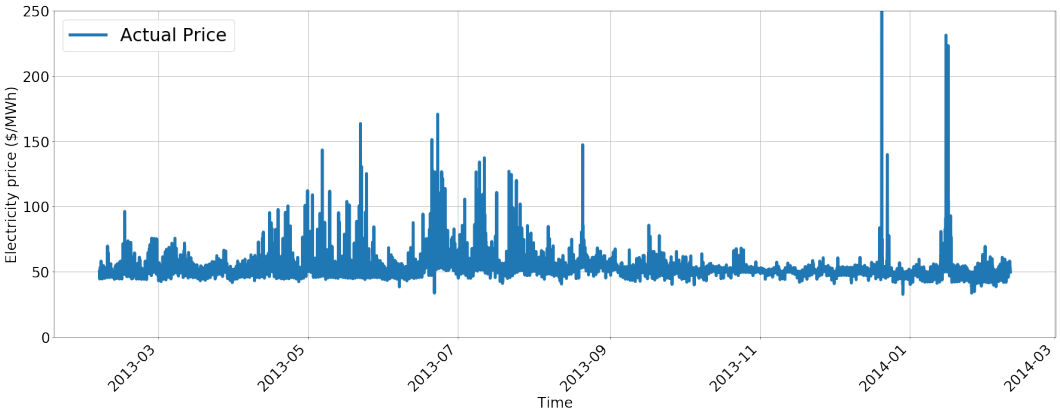


Figure 2.8: Electricity price data from New South Wales, Australia, in 2013 [1].

2.4 Electricity Price Forecasting

This section describes the background and problem statement of electricity price forecasting, followed by an evaluation of the proposed forecasting method through simulation experiments.

2.4.1 Problem Definition

In a typical power system, it is essential to balance supply and demand. Usually, electricity generated in power plants is supplied to each household through the power grid. If the generating side transmits more power than demand or a shortage of power to be transmitted, the voltage and frequency at the end of the grid will fluctuate significantly. Since such voltage and frequency fluctuations would create major problems for consumer electrical equipment, it is required to supply power at the rated voltage and frequency. Therefore, electric utilities continuously forecast electricity demand and schedule generation levels for each power plant to maintain the balance between supply and demand. With the massive introduction of renewable energy in recent years, ensuring the flexibility of the power supply side is a crucial issue [58]. Flexibility is the ability to adjust the amount of power generation to balance supply and demand, and is essential for a stable supply of electricity. Renewable energy cannot adjust the power generation output, and, moreover, production is very dynamic and partly unavailable during the day. Therefore, as renewable energy is introduced in large quantities, the required flexibility will also increase. Today, with the massive introduction of solar energy, balancing supply and demand by adjusting output on the supply side alone is becoming nearly impossible. Accordingly, demand response has gained increasing attention as a potential solution to this issue [59] [60] [61], as it involves modifying electricity consumption patterns on the demand side. These include peak shaving, which shifts the time of peak demand [62] [63] [64], and bottom-up, which increases demand during periods of low demand.

One of the most promising demand response mechanisms is dynamic pricing [65] [66] [67], where electricity prices vary over time and have been implemented in many regions, including Europe, the United States, and Australia. Dynamic pricing adjusts the electricity demand indirectly by changing the price of electricity. For example, when high electricity demand or low electricity generation is expected, electricity prices are set higher, thus indirectly lowering demand. In contrast, when low electricity demand or high electricity generation is expected, electricity prices are set low, thereby indirectly raising demand. In a dynamic electricity pricing system, prices are determined by the electricity market, but the method and frequency of this determination varies across countries and regions, and even within the same country or region, depending on the type of market. National or regional electricity markets can be classified into two categories: those introduced mainly in Europe, which consist of day-ahead and hour-ahead

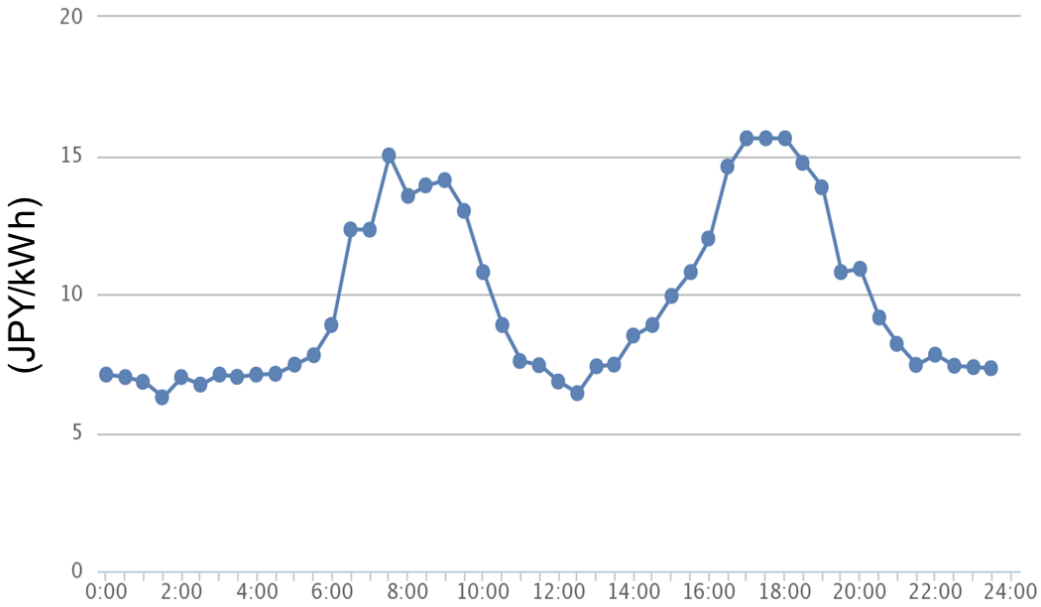


Figure 2.9: Example of the JEPX wholesale electricity price transition (January 28, 2021) [2].

markets, and those introduced mainly in the United States, which consist of day-ahead and real-time markets. For example, in the Japanese electricity market, as in Europe, there is a day-ahead market and a hour-ahead market. In this case, the day-ahead market is the primary market, where power to be generated the next day is bid on the day before. The minimum transaction unit is 50 kWh per frame (30 minutes). Sellers, such as power plants, and buyers, such as electric utilities, bid on the combination of quantity and price they wish to sell or buy by the trade date through an online trading system. After the deadline, the exchange calculates the equilibrium point where the demand and supply curves intersect, based on the quantity and price of trades, and determines the contract price. Fig. 2.9 shows the wholesale prices in Japan's day-ahead electricity market on January 28, 2021. The horizontal axis represents time, and the vertical axis represents electricity prices. The wholesale price is determined by Japan Electric Power eXchange (JEPX), the only wholesale power exchange in Japan, and the price fluctuates in increments of 30 minutes as shown in Fig. 2.9, depending on the daily demand and supply of electricity. Another electricity market, the hour-ahead market, trades electricity as a place to adjust generation and demand due to power generation malfunctions and temperature changes. On the generation side, if a power plant is shut down due to an accident and cannot generate the planned amount of electricity, the shortfall can be met in this hour-ahead market. On the demand side, if demand is expected to increase due to rising temperatures and the amount purchased in the day-ahead market is not expected to be sufficient, additional supplies can be purchased in this hour-ahead market. While

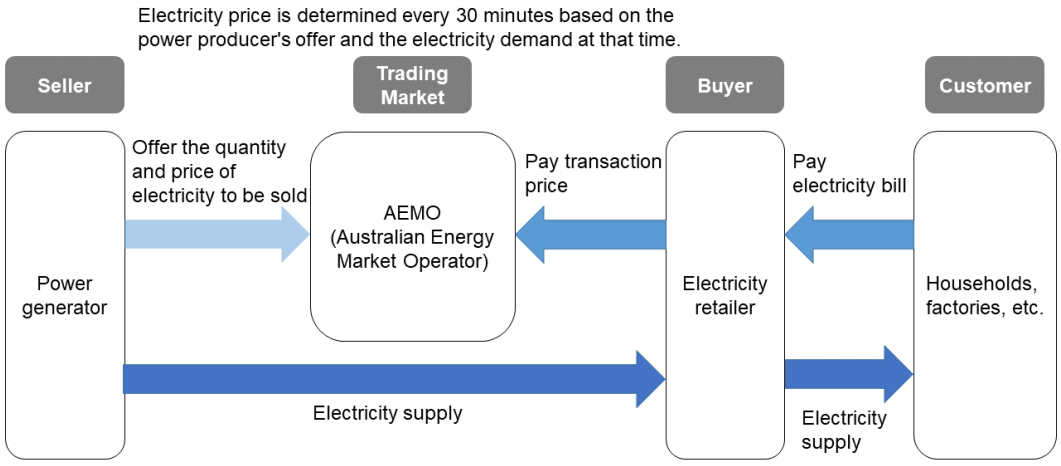


Figure 2.10: Overview of Electricity Trading in Australia.

the day-ahead market prices 48 frames for one day at a time, the hour-ahead market is traded on a half-hourly basis with time and price priority. In Japan, final retail prices may still be fixed, but dynamic pricing services for consumers have been increasing in recent years.

On the other hand, the Australian electricity market, for example, consists of a day-ahead market and a real-time market, just as in the United States. Unlike Japan and Europe, a real-time market exists instead of the hour-ahead market, which is the primary market. Although the hour-ahead market introduced in Japan and Europe is close to real time, it cannot cope with changes in supply and demand that occur after the bidding deadline. The real-time market, on the other hand, can respond to changes in supply and demand in real time. The actual electricity prices and electricity demand in New South Wales, Australia, from May 25 to May 31, 2013 are shown in Fig. 2.4. The horizontal axis represents time, and the left and right vertical axes represent electricity prices and electricity demand, respectively. The green graph shows electricity prices and the red graph shows electricity demand. From Fig. 2.4, it can be seen that fluctuations in electricity prices and electricity demand have a certain correlation with the location of peaks and other factors. The electricity trading market in Australia is shown in Fig. 2.10. First, each power generator presents the available electricity supply and the price of electricity to Australian Energy Market Operator (AEMO). This offer may be changed at any time. AEMO decides which power generators are to be operated in order to meet the demand for electricity and to be the most cost-effective, based on the proposals from the power generators. The wholesale electricity price is determined every 30 minutes based on the cost at this time, and in most cases the retailer purchases the electricity. Electricity is then supplied to homes, buildings, factories, etc [68]. As discussed thus far, the method of determining electricity prices in dynamic pricing differs from country to country and market to market, so it is necessary to consider input data and forecasting

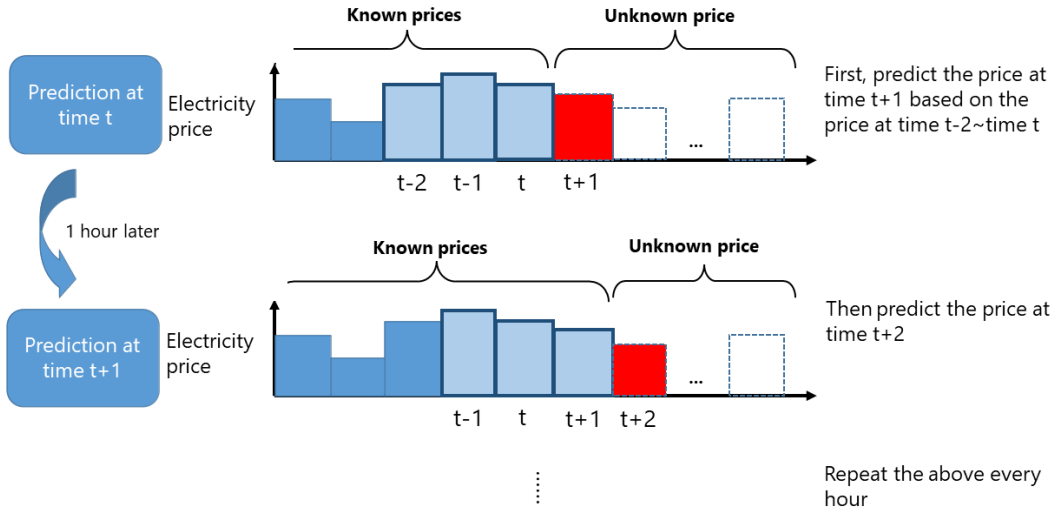


Figure 2.11: Overview of one-step-ahead prediction.

methods appropriate to each pricing method. In forecasting electricity prices, this study focuses on the real-time electricity market in Australia, particularly the market in New South Wales, which has the largest city in Australia, Sydney, due to the availability of data.

As electricity prices fluctuate over time under dynamic pricing schemes, accurately forecasting price movements becomes increasingly important for consumer decision-making. This is particularly critical for prosumers—consumers who also generate electricity—whose numbers are growing with the widespread adoption of solar power.

2.4.2 Simulation Setup

In this subsection, simulation experiments are conducted to demonstrate the effectiveness of the proposed forecasting method. First, the experimental setup is outlined, followed by the evaluation of two key aspects of the proposed method: (1) incorporating auxiliary features beyond the target variable, and (2) dynamically selecting MW to improve the decomposition process.

It was compared with Chang's model [3], which uses the same WT-LSTM model but forecasts solely from past prices and with a fixed MW. As in the study by Chang et al., the experiment was carried out using data on electricity price and grid demand data for the state of New South Wales, Australia, in May 2013. This data is published by AEMO [1], and although the original data is every 30 minutes, hourly data was used as in Chang et al. In the experiment, one-step-ahead (hourly) forecasting was used to predict the price of electricity for the next hour every hour. Fig. 2.11 illustrates the one-step-ahead forecasting procedure at the current time t. In both the upper and lower panels, time is shown on the horizontal axis and electricity price on the vertical axis.

Solid lines indicate observed historical prices, whereas dotted lines represent future prices that have not yet been observed. For simplicity, Fig. 2.11 uses electricity price as a representative input feature. At time t, the price at $t+1$ is forecast using the price data from $t-2$ to t. Subsequently, one hour later at time $t+1$, the updated price series from $t-1$ to $t+1$ is used to predict the price at $t+2$. This one-step-ahead prediction process is repeated sequentially at each hourly time step. The evaluation metrics are mean squared error (MSE) and mean absolute error (MAE) expressed by the following equations.

$$MSE = \frac{1}{n}\sum_{i=1}^{n}(f_i - y_i)^2, \tag{2.6}$$

$$MAE = \frac{1}{n}\sum_{i=1}^{n}|f_i - y_i|, \tag{2.7}$$

where n is the number of data, y_i is the actual value, and f_i is the predicted value.

The decomposition level of WT was set to level 5, following the previous studies [3] [69] [70]. As the optimization method, adaptive moment estimation (Adam) optimizer [71] was employed. Hyperparameters such as the number of neurons in the LSTM layer, the number of training epochs, the batch size, and the learning rate of Adam were automatically determined to ensure an objective evaluation of model performance [33]. Specifically, parameter tuning was performed using the tree-structured parzen estimator (TPE) [72], a Bayesian optimization method. The TPE method was selected due to its ability to flexibly handle not only continuous parameters but also discrete, categorical, and conditional variables, which are often challenging for traditional Bayesian optimization techniques. Moreover, it offers relatively low computational cost compared to other optimization methods [73].

2.4.3 Simulation Results

Effect of Incorporating Auxiliary Features Beyond the Target Variable

Electricity demand is introduced as an auxiliary feature to enhance forecasting accuracy. While the previous study by Chang et al. predicted electricity prices solely based on historical price data, the proposed method incorporates both past prices and electricity demand to capture the underlying relationship between market behavior and consumption patterns. The evaluation was conducted over a single day, and the specific training, validation, and test periods are summarized in Table 2.1.

Fig. 2.12 shows the actual price, the forecast results of the Chang et al. model reproduced from the paper, and the forecast results of the proposed model with the added electricity demand. The horizontal and vertical axes indicate time and electricity prices, respectively. The light blue graph represents the Chang et al. model, the yellow graph represents the proposed model, and the green graph represents the actual electricity prices. Fig. 2.12 shows that the model of Chang et al. that is reproduced does not follow

Table 2.1: Training, validation, and test data period

Training	Validation	Test
May 1 - May 29	May 30	May 31

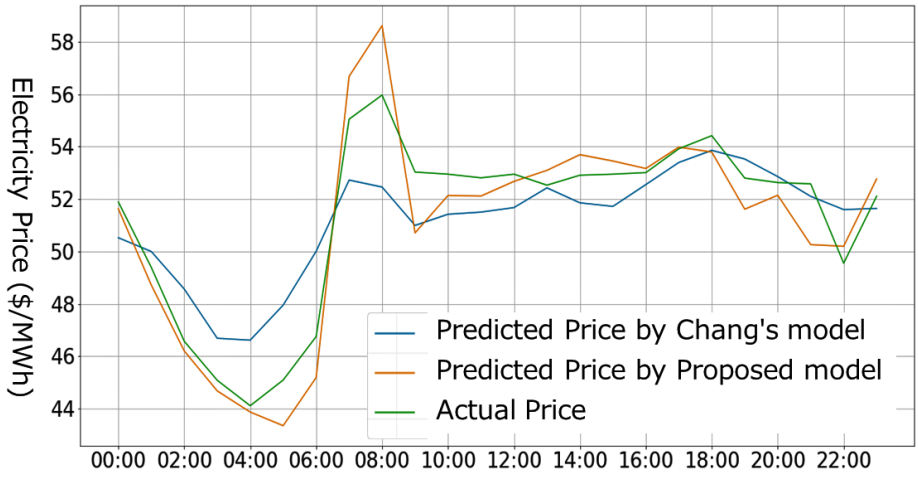


Figure 2.12: Actual prices, predicted prices of the replicated Chang et al. [3] model, and predicted prices of the proposed electricity demand addition model.

the fluctuation of the price in the morning, while the proposed model with the electricity demand gives predictions that are closer to the actual prices. Table 2.2 shows MSE and MAE of the model of Chang et al. published in the paper, the values reproduced based on the paper, and MSE and MAE of the proposed model. Based on the above experimental results, it is considered that the accuracy of forecasting future electricity prices can be improved by decomposing the grid electricity demand time series by frequency and utilizing the component series of the time series.

Effect of Flexible Forecasting by Switching Mother Wavelets

This experiment was carried out to evaluate the flexible forecasting capabilities of the proposed method through dynamic MW selection. The main experimental setup is the same as in the previous section. This experiment was performed with each of the following 19 MWs: Nine ways to fix MW with db1 to 6 and sym3 to 5 and 10 ways when n, the number of weeks to be considered in switching MW, is changed from 1 to 10 in the proposed method. The evaluation metrics was mean absolute percentage error

Table 2.2: The published and reproduced values of the prediction error of the model of Chang et al. [3] and the prediction error of the proposed model

	Chang's model [3] (Described)	Chang's model [3] (Replicated)	Proposed model
MSE	2.80	2.92	1.35
MAE	1.45	1.42	0.84

(MAPE), which is expressed by the following equation.

$$MAPE = \frac{100}{n}\sum_{i=1}^{n}\left|\frac{\hat{y}_i - y_i}{y_i}\right|, \tag{2.8}$$

where n is the number of data, y_i is the actual value, and $\hat{y}_i$ is the predicted value. Throughout the experiment, forecasting was conducted by repeating time-series decomposition and model training on a weekly basis, as illustrated in Fig. 2.13. Specifically, the forecasting model is first trained using electricity price and demand data from the four-week period spanning January 1 to January 28, 2013. Data from January 29 to February 4 are then used for validation to assess the training status of the model, followed by performance evaluation using data from February 5 to February 11. After this process, the entire data window is shifted forward by one week, and the decomposition, training, validation, and testing procedures are repeated. This rolling forecasting process is performed for 53 consecutive weeks, corresponding to approximately one year of evaluation.

Table 2.3 shows MAPE throughout the experimental period for each MW. The second line, "switching to the best MW" corresponds to an idealized scenario in which the proposed method always selects the mother wavelet that yields the highest prediction accuracy at each time period. This case therefore represents the theoretical upper bound of the proposed approach. As shown in Table 2.3, forecasting accuracy depends strongly on the choice of mother wavelet used for time-series decomposition. Several mother wavelets, including those selected by the proposed method, achieve higher accuracy than db5, which was adopted in the previous study [3]. Among these, the lowest MAPE of 2.148% is obtained by one variant of the proposed method that determines the mother wavelet based on forecasting performance over the preceding three weeks. Nevertheless, even under the "switching MW (n=3)" setting, a gap of approximately 0.07% ppt remains compared with the "switching to the best MW" case, which represents the theoretical optimum. The underlying reasons for this discrepancy are discussed in the following section.

Fig. 2.14(a) presents the electricity price results for the period from July 22 to July 23, including the actual price (blue), the predicted price with a fixed mother wavelet db5 (light blue), the prediction using sym5 (gray), and the prediction obtained by

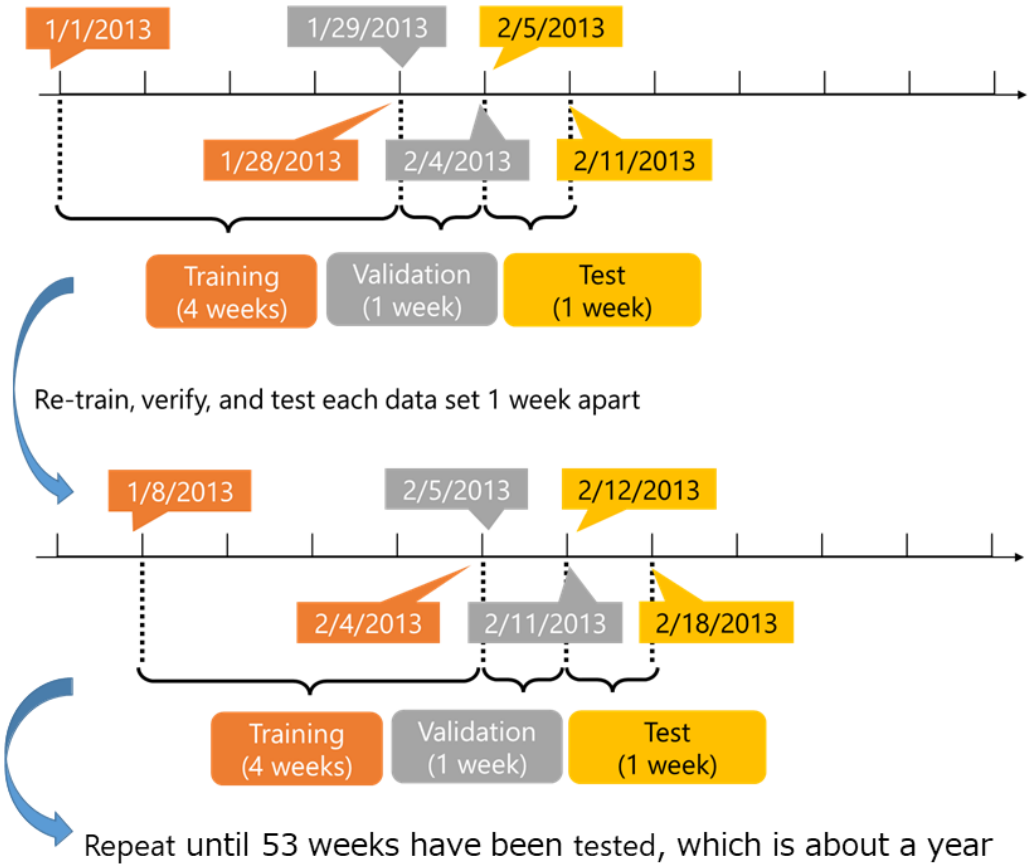


Figure 2.13: Details of the experimental period.

the proposed MW-switching method (red). The vertical axis represents the electricity price, while the horizontal axis denotes time in the format of "month-day hour." In Fig. 2.14(a), July 23 corresponds to the weekly update point of the mother wavelet in the proposed method. Specifically, db4 is used as the mother wavelet up to July 22, after which the method switches to sym5 on July 23, as it achieved the highest forecasting accuracy over the preceding three weeks. As shown in the figure, switching the mother wavelet to sym5 from the week starting on July 23 yields predictions that more closely follow the actual price trajectory than those obtained by continuously using db5. Fig. 2.14(b) illustrates the absolute prediction errors corresponding to the forecasts shown in Fig. 2.14(a). Although the proposed method exhibits a relatively large error at 7:00 on July 23, its prediction error is smaller than that of db5 at many other time points. These results indicate that adapting the mother wavelet based on recent forecasting performance effectively mitigates accuracy degradation over time.

Fig. 2.15(a) depicts the weekly MAPE values for each mother wavelet, while Fig. 2.15(b) presents the corresponding weekly rankings of the mother wavelets based

Table 2.3: MAPE of each mother wavelet (MW) in electricity price forecast over entire experimental period

Mother wavelet	MAPE (%)	Description
switching to best MW	2.074660	Ideal case of proposed method.
switching MW (n=3)	**2.148150**	Proposed method.
switching MW (n=8)	2.152941	
switching MW (n=6)	2.158812	
switching MW (n=9)	2.163366	
switching MW (n=5)	2.164564	
switching MW (n=7)	2.172413	
switching MW (n=10)	2.174297	
switching MW (n=4)	2.178161	
switching MW (n=2)	2.182103	
Symlet 5	2.196947	
switching MW (n=1)	2.206786	Proposed method.
Daubechies 4	2.212410	
Daubechies 6	2.295169	
Daubechies 5	2.307206	Used in previous studies [3].
Symlet 4	2.399550	
Daubechies 3	2.445557	
Symlet 3	2.545998	
Daubechies 2	2.703441	
Daubechies 1	2.858116	

on predictive accuracy. For clarity, only selected periods are shown, and the case with n=3, which achieved the best performance in Table 2.3, is presented as a representative example of the proposed method. In addition, mother wavelets that outperform db5, which was adopted in the previous study [3], are highlighted with solid lines. In Fig. 2.15(a), the horizontal axis denotes the week and the vertical axis indicates the MAPE, where lower values correspond to higher forecasting accuracy. The figure shows that the proposed method, represented by the solid red line, is able to reduce the average prediction error over many weeks. For example, during the period from April 30 to May 6, the MAPE reaches 6.91% when db1 is used as a fixed mother wavelet (dotted blue), whereas it decreases to 3.95% with the proposed method, corresponding to an accuracy improvement of approximately 42.8%. Fig. 2.15(b) uses the same weekly intervals as Fig. 2.15(a). Here, the vertical axis represents the ranking of each mother wavelet in descending order of prediction error, such that higher ranks indicate better accuracy. While several fixed mother wavelets fall to 15th place or lower in some weeks, the proposed method consistently maintains a rank of fourth or higher, as shown by the solid red line. Notably, during the periods from April 2 to April 8 and from May 7 to



Figure 2.14: Actual and predicted electricity prices for July 22–23, along with the corresponding absolute prediction errors for each mother wavelet.

May 13, db5 temporarily achieves the highest accuracy. This behavior explains why the best performance of the proposed method in Table 2.3 remains slightly inferior to the theoretical optimum. Since the proposed method selects the mother wavelet based on forecasting performance over previous weeks, it cannot immediately adopt a wavelet whose accuracy improves abruptly within a single period.

Fig. 2.16 presents the average accuracy ranking of the mother wavelets shown in Fig. 2.15 over the entire experimental period. In this figure, lower bars correspond to higher average rankings, indicating better overall forecasting accuracy. The results demonstrate that the proposed method achieves superior average accuracy compared with the other mother wavelets, not only during the periods highlighted in Fig. 2.15 but consistently across the full evaluation horizon. In addition, Fig. 2.17 shows the standard deviation of the precision rankings of MW shown in Fig. 2.15 for the entire experimental period. The lower the bar on this graph, the lower the standard deviation of the ranks, meaning lower variation in the rankings. From this figure, it can be seen that the proposed method achieves a higher average rank than the other MW with the least variation. These results suggest that switching MW may continuously suppress the decrease in forecast accuracy from week to week.

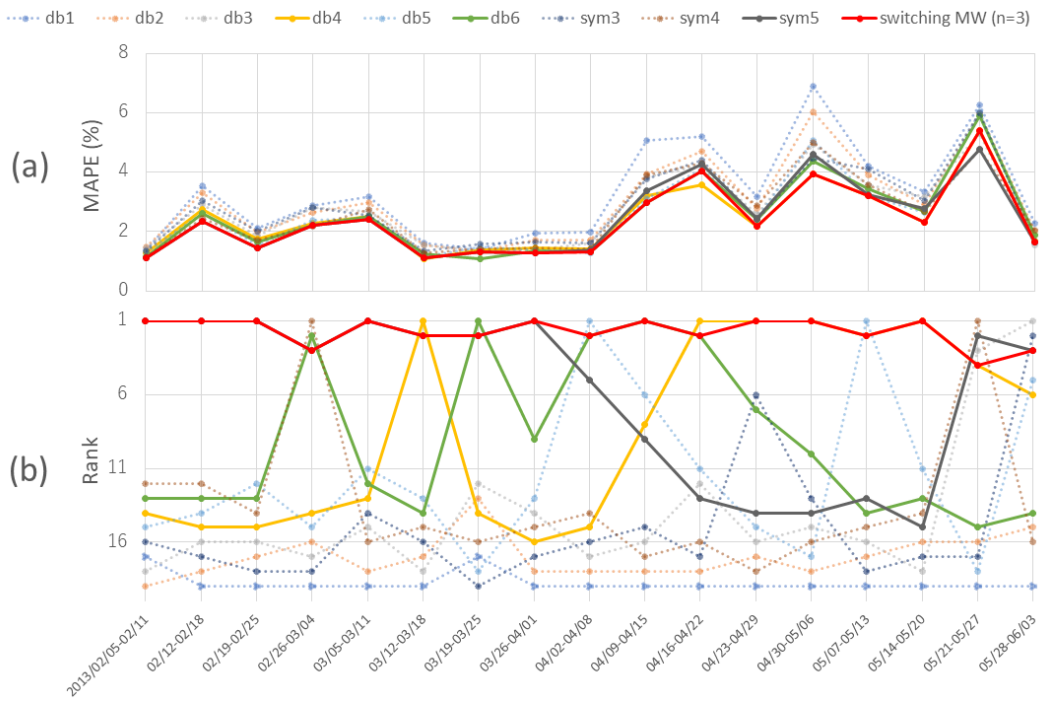


Figure 2.15: Weekly forecast accuracy (MAPE) and rank of each mother wavelet in forecasting electricity price.

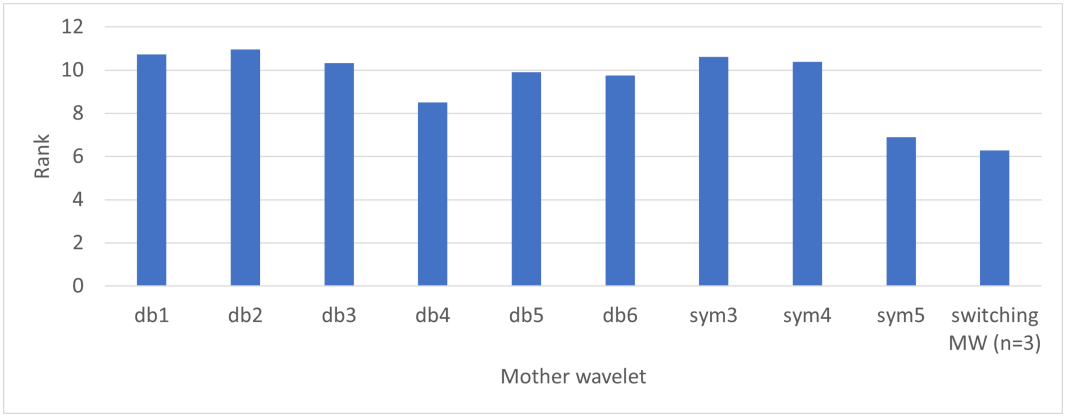


Figure 2.16: Average rank of accuracy of electricity price forecasts over the entire experimental period.

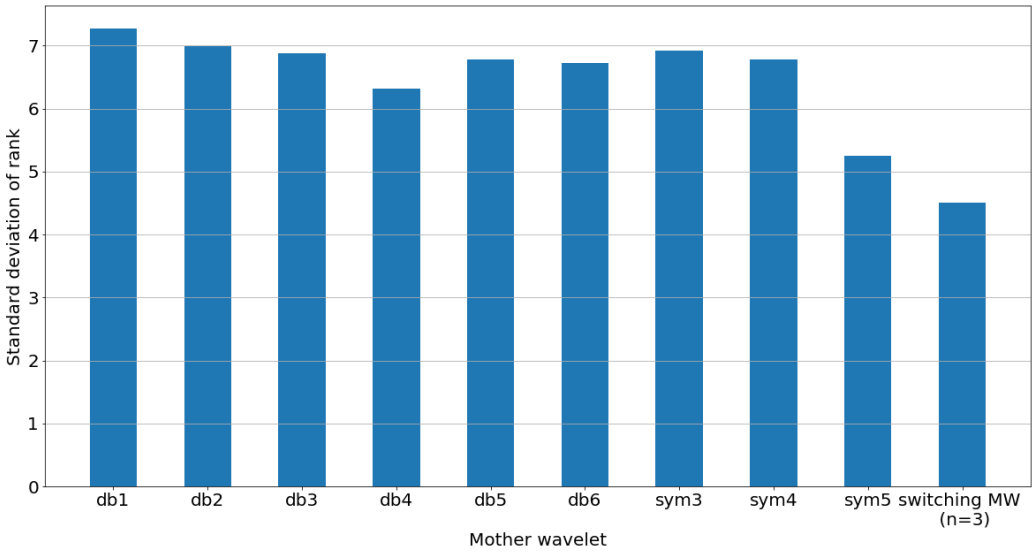


Figure 2.17: Standard deviation of the accuracy ranking of electricity price forecasts over the entire experimental period.

2.5 Electricity Demand Forecasting

In this section, the background and challenges of electricity demand forecasting are described, followed by the evaluation of the proposed forecasting method through simulation experiments.

2.5.1 Problem Definition

Energy management systems (EMS) have attracted significant attention as an effective means of utilizing solar energy more efficiently. An EMS is a system that installs photovoltaic (PV) panels and battery storage, and centrally manages facilities within a power network using information and communication technologies. An overview of the EMS is shown in Fig. 2.18. As illustrated in the figure, the EMS determines the operation schedules of demand-side equipment such as air conditioning systems and supply-side resources such as battery storage. These operations are controlled and monitored based on both the predicted electricity prices and the building's electricity demand. Future electricity demand in buildings is predicted by collecting environmental information from various sensors, including thermometers, and by utilizing this data together with past electricity demand records. Afterward, the EMS uses the actual electricity consumption data to update the forecasts of future electricity prices and demands, and accordingly determines optimal operation plans based on the newly predicted data. Thus, after analyzing past energy usage, the EMS can forecast future electricity prices and energy demand, and establish optimal operation strategies for facilities such as air conditioning systems. This enables electricity consumers not only to optimize the use of resources such as gas, electricity, and water, but also to reduce electricity costs by controlling peak power consumption. Considering these complex factors, the EMS is expected to serve as an autonomous mechanism to improve energy efficiency automatically.

However, this potential can be realized only if the automated methods achieve sufficiently high accuracy and can respond to highly dynamic real-world conditions. Fig. 2.19 shows the electricity demand of one of the buildings at the Graduate School of Information Science and Technology, the University of Osaka, over the course of a year. As shown in the figure, the degree of demand fluctuation varies depending on the season. For instance, the demand shows significant variations in the summer months (July and August), while the fluctuations are relatively moderate in the winter months (January and February). Therefore, achieving highly accurate electricity demand forecasting that can cope with such non-stationary characteristics is a crucial element in realizing effective EMS.

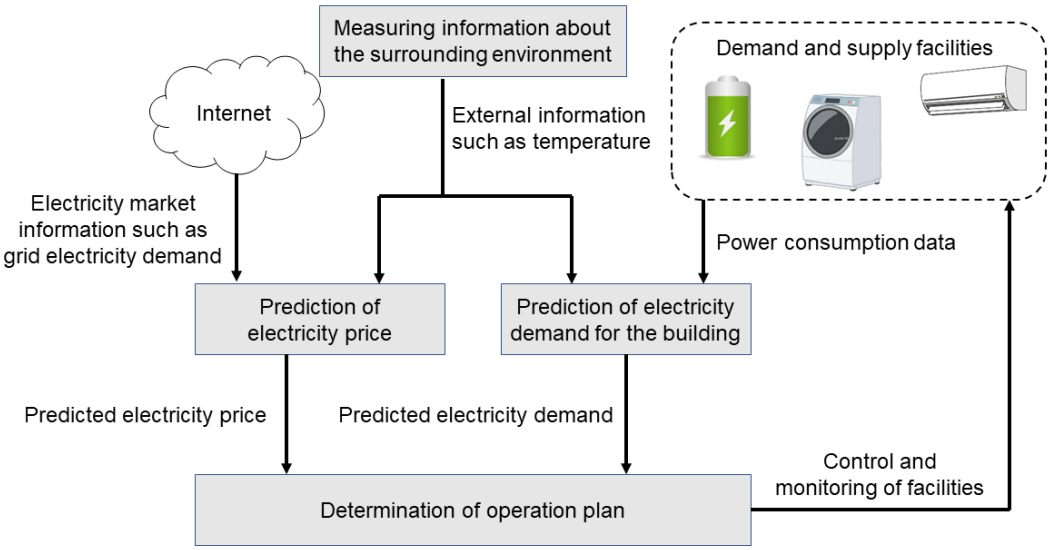


Figure 2.18: Energy management system overview.

2.5.2 Simulation Setup

To verify the proposed forecasting method for electricity demand forecasting, electricity demand data from the 2019 fiscal year for buildings at Osaka University's Graduate School of Information Science and Technology are used. Training with four weeks of data and one-step-ahead prediction test with one week of data are repeated for a year. The experiment is conducted using a total of 19 MW configurations. These include nine cases in which the mother wavelet is fixed to db1–db6 or sym3–sym5, as well as ten cases of the proposed method, where the switching window length n is varied from 1 to 10 weeks.

To evaluate the effectiveness of combining feature selection by mRMR with flexible forecasting by WT-LSTM, the proposed method was compared with two baseline cases: (1) forecasting using only past demand data, and (2) forecasting using all candidate features without selection. The available data, which included electricity demand, solar irradiance, temperature, humidity, and their respective lag features, are used as candidate features. All datasets used in this experiment—including electricity demand and meteorological variables—are aligned to the same temporal resolution of one hour. MAPE is introduced as performance metrics. This experiments was conducted on an environment equipped with an Intel Core i7-8700 CPU (3.20 GHz) and 16 GB of memory.

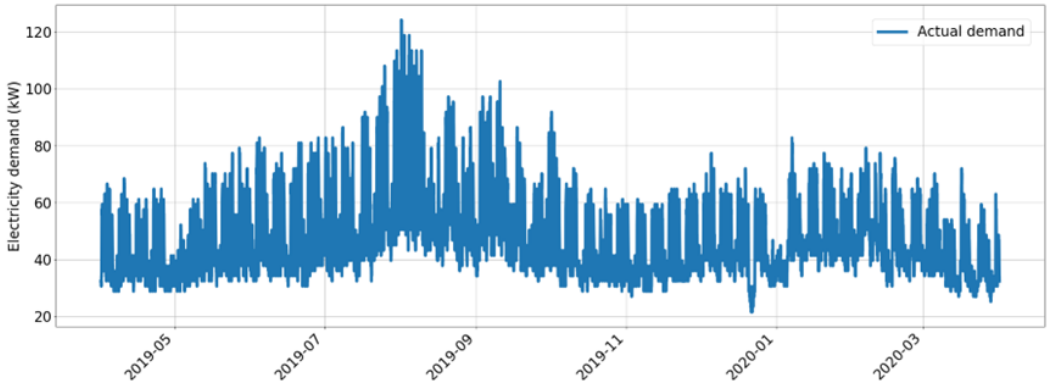


Figure 2.19: Electricity demand change in one building at the Graduate School of Information Science and Technology, the University of Osaka for one year in FY2019.

Table 2.4: MAPE of each mother MW in electricity demand forecast over entire experimental period

Mother wavelet	MAPE (%)	Description
switching MW (n=8)	**1.569602**	Proposed method.
Symlet 5	1.588242	
Daubechies 6	1.652728	
Daubechies 4	1.660685	
Daubechies 5	1.667753	
Symlet 4	2.340044	
Symlet 3	2.481672	
Daubechies 3	2.519659	
Daubechies 2	2.924541	
Daubechies 1	3.063592	

2.5.3 Simulation Results

MAPE of the proposed method for switching the MW and the method for fixing to a specific MW are shown in Table 2.4. The best accuracy of $n = 8$ is shown as a representative value of the proposed method. Table 2.4 shows that the proposed method of switching the MW improves the error by 1.17% to 48.8% compared with the method of fixing it to a specific MW. Fig. 2.20 shows the weekly accuracy ranking of each MW, with the higher position indicating higher accuracy. The proposed method and MW that were highly accurate when fixed are shown as solid lines. Fig. 2.20 shows that the proposed method always maintains the 8th place or higher, while all other methods fall below the 9th place depending on the week. This result indicates that switching the MW periodically is useful for reducing the deterioration of prediction accuracy in electricity demand forecasting.

Fig. 2.21 shows a comparison between the proposed method of selecting features

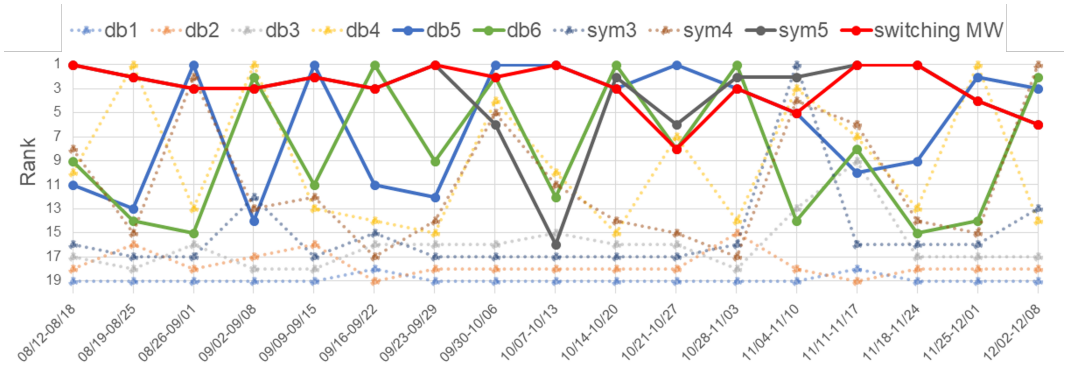


Figure 2.20: Accuracy ranking of each mother wavelet by week.

with mRMR and the case of selecting only historical power demand data as features or all feature candidates. The vertical axis is the maximum weekly MAPE. For the proposed method with mRMR, electricity demand without time shift, 2 days, 6 days, and 4 weeks ago, and solar irradiance without time shift were selected. From Fig. 2.21, the maximum MAPE of mRMR is the smallest, and this means that appropriate feature selection by mRMR is effective for prediction by WT-LSTM.

In terms of computational efficiency, generating one week of electricity demand forecasts requires an average inference time of 0.1819 s (Intel Core i7-8700). This time corresponds only to the inference process and does not include model training. Although the demand forecasting experiments in this chapter were conducted at an hourly resolution due to data availability, the low inference time indicates that the proposed WT–LSTM framework can be applied to higher temporal resolutions, potentially beyond those required for real-time ramp rate control. In this context, different time resolutions naturally correspond to different operational objectives: second-level forecasting is suitable for fast ramp rate control, minute-level forecasting can support production-side or fast load balancing, and quarter-hour or hourly forecasting is appropriate for slower load balancing and higher-level energy management decisions.



Figure 2.21: Maximum weekly MAPE of each feature selection.

2.6 Solar Irradiance Forecasting

In this section, the background and challenges of solar irradiance forecasting are discussed, followed by an evaluation of the proposed forecasting method through simulation experiments.

2.6.1 Problem Definition

Solar energy is one of the most abundant energy resources available on Earth. The average solar irradiance reaching the Earth's surface is approximately $1367 W/m^2$, which corresponds to an annual potential power generation of about $1.74 \times 10^{17} W$ [74]. Such a vast and widely distributed energy source is sufficient to meet the total global electricity demand. Therefore, solar energy is regarded as one of the best alternatives to conventional energy sources for PV systems that supply industrial, commercial, and residential energy demands. In recent years, the installation of PV power plants has been rapidly increasing worldwide. Although solar energy is considered one of the most promising substitutes for fossil fuels in both industrial and scientific communities, several challenges remain for ensuring reliable and stable integration of PV systems into power grids. The primary challenge in achieving large-scale penetration of solar energy into the electricity market lies in its highly variable and intermittent nature. Hence, accurately forecasting the availability of solar energy has become highly desirable for the energy industry.

Generally, global horizontal irradiance (GHI) data are predicted over different time horizons depending on the application of solar energy. For example, long-term GHI forecasts are useful for PV site selection and system installation planning. The long-term variations due to solar motion exhibit high predictability. Conversely, very short-term GHI forecasts are essential for real-time monitoring and operation of energy systems. Short-term fluctuations in solar irradiance, often caused by rapid cloud movements, introduce significant uncertainty into PV power output. Considering the increasing deployment and cumulative penetration of large-scale PV systems, such fluctuations can compromise the transient stability of power grids, leading to voltage flicker or even blackouts. Therefore, from the perspective of mitigating PV power variability and ensuring grid stability, the need for highly accurate short-term solar irradiance forecasting has become more critical than ever.

2.6.2 Simulation Setup and Results

This section describes the experimental setup used to evaluate the proposed forecasting method for solar irradiance prediction. High-resolution meteorological data collected in Oldenburg, Germany, is used. The dataset includes solar irradiance and auxiliary meteorological variables measured at 1-second intervals. The training period is June 17 – June 30, 2015 (14 days) and the evaluation period is July 7, 2015, 12:00–13:00. The input to the forecasting model includes the following 11 features:

- Temperature
- Humidity
- Wind direction
- Wind speed
- Cloud cover
- Solar altitude angle
- Time (hour, day, month)
- Cloud flag (quality indicator)
- Wavelet-decomposed irradiance components (from wavelet transform)

Each input instance uses the most recent 60 seconds of data as input to predict irradiance values over a specified forecast horizon (e.g., 10–120 seconds ahead). In this experiment, the variation of forecasting accuracy with respect to different prediction horizons is evaluated, with a particular focus on its potential application to ramp-rate control. Forecasting is performed every second, with forecast horizons of 10, 30, 60, and 120 seconds evaluated. Evaluation metrics are root mean squared error (RMSE), MAE and MAPE.

Table 2.5 shows the values of each of the evaluation metrics in each of the forecast horizons. As expected, forecasting error increases with longer prediction horizons due to error accumulation. MAPE is 9% even when forecasting 30 seconds ahead and 5% when forecasting 10 seconds ahead, which is considered sufficient for practical pur-

Table 2.5: RMSE, MAE, MAPE at each forecast horizon.

	Forecast Horizon [*sec*]			
Evaluation Metrics	10	30	60	120
RMSE [W/m^2]	21.26	39.94	66.91	120.81
MAE [W/m^2]	20.44	36.61	59.70	105.10
MAPE [%]	5.15	9.20	15.16	26.89

poses.

2.7 Summary

In this chapter, a WT-LSTM–based forecasting method for behind-the-meter applications was proposed. The proposed approach aims to achieve high-accuracy forecasting of power price, power demand, and solar irradiance, which are essential for efficient energy management and control in behind-the-meter systems. Specifically, the method integrates WT for decomposing non-stationary time-series data and LSTM networks for flexible temporal prediction. A key advantage of the proposed method lies in the following three contributions: (i) incorporating auxiliary features beyond the target variable, (ii) applying a quantitative feature selection method to identify the most relevant inputs, and (iii) dynamically selecting MW to improve the decomposition process. These components enable the model to more effectively capture non-stationary behaviors and relevant temporal patterns within power system time-series data. Simulation results demonstrated that the proposed method outperforms conventional and baseline models in capturing non-stationary characteristics, thereby validating its effectiveness and robustness for behind-the-meter forecasting tasks.

As an extension of this work, the development of a ramp rate control method is considered. The forecasting studies presented in this chapter, while demonstrating high prediction accuracy, serve as a foundational step rather than an end in themselves. In practical energy systems, forecasting alone is insufficient to address real-world challenges — it is only through the application of these forecasts to energy management and ramp-rate control that the benefits of accurate prediction can be fully realized. To address this limitation, Chapter 3 proposes a ramp-rate control strategy using PV cooling, and first evaluates it under the assumption of perfectly predicted power demand and solar irradiance.

For future research on forecasting, it aims to enhance real-time adaptability and robustness against uncertainty. Specifically, the current deterministic framework will be extended to a probabilistic forecasting model that can represent the range and likelihood of possible outcomes rather than a single point estimate. Such a probabilistic approach would allow EMS to make risk-aware decisions under variable solar irradiance and demand conditions. In addition, the forecasting model will be upgraded to support online learning and adaptive model updates, enabling it to respond promptly to environmental and seasonal changes without the need for complete retraining. This would significantly improve the model's applicability to long-term, real-world behind-the-meter operations where data distributions evolve over time. Furthermore, although this chapter focuses on electricity price, demand, and solar irradiance, the underlying WT-LSTM methodology could potentially be extended to other renewable generation sources—such as wind power or geothermal output—because they also exhibit multi-scale and non-stationary temporal behavior. Verifying this broader applicability and tailoring the model to these additional domains remains an important direction for future work.

Chapter 3

Cooling-Based Optimization for PV Ramp Rate Minimization

Rapid variations in solar irradiance cause pronounced fluctuations in photovoltaic (PV) power generation. Conventional ramp rate control approaches typically rely on battery energy storage systems (BESS) to smooth PV output and maintain a stable power supply to the grid. However, such approaches involve high capital investment and considerable maintenance requirements. This chapter introduces a novel ramp rate control strategy for PV systems based on cooling technology, aimed at enhancing grid stability and supporting ancillary services[1]. The proposed approach exploits the thermoelectric characteristics of PV modules by regulating panel temperature in real time, thereby adjusting generation efficiency and mitigating rapid output changes. Beyond ramp-rate mitigation alone, this approach introduces an effective production control knob for PV systems: PV modules are actively cooled during periods of temporary production excess, and the resulting lower module temperature increases conversion efficiency, enabling the system to supply more energy during subsequent periods when demand exceeds instantaneous PV output. This dual effect—reducing excessive ramps while improving the timing and usability of PV energy—extends the functionality of cooling from a purely stabilizing mechanism to a proactive energy management tool. The performance of the proposed approach was evaluated through simulations using real-world data. The results demonstrate reductions of 43.5% in the mean ramp rate and 76.2% in the maximum ramp rate compared with conventional battery-based control strategies. Importantly, these improvements were achieved using a cooling unit with a coefficient of performance (COP) below 10 and a small battery capacity of only 20 kWh. This highlights the efficiency of the proposed method and its potential to substantially reduce system costs and environmental impacts relative to traditional ramp rate control solutions.

[1]This chapter is a refined and reproduced version of the paper to be published in Applied Energy [75], copyrighted by Elsevier.

3.1 Introduction

Solar energy is widely regarded as a promising renewable alternative to fossil fuels for reducing greenhouse gas emissions and mitigating global warming. However, the increasing penetration of PV generation introduces new operational challenges for power systems. PV power output is influenced by temperature, solar irradiance, and other meteorological conditions. Among these factors, solar irradiance—directly converted into electrical energy by PV modules—exhibits rapid and significant fluctuations depending on weather conditions and geographic location. Such variability can induce steep power output ramp rates and frequency deviations, raising concerns about grid stability. To address these challenges, a wide range of mitigation and control strategies has been investigated in previous studies.

To mitigate short-term power fluctuations in PV generation, three main approaches have been extensively studied. The first approach combines PV systems with BESS [76]. While BESS can provide large capacity and effectively absorb rapid power ramps, it suffers from high installation and maintenance costs as well as considerable environmental impact. The second approach relies on controllable fuel-based generation, such as gas turbines [77]. Although fuel-based generators offer fast and flexible power output adjustment, they also entail high system costs and significant environmental burdens, similar to large-scale battery systems. The third approach employs dump loads to limit power injection into the grid during periods of high variability [78]. Dump loads typically consist of resistive elements and controllers that dissipate excess power. This method benefits from low system complexity and cost; however, the consumed energy is irrecoverably wasted. Overall, these conventional approaches are associated with either high economic and environmental costs or inefficient use of generated power. In contrast, the proposed method regulates ramp rates by directly adjusting PV generation itself, without relying on large-capacity batteries, fuel-based generators, or dump loads. As a result, the proposed approach achieves lower system costs and environmental impact while enabling more effective utilization of generated energy compared with existing methods.

The proposed approach exploits the temperature dependence of PV generation efficiency to enable direct regulation of PV power output. At elevated panel temperatures, increased carrier concentration at the p–n junction leads to a reduction in module efficiency [79]. Although previous studies have investigated PV cooling techniques [80], their primary objective has been to enhance energy conversion efficiency rather than to control power output ramp rates.

This chapter proposes a ramp rate control strategy that mitigates power output fluctuations of a specific PV plant or installation by actively regulating PV generation through on-site cooling. In the proposed framework, the energy management of the PV system—including the operation of PV cooling units—is performed within a microgrid environment based on electricity demand, weather information, and PV generation

forecasts. The proposed approach achieves low system cost and reduced environmental impact, as it does not require the operation of gas turbines or large-capacity battery systems. Moreover, surplus energy during output fluctuations is not dissipated through curtailment; instead, it is effectively utilized by the PV cooling units. The main contributions and novelties of this work are summarized as follows:

- **Effective ramp rate reduction**: The proposed method reduces the mean ramp rate by 43.5% and the maximum ramp rate by 76.2% compared with a battery-only control strategy. These results demonstrate the effectiveness of the proposed approach in stabilizing PV power output and alleviating grid disturbances.
- **Cost and environmental benefits**: By eliminating the need for gas turbines and large-capacity batteries, the proposed method lowers operational costs and reduces the environmental footprint associated with managing PV output variability.

The remainder of this chapter is as follows. First, related studies on ramp rate control techniques and PV cooling approaches are reviewed separately in Section 3.2. Next, Section 3.3 provides an overview of the proposed ramp rate control framework based on PV cooling. Section 3.4 then details the system model and formulates the optimization problem for PV system operation, explicitly incorporating the PV cooling unit. Finally, Section 3.5 presents simulation results to evaluate the effectiveness of the proposed method, and Section 3.6 concludes the chapter with a summary of the findings.

3.2 Related Works

Related studies on ramp rate control are reviewed and broadly categorized into three groups: approaches based on BESS, methods relying on fuel-based power generation, and techniques that regulate power output through energy consumption or curtailment using dump loads. In addition, prior research on PV cooling technologies is summarized at the end of this section.

3.2.1 Ramp rate control methods

Among existing ramp rate control approaches, methods based on BESS have been the most extensively studied. Amorim et al. [76] proposed a detailed BESS sizing methodology that evaluates energy capacity, power rating, and discharge characteristics. Using one-year mission profiles of solar irradiance and ambient temperature in Goiânia, Brazil, their approach reduced the required BESS volume by 57.14% compared with previously reported designs. It has also been shown that the solar irradiance profile strongly influences the required power and energy capacity of BESS [81]. In particular, a BESS power rating equivalent to approximately 60% of the nominal PV string power was found to be sufficient to smooth most detected PV power ramps, even under

strict ramp-rate constraints. For BESS-based ramp rate control, accounting for battery degradation is a critical consideration. Martins et al. [82] compared commonly used control algorithms with a focus on battery operating status, which directly affects battery lifetime. Their analysis included the required BESS capacity for each algorithm and demonstrated that a second-order low-pass filter–based control strategy required less battery capacity, induced fewer charge–discharge cycles, and reduced the magnitude of charge variation, thereby extending battery lifetime. Additional studies have emphasized the importance of battery operating temperature, as well as the influence of battery size and ramp rate limits on degradation behavior [83]. To further mitigate degradation, hybrid energy storage and management strategies have been proposed. For example, Abdelghany et al. [84] employed a model predictive control framework to manage battery and hydrogen storage systems, extending overall system lifetime. Similarly, Gonzalez et al. [85] proposed a control algorithm with objectives of reducing battery cycling, minimizing storage capacity requirements, and preventing ramp rate violations, resulting in improved battery longevity and cost-effective smoothing. Various signal-processing-based smoothing techniques using BESS have also been investigated. Atif et al. [86] compared low-pass, moving average, Gaussian, and Savitzky–Golay filters for PV output smoothing. Their results indicated that moving average and low-pass filters perform poorly when large window sizes or time constants are used, as these conditions degrade BESS performance. In contrast, the Savitzky–Golay filter effectively reduced both battery ramp rates and charge–discharge power while smoothing PV fluctuations. In systems combining PV generation with BESS, strategies that explicitly consider the battery state of charge (SOC) have been proposed. Jiménez et al. [87] introduced a dual-algorithm approach consisting of moving average control to estimate a smooth reference trajectory and SOC control to maintain flexibility around a desired SOC level. Simulation results demonstrated the effectiveness of this method in mitigating PV-induced variability in distribution grids. Beyond battery-only systems, hybrid storage configurations have also been explored. Álvaro et al. [88] controlled renewable power plant ramp rates using a combination of batteries and capacitors. Hybrid solutions integrating batteries with ultracapacitors or supercapacitors can reduce overall system cost by limiting the amount of unused battery capacity required to handle short-duration, high-power fluctuations. Arevalo et al. [89] demonstrated that a hybrid supercapacitor–battery system reduced supercapacitor operation compared with conventional smoothing techniques. Similarly, Benavides et al. [90] compared ramp rate–based and moving average smoothing methods in a hybrid storage system and showed that the ramp rate method resulted in fewer supercapacitor cycles, even when renewable generation capacity was varied. BESS-based approaches have also been studied in the context of electricity market participation. Abdelghany et al. [91] proposed a two-layer model predictive control framework for wind–solar microgrids operating in both grid-connected and islanded modes. Their hierarchical control structure integrates high-level and low-level controllers to optimize BESS operation and market participation simulta-

neously. Overall, these studies demonstrate that BESS is highly effective in mitigating PV output variability, particularly when large-capacity batteries are available to handle steep ramp events. However, despite their technical effectiveness, BESS-based solutions are associated with high capital and maintenance costs, as well as significant environmental impacts, motivating the exploration of alternative ramp rate control strategies.

Another approach to alleviating the adverse impacts of rapid power fluctuations is the use of dispatchable generation sources, such as gas turbines. To address the intermittency of solar power, Abudu et al. [77] investigated compressed air injection as a means to enhance the fast-response capability of gas turbine–based on-demand generation systems. Their study highlighted that the increasing penetration of renewable energy sources, together with stricter grid operation requirements, necessitates higher ramping capabilities from backup power units such as gas turbines. Using quasi-steady-state simulations based on a constant mass flow method, they demonstrated that, independent of the initial load condition, injecting compressor outlet air at a rate of 2% during ramp-up operation improves the ramp-up rate of a large gas turbine by approximately 10% on average. Despite this improvement in dynamic performance, the approach was estimated to result in annual fuel consumption exceeding one million liters. Gas turbine–based generation offers the advantage of high controllability and rapid adjustment of power output. However, similar to large-capacity battery-based solutions, such systems are associated with high capital and operational costs, as well as substantial environmental impacts, which limit their attractiveness as a sustainable long-term solution for mitigating PV-induced power fluctuations.

Power curtailment using dump loads has been shown to be a comparatively effective option when larger power fluctuations are permissible, resulting in smaller revenue losses than battery energy storage–based approaches [78]. The effectiveness of dump load controllers in mitigating voltage flicker caused by passing clouds over PV arrays has also been demonstrated [92]. Although dump load–based control combined with maximum power point tracking (MPPT) is regarded as highly reliable and relatively low-cost, it is generally not recommended for suppressing PV power fluctuations in large-scale PV plants [93]. This limitation arises because intentional power curtailment directly reduces the revenue of PV system owners. Nevertheless, such methods can be suitable for smaller PV installations at the residential or community scale, where economic impacts are more limited. In addition, droop-based excess power curtailment control has been employed to regulate inverter output and maintain system voltage within predefined limits [94]. This control strategy relies on the relationship between system frequency and excess generation power. However, in these approaches—whether based on dump loads, MPPT-based curtailment, or droop control—the curtailed or consumed power cannot be recovered or reutilized. Table 3.1 summarizes the key advantages and limitations of the three major categories of ramp rate control methods discussed above.

3.2.2 PV cooling methods

A wide range of PV cooling techniques has been investigated in the literature. Cooling approaches based on phase change materials (PCMs), nanofluids, and hybrid combinations of both have been extensively studied. In particular, passive cooling using PCMs has been reported to enhance PV efficiency by up to 20% [80]. Several studies have focused on PCM models driven by natural convection and numerical simulations [95], demonstrating that PCM-based thermal energy storage can consistently reduce energy consumption, with efficiency gains of approximately 20%, especially during peak demand periods. Innovative PCM materials have also been explored. For example, sheep fat was introduced as a novel PCM and shown to cool PV modules more effectively than conventional paraffin wax [96]. Passive cooling systems relying on natural coolant circulation induced by buoyancy and gravity have also been proposed [97], where composite PCMs composed of coconut oil and sunflower oil significantly improved PV efficiency in experimental evaluations. Other studies have examined passive cooling using static water combined with PCM [98]. In this approach, both the latent heat of PCM melting and water evaporation contribute to thermal regulation, resulting in daily power output increases of 8.12% and 9.39% over two observation days compared with uncooled PV panels. Shape-stabilized PCMs with high energy storage capacity and rapid charge–discharge characteristics are also under active investigation [99]. For instance, salt hydrate–based shape-stabilized PCMs incorporating functionalized graphene nanoplatelets have been synthesized, achieving enhanced solar absorption and a photothermal efficiency of 92.6%. Nanofluids have additionally been studied as both coolants and optical filters [100]. Their application in PV–thermal systems has been shown to improve PV efficiency by more than 60%, while combining nanofluids with PCMs yields efficiency improvements of approximately 32%. The performance benefits of nanoparticles have also been experimentally confirmed [101], where nano-enhanced PCM-based thermal energy storage systems significantly improved both electrical and thermal outputs of PV–thermal air collectors, particularly at higher airflow rates. However, high development costs and long-term stability issues remain major challenges for nanofluid- and nano-PCM-based cooling technologies [100]. Beyond cooling, innovative applications of PV waste heat have been explored. For example, solar cell waste heat has been utilized for desalination, enabling simultaneous freshwater and electricity production [102]. A five-stage PV–membrane distillation–evaporative crystallizer demonstrated stable freshwater output, reduced PV cell temperatures, and an associated 8% increase in electrical power generation. Geometric cooling enhancements have also been investigated. Studies focusing on fin plate configurations on the rear side of PV modules evaluated pin fins, Y-shaped fins, and spring fins through numerical and experimental analyses [103]. Additionally, comparative evaluations of PCM-based, thermoelectric, and aluminum-fin cooling systems revealed that while fin-based solutions generally achieved the highest power output, improperly selected PCMs could act as thermal insulators, raising panel temperature and degrading performance [104].

Atmospheric water-based cooling strategies have also been proposed. An adsorption atmospheric condenser was shown to provide an average cooling power of 295 Wm^{-2} reduce PV module temperatures by at least 10°C under irradiance of 1.0 kWm^{-2} [105]. Outdoor field experiments demonstrated power generation increases ranging from 13% to 19%, with the added advantage of minimal geographical constraints. Finally, active water cooling remains one of the simplest and most effective PV cooling techniques and has been widely studied [106]. However, its practical deployment is often limited by the requirement for a stable water supply and sufficiently large cooling systems to offset the associated energy consumption. Importantly, all PV cooling technologies reviewed in this section primarily aim to maximize PV power generation efficiency. In contrast, the focus of the present study is fundamentally different: it explores the use of PV cooling as a means of actively regulating power output for ramp rate control, which lies outside the scope of existing PV cooling research.

Table 3.1: Pros and cons of typical ramp rate control approaches.

Ramp rate control methods	Pros	Cons
Battery energy storage systems (BESS)	• A larger battery capacity enables better accommodation of large ramp-rate variations. • Capable of responding to both rapid increases and rapid decreases in PV power output. • Surplus energy that is mitigated can be effectively reutilized.	• Increasing battery capacity leads to higher equipment and maintenance costs. • Larger batteries are associated with greater environmental impacts. • Repeated fast charging and discharging accelerate battery degradation.
Power generation from fuels	• Capable of rapidly supplying large amounts of power.	• High capital and maintenance requirements. • Significant environmental burden. • Limited ability to address sudden increases in PV generation output.
Power consumption or limitation by dump loads	• Significantly lower equipment and maintenance costs.	• Suppressed or consumed power cannot be recovered or reused. • Limited capability to handle sudden decreases in PV generation output.

3.3 Cooling-Based Control Methodology

This section outlines the proposed ramp rate control strategy and the role of PV cooling as a core element of the approach, together with the target microgrid illustrated in Fig. 3.1. The microgrid can operate either connected to the main grid or in an isolated mode through a breaker. It represents a localized energy system composed of generation resources and electricity consumers. Fig. 3.1 presents a schematic representation of the microgrid model considered in this study. The microgrid primarily consists of a PV plant and electrical loads that represent power consumption facilities. The PV plant includes PV modules, PV cooling units, and battery storage systems as its main components. Power flow within the PV plant is coordinated by a controller based on the system state and power balance conditions. Notably, this controller monitors only the power ramp behavior of the PV plant rather than the overall grid state. When a power deficit occurs, electricity is supplied from the main grid. Conversely, when surplus power is available, it is exported to the main grid or utilized by the PV cooling units or batteries; however, depending on ramp-rate constraints, a portion of the excess energy may be curtailed within the PV plant.

It should be noted that the proposed ramp rate control strategy is both modular and scalable, since it is intended to operate at the subsystem level rather than controlling the entire PV system centrally. The PV cooling mechanism and the corresponding battery bank are inherently scalable and are designed to function starting from a minimal number of units. This decentralized configuration eliminates the need for a centralized cooling infrastructure. Once the design of an individual unit is defined, the same unit can be replicated to expand the system capacity up to that of a full-scale power plant. It is also worth emphasizing that the cooling unit performance and battery capacity adopted in this study are deliberately kept modest, making them suitable as a basic unit size for scalable deployment. Under this design philosophy, the proposed method can be readily adapted to PV installations with different scales and system configurations.

3.3.1 Overview of the proposed ramp rate control method

An overview of the proposed framework is shown in Fig. 3.2. The primary goal of the proposed approach is to suppress short-term ramp rates in PV power output, such as those caused by transient cloud movements. The method takes power demand information and weather-related data as inputs, where the weather data include variables such as ambient temperature and solar irradiance. Its output is an operational plan specifying the control actions for PV cooling units, battery charging and discharging, and power exchanges with the main grid. The method determines an optimal control solution over a finite prediction horizon by minimizing a predefined objective function. Specifically, the proposed strategy formulates detailed operating schedules for cooling units and batteries at the subsystem level where the PV plant is connected, considering both surplus

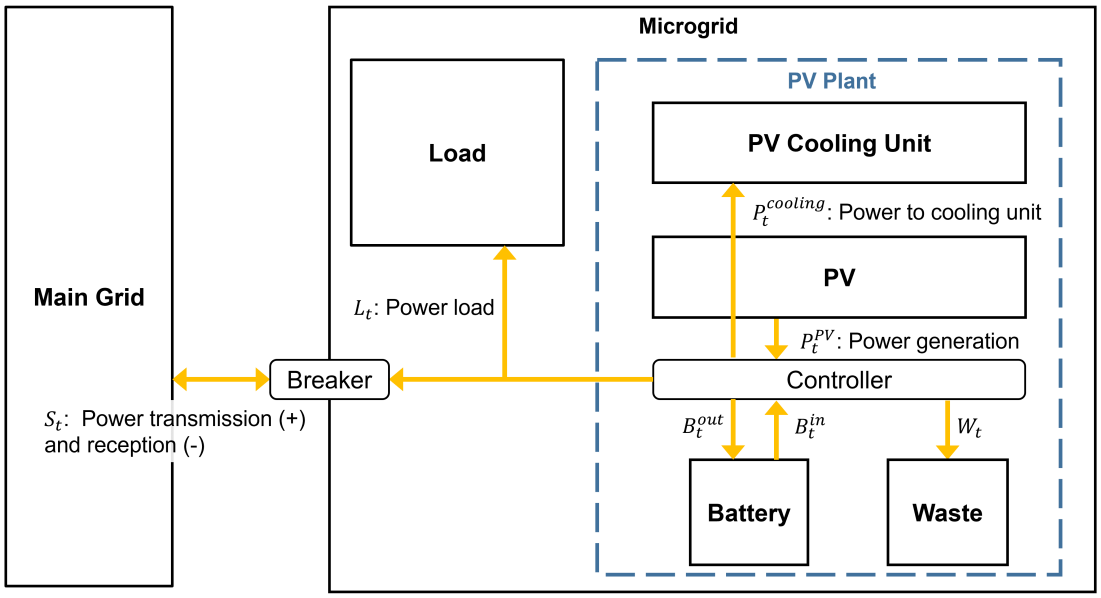


Figure 3.1: Schematic of the target microgrid with mathematical notation for each system variable.

generation and power shortage conditions. By dynamically regulating cooling actions in response to real-time PV generation and load conditions, the method enables flexible power injection to and withdrawal from the grid while maintaining grid stability.

The proposed method operates through the following sequence of steps. First, load demand and weather information are collected for a short time window during which PV output fluctuations are expected, such as a 15-minute interval. Using this weather data, a PV model generates forecasts of power output and panel temperature. Based on these forecasts, an energy optimization problem is formulated with the primary objective of minimizing ramp rates. Although ramp rates could be reduced by curtailing power output or dumping excess energy, such measures are undesirable; therefore, the optimization also aims to maximize power supplied to the grid while minimizing wasted energy. The decision variables include the operation of PV cooling units and batteries, as well as power exchanges with the main grid. This optimization problem is expressed in mathematical form and solved using a numerical optimization solver to obtain an optimal operational plan. Finally, the resulting control actions are implemented in the system, and the updated system state is fed back into the mathematical model for subsequent operation.

The proposed method is intended for online operation through the formulation of a mathematical optimization problem. This design is fundamental to the method, as it allows real-time control actions to be updated using current weather information and PV output predictions. Moreover, the system is designed to run efficiently on low-cost and commonly available hardware platforms, such as the Raspberry Pi.

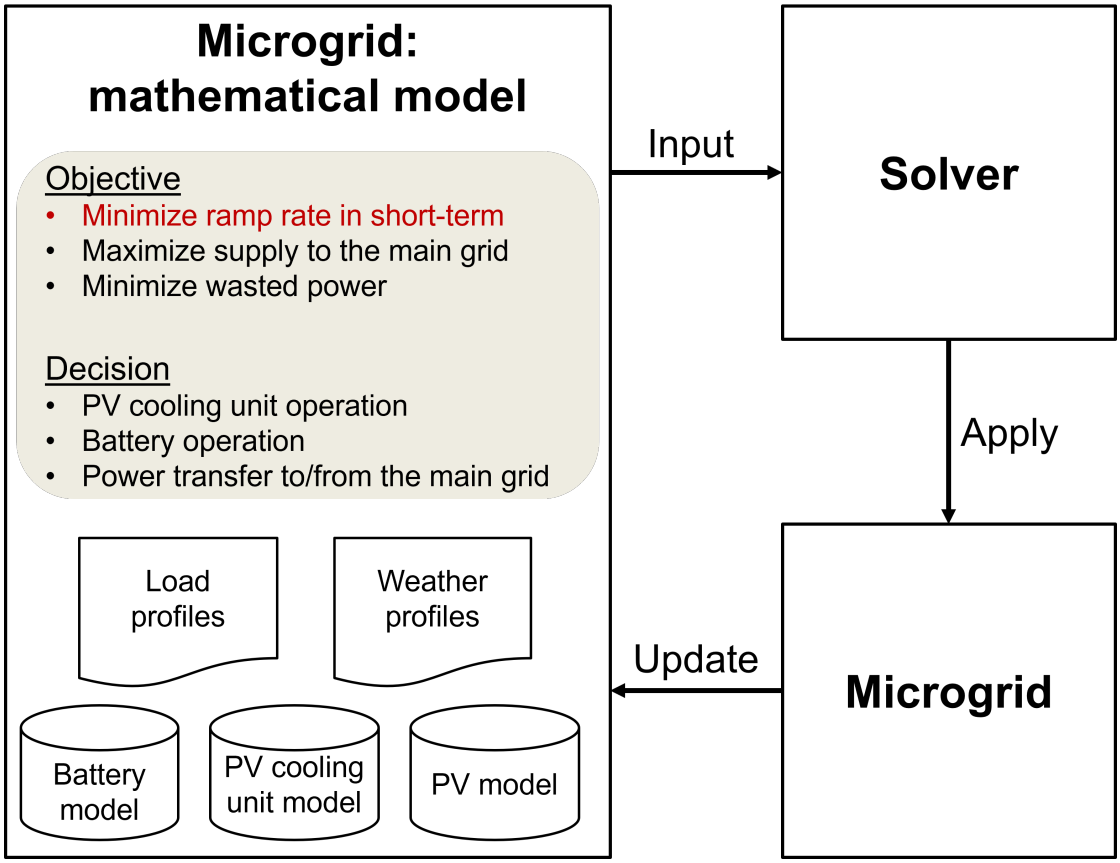


Figure 3.2: Overview of the proposed optimization-based control framework for PV systems incorporating PV cooling units.

3.3.2 How to utilize PV cooling units

This section describes the operation of the PV cooling unit, which constitutes the core component of the proposed method. Depending on the PV cell technology, previous studies have reported that the maximum power output decreases by approximately 0.25%–0.5% for each 1 °C rise in panel temperature [100]. By incorporating an active cooling mechanism, the proposed approach alleviates efficiency degradation caused by temperature increases and enables more stable PV power output. When PV generation rises rapidly during output fluctuations, the cooling unit is activated to absorb surplus power while simultaneously lowering the panel temperature. Conversely, when PV output drops sharply, cooling operation is reduced or suspended, allowing more power to be delivered to the grid. Through this bidirectional coordination, the method stabilizes grid power injection and enhances the overall efficiency and reliability of the PV system. Rather than operating in an on/off manner, the power supplied to the cooling unit is continuously modulated to keep the ramp rate as close as possible to the specified limit.

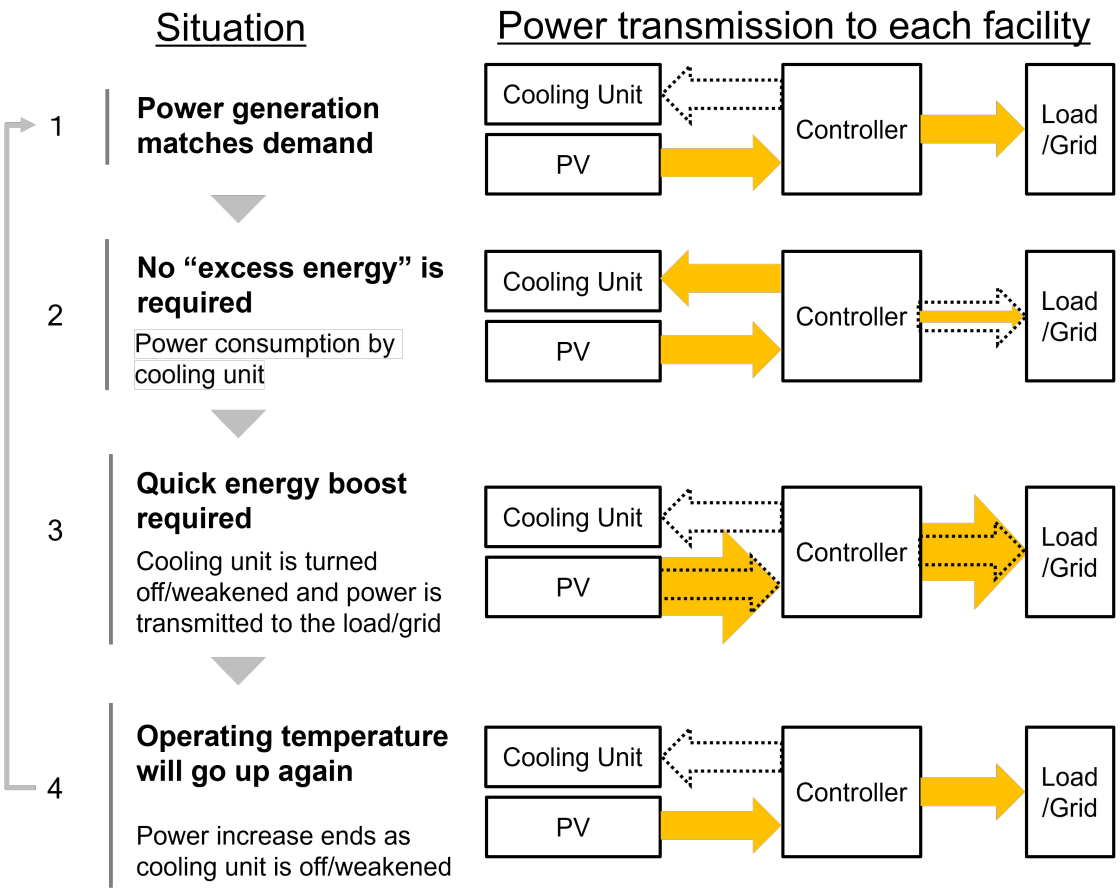


Figure 3.3: PV cooling–based control strategy for regulating power generation.

Fig. 3.3 illustrates a more detailed example of how the PV cooling unit is utilized. In Situation 1, PV power generation is balanced with demand, or output fluctuations are negligible; therefore, the cooling unit remains inactive. In Situation 2, when solar irradiance increases and PV generation exceeds demand, the cooling unit is activated to cool the panels while consuming the surplus power, thereby suppressing sudden power injections into the grid. In Situation 3, if solar irradiance drops sharply or demand rises abruptly, requiring an immediate increase in supplied power, the cooling unit is reduced or switched off so that power can be delivered to the grid. At this stage, the previously cooled panels operate at higher efficiency, enabling increased power generation and preventing an abrupt reduction in power supplied to the load or the grid. In Situation 4, as cooling operation is suspended, the panel temperature gradually increases and the temporary power enhancement diminishes. This duration is considered sufficient to mitigate excessive ramp rates caused by PV output variability. The detailed operating schedule of the PV cooling unit is determined by solving an optimization problem based on prevailing weather conditions and load demands, as illustrated in Fig. 3.2.

3.4 System Model

This section presents the mathematical formulations used in the proposed approach. It details the models of the microgrid, photovoltaic system, PV cooling unit, and battery.

3.4.1 Targeted microgrids

When a power deficit occurs, the microgrid draws electricity from the main grid. Whenever surplus power is available, it is exported to the main grid, absorbed by PV cooling units and batteries, or, if necessary, dissipated within the plant. Accordingly, the microgrid is required to satisfy power balance at every time instant t, which can be expressed as follows:

$$S_t = P_t^{PV} + B_t^{out} - L_t - P_t^{cooling} - B_t^{in} - W_t, \ \forall t, \tag{3.1}$$

where S_t is power transmitted/received, P_t^{PV} is PV generation, B_t^{out} is battery discharge, L_t is power load, $P_t^{cooling}$ is power consumed by the PV cooling unit, B_t^{in} is battery charge, and W_t is wasted power. The power transmitted/received S_t is positive when transmitted and negative when received. In addition, power consumed by the PV cooling unit $P_t^{cooling}$ and wasted power W_t cannot be negative, as given by Eq. 3.2 and 3.3:

$$0 \leq P_t^{cooling}, \ \forall t, \tag{3.2}$$

$$0 \leq W_t, \ \forall t. \tag{3.3}$$

3.4.2 PV and PV cooling unit model

In this work, a mathematical PV electrical model together with an equivalent circuit–based PV thermal model is employed to estimate the electrical and thermal time constants of the PV cell. Fig. 3.4 illustrates the PV electrical model, the PV thermal model, and the PV cooling unit model adopted in this study, along with their respective input–output relationships. The behaviors of the PV electrical and thermal models are described by the following equations:

$$P_t^{PV} = \alpha \cdot (0.2047 \cdot I_t - 3.379) \cdot \{1.36464 - 0.36423 \cdot exp(0.00991 \cdot T_t^{PV})\} \cdot \frac{1}{1000}, \ \forall t, \tag{3.4}$$

$$T_{t+1}^{PV} = exp(-\frac{t}{\tau}) \cdot T_t^{PV} + \{1 - exp(-\frac{t}{\tau})\} \cdot T_t^{ambient} + R \cdot (-\frac{\alpha}{H_t} \cdot 1000 + I_t), \ \forall t, \tag{3.5}$$

where α is number of panels, I_t is solar irradiance at time t, T_t^{PV} is PV panel temperature at time t, τ is the PV panel thermal constant time, $T_t^{ambient}$ is ambient temperature at time t, R is panel thermal resistance, H_t is heat produced by cooling unit at time t. The PV electrical model was constructed by fitting empirical data obtained from a

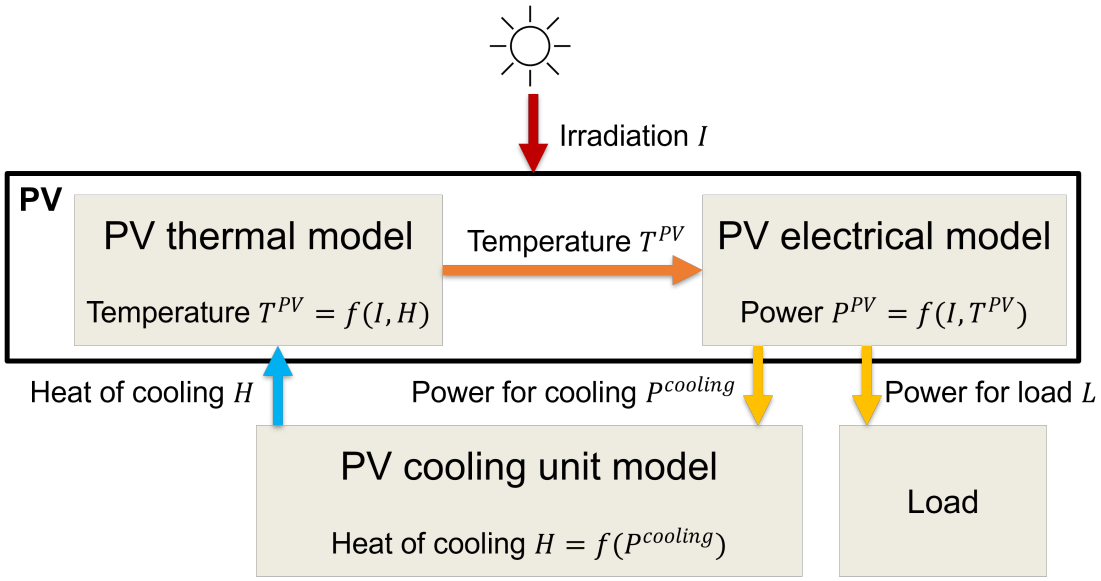


Figure 3.4: PV-electrical, PV-thermal, and PV cooling unit model.

real PV module[2], and is used to estimate PV power output under varying levels of solar irradiance and panel temperature. The PV thermal model was adapted from prior studies on energy management systems [107]. In addition, the panel temperature is constrained not to drop below a specified minimum value, as defined in Eq. 3.6, since excessively low temperatures may impair proper panel operation.

$$T^{PV,lower} \leq T_t^{PV}, \quad \forall t. \tag{3.6}$$

To simplify the modeling and optimization process, the simple COP model was utilized for the PV cooling unit:

$$H_t = P_t^{cooling} \cdot COP, \quad \forall t, \tag{3.7}$$

where the H_t is calculated by an coefficient COP and power consumption of cooling unit $P_t^{cooling}$. For example, COP of a single-stage thermoelectric (Peltier) cooler typically falls in the range of 0.3–0.7, whereas conventional air-conditioning systems generally exhibit COP values between 5 and 8. Similar to the PV thermal model, this cooling model is adapted from prior work on online energy management for heating and cooling systems [108]. Although no specific cooling technology is prescribed in this study, the model is broadly applicable because it characterizes cooling performance as the ratio between the electrical energy consumed per unit time and the corresponding thermal energy removed by the cooling unit. For simplicity, the COP is assumed to be constant across all environmental conditions in this work.

[2]Kyocera KC200GT

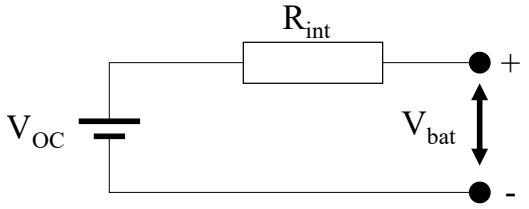


Figure 3.5: Internal resistance battery model [109].

3.4.3 Battery model

In this study, a simple internal-resistance-based battery model [109] is employed to represent the charging and discharging behavior of the battery. Figure 3.5 illustrates a standard internal resistance battery model, consisting of an ideal open-circuit voltage source V_{OC} connected in series with an equivalent internal resistance R_{int}. Both the open-circuit voltage V_{OC} and the internal resistance R_{int} are functions of SOC.

The SOC in the internal resistance model is calculated using the coulomb counting method, as expressed in Eq. 3.8,

$$SOC = \frac{Ah_{rate} - Ah_{used}}{Ah_{rate}}, \tag{3.8}$$

with Ah_{rate} a rated maximum charge of the battery, and where

$$Ah_{used} = \int_0^t I(t)dt. \tag{3.9}$$

The change in the SOC level is calculated based on the battery current:

$$SOC_1 = SOC^{init}, \tag{3.10}$$

$$SOC_{t+1} = SOC_t + \frac{\gamma \cdot B_t^{in} - B_t^{out}}{B^{cap} \cdot 3600} \cdot \Delta t, \ \ \forall t, \tag{3.11}$$

$$SOC^{min} \leq SOC_t \leq SOC^{max} \ \ \forall t, \tag{3.12}$$

where γ is the charging efficiency, B^{cap} is the battery capacity, and Δt is the step length in the optimization calculation. In addition, the charging and discharging rates are constrained to constant limits, and charging and discharging are not allowed to take place at the same time, given by Eq. 3.13, Eq. 3.14 and 3.15, respectively.

$$0 \leq B_t^{in} \leq C^{rate}, \ \ \forall t, \tag{3.13}$$

$$0 \leq B_t^{out} \leq C^{rate}, \ \ \forall t, \tag{3.14}$$

$$B_t^{in} \cdot B_t^{out} = 0, \ \ \forall t, \tag{3.15}$$

where C^{rate} is the maximum charging/discharging power.

3.4.4 Mathematical formulation of PV system operation optimization

This section provides a detailed mathematical formulation for scheduling the operation of the PV cooling units and batteries, as well as power exchanges with the main grid. The scheduling optimization problem is formulated as follows:

$$\begin{aligned}
&\text{minimize} && \sum_{t=1}^{l}(S_{t+1}-S_t)^2-\beta\sum_{t=1}^{l}S_t+\sum_{t=1}^{l}W_t, && (3.16)\\
&\text{subject to} && (3.1)-(3.15),\ \forall t,\\
&\text{input} &&\\
&&& \{L_t, I_t, T_t^{ambient}\},\ \forall t,\\
&\text{decision variables} &&\\
&&& \{S_t, P_t^{cooling}, B_t^{in}, B_t^{out}\},\ \forall\{t\},
\end{aligned}$$

where β is the coefficiency for scaling and l is the planning period. The objective function primarily aims to minimize ramp rates, while also incorporating terms that promote maximizing power supplied to the main grid and reducing wasted energy. This nonlinear optimization problem is solved using an appropriate solver, yielding optimal schedules for PV cooling operation, battery charging and discharging, power curtailment, and power exchange with the main grid.

3.5 Simulation Experiments

This section presents a series of representative simulations conducted to evaluate the effectiveness of the proposed method under realistic operating conditions. First, the simulation setup is outlined, after which several case studies are introduced. In addition, the impacts of battery capacity and COP of the cooling unit on ramp rate control performance are examined.

3.5.1 Simulation Setup

This subsection summarizes the parameter settings used in the proposed method. In all simulations, the evaluation window is set to 15 minutes with a temporal resolution of 1 second. The parameter β in Eq. 3.16 is fixed at 0.0000982. The battery-related parameters adopted in the optimization problem are summarized in Table 3.2. The battery-related parameters are determined based on prior studies on battery-based energy management [107]. Outdoor temperature and solar irradiance data for Oldenburg are obtained at a 1-second temporal resolution. As illustrated in Fig. 3.6, the dataset corresponds to a 15-minute interval characterized by pronounced PV output variability.

Table 3.2: Parameters settings of battery.

Description	Symbol	Value
Initial SOC	SOC^{init}	0.9
Min. SOC	SOC^{min}	0.2
Max. SOC	SOC^{max}	1.0
Max. charging/discharging power	C^{rate}	10 [kW]
Charging efficiency	γ	0.9

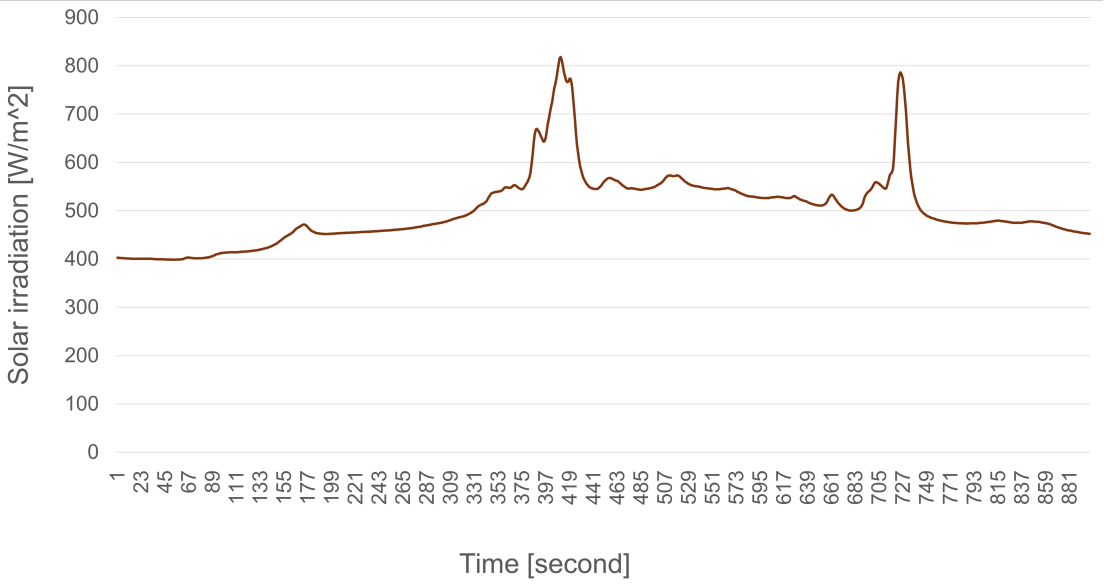


Figure 3.6: Solar irradiance in Oldenburg on July 7, 2015 from 12:30 to 12:45.

The specific 15-minute segments selected for simulation in each season and time-of-day category are summarized in Table 3.3. The morning period is defined as two hours after sunrise, while the evening period is defined as two hours before sunset for each day. The PV-related parameters used in the optimization problem are summarized in Table 3.4. The number of PV panels is chosen so as to represent a PV plant with a rated capacity of 1 MW. The thermal resistance and thermal time constant of the PV panels are determined based on a previous study on PV modules [110]. Load profiles are generated using actual grid frequency data from Oldenburg. The fundamental components of the load profiles are defined according to the assumed PV plant size and are summarized in Table 3.5 for each season and time-of-day condition. Fig. 3.7 illustrates the noise component derived from Oldenburg grid frequency data when superimposed on the fundamental load component. This synthesized load profile is then used as an

[3] When PV panel temperature is originally less than 10°C, T^{lower} is 0.

Table 3.3: Date and time of selected 15 minutes of temperature and solar irradiance data for each season and time of day.

Season	Time of day		
	Morning	Noon	Evening
Autumn	October 7, 2014 9:30–9:45	October 7, 2014 12:00–12:15	October 7, 2014 16:00–16:15
Winter	January 7, 2015 10:45–11:00	January 7, 2015 12:30–12:45	January 7, 2015 14:00–14:15
Spring	April 7, 2015 10:00–10:15	April 7, 2015 12:00–12:15	April 7, 2015 16:45–17:00
Summer	July 7, 2015 7:30–7:45	July 7, 2015 12:30–12:45	July 7, 2015 18:45–19:00

Table 3.4: Parameters settings of PV.

Description	Symbol	Value
Lower temperature limit of PV panel	T^{lower}	10 [°C] [3]
Nominal solar irradiance	$I^{nominal}$	800 [W/m^2]
PV panel thermal resistance	R	0.01874 [K/W]
Number of PV panels	α	5000
PV panel thermal constant time	τ	1128 [sec]

input to the simulation. The performance metric, namely the ramp rate, is defined as follows:

$$Ramp\ rate = \frac{|\Delta P| \cdot T_s}{timescale}, \tag{3.17}$$

where ΔP describes the change in power S_t, i.e., $\Delta P = |S_{t+1} - S_t|$, exchanged between the microgrid and the main grid, T_s describes data resolution ($T_s = 1$ in this study), $timescale$ describes the time scale for calculating ramp rate ($timescale = 1$ in this study).

3.5.2 Simulation Results

Effect of PV cooling on ramp rate

This section analyzes how PV cooling influences ramp-rate behavior. The simulations were conducted for each season and time of day. In all cases, the battery capacity was fixed at 10 kWh, and the cooling unit was assumed to have a COP of 15.

Focusing on the summer noon period (July 7, 12:30–12:45), when solar irradiance is particularly high, Table 3.6 compares the mean and maximum ramp rates for cases

Table 3.5: Baseline load profile components categorized by season and time of day [kW].

	Time of day		
Season	Morning	Noon	Evening
Autumn	20	400	20
Winter	500	400	60
Spring	300	400	40
Summer	500	400	60

Table 3.6: Mean and maximum ramp rates under summer noon conditions, with and without cooling.

Valuation index	w/o cooling	w/ cooling
Mean ramp rate [kW/sec]	0.6850	0.3871
Maximum ramp rate [kW/sec]	8.111	1.929

with and without PV cooling. From Table 3.6, it is evident that the introduction of PV cooling leads to reductions in both the average and peak ramp rates. In particular, the mean ramp rate is reduced by 43.5%, while the maximum ramp rate is reduced by 76.2%.

To illustrate the mechanism behind these improvements, Fig. 3.8 presents a detailed view of the simulation results over a 200-second interval within the 15-minute simulation window, during which solar irradiance exhibits pronounced fluctuations. Figure 3.8(a) depicts the power flow behavior, while Fig. 3.8(b) shows the corresponding ambient temperature, PV panel temperature, and solar irradiance. The dotted curves represent the case without cooling, and the time axis is shared between the two subfigures. A comparison of grid power profiles in Fig. 3.8(a) reveals that power variations—and hence ramp rates—are substantially smoother when PV cooling is applied. Around 375 seconds, solar irradiance (shown in brown in Fig. 3.8(b)) begins to rise sharply, which in turn increases PV power output, as observed in Fig. 3.8(a). To suppress the resulting ramp-up, the cooling unit is activated, as indicated by the light-blue region, simultaneously consuming power and reducing panel temperature. This coordinated action mitigates the surge in power injected into the grid. Furthermore, pre-cooling plays an important role in alleviating ramp-down events. As shown in Fig. 3.8(b), solar irradiance drops abruptly around 420 seconds, leading to a decrease in PV generation. However, owing to the lower panel temperature achieved through prior cooling, the reduction in output is smaller than in the no-cooling case, represented by the dotted line. In addition, by gradually relaxing the cooling operation and redirecting the power previously

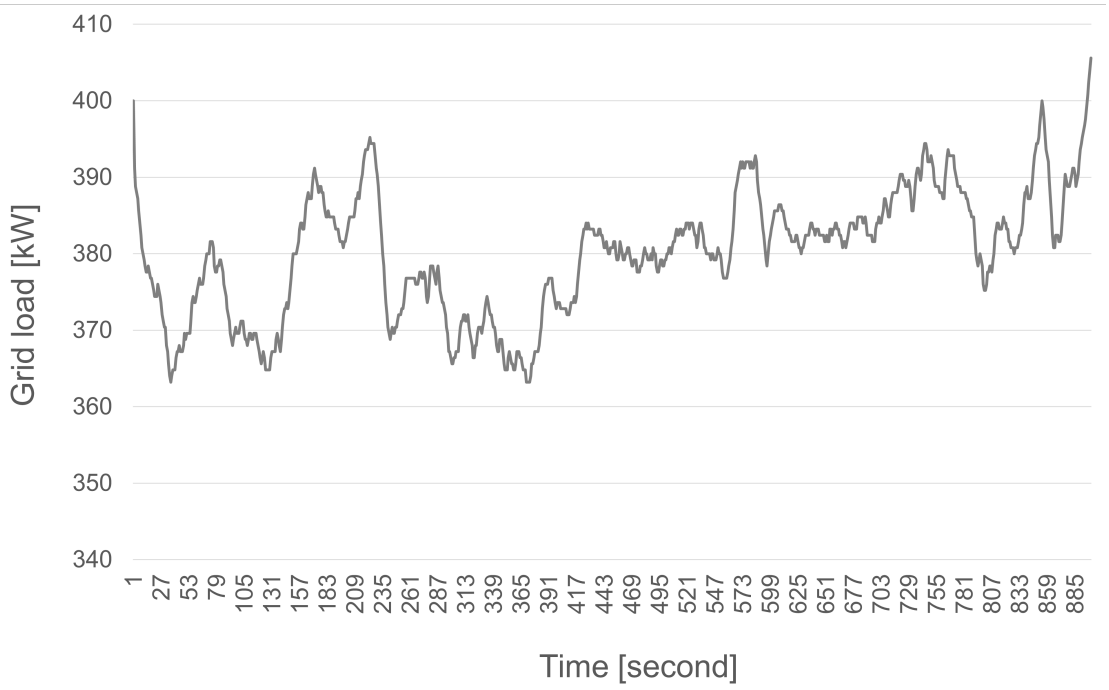


Figure 3.7: Load profile for summer noon derived from grid frequency data in Oldenburg.

consumed by the cooling unit back to the grid, the transition in grid power becomes smoother. This effect is more clearly observed in Fig. 3.9, which provides a magnified view of the relevant portion of Fig. 3.8.

Fig. 3.10 shows the mean and maximum ramp rates for each season and time period. Because solar irradiance levels and ramp-rate characteristics vary substantially across seasons and times of day, the results are normalized with respect to the no-cooling case for each condition, which is set to 1. As shown in Fig. 3.10, the proposed method achieves ramp-rate reduction consistently across all seasons and times of day. Larger relative reductions are observed during morning and evening periods and in winter, likely because baseline ramp rates in these conditions are comparatively lower, making them easier to suppress.

Effect of battery size and cooling unit COP

This section examines the influence of battery capacity and the coefficient of performance (COP) of the cooling unit on ramp-rate mitigation performance. The evaluated battery capacities are 0 (no battery), 10, 20, 30, 40, 70, and 100, while the COP values considered are 1, 3, 5, 10, and 15. The simulations are conducted using a 15-minute dataset corresponding to summer noon conditions (July 7, 2015, 12:30–12:45).

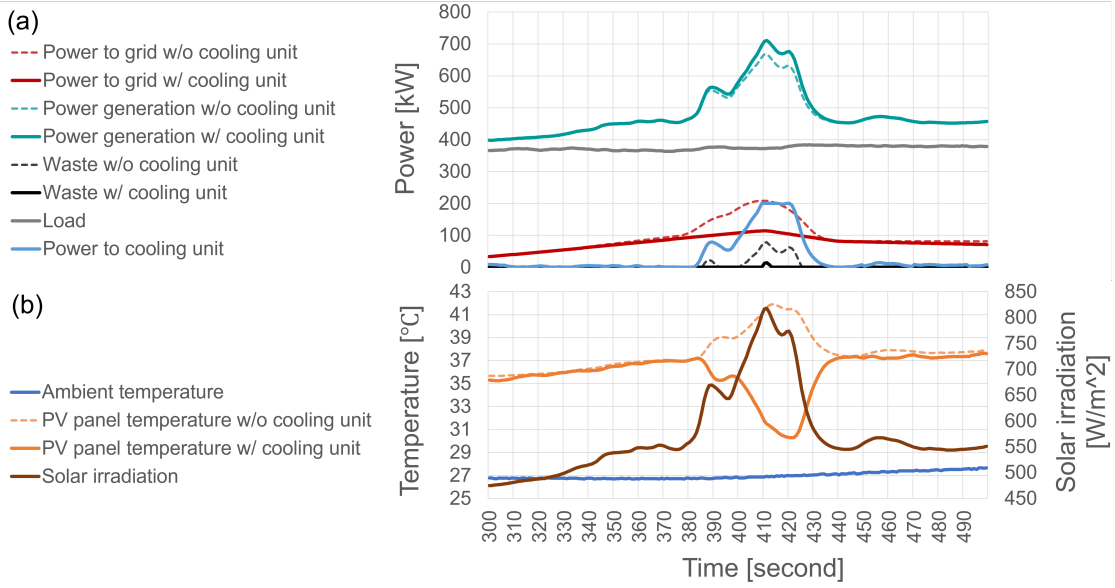


Figure 3.8: Changes in power (a) and temperature (b) over a 200-second interval during summer noon under rapidly changing solar irradiance conditions.

When a cooling unit with a low COP is used, ramp-rate reduction may be achieved mainly through power consumption rather than through an actual improvement in PV generation efficiency, which is not desirable. To capture this effect, accumulated energy—defined as the total energy transferred from the microgrid to the main grid over the planning horizon (i.e., equals $\sum_{t=1}^{l} S_t$, with l still the planning period) is introduced as an additional evaluation metric alongside ramp rate. This metric tends to take smaller values when the cooling unit fails to enhance PV generation efficiency through effective cooling.

Fig. 3.11 illustrates the mean ramp rate (a), maximum ramp rate (b), and accumulated energy (c) for different combinations of battery capacity and cooling unit COP. In all subfigures, the horizontal axis represents battery capacity, and the dotted lines indicate the results obtained without cooling. As shown in Fig. 3.11(a) and (b), the introduction of PV cooling reduces both the mean and maximum ramp rates across all tested battery capacities and COP values compared to the no-cooling case. Focusing on battery capacities up to 40 kWh, ramp-rate reductions exceeding 50% are achieved relative to the case without cooling, while the associated loss in accumulated energy remains limited to approximately 10 kWh. Even with a very modest cooling performance (COP = 1), substantial ramp-rate mitigation is obtained, although the total power delivered to the grid is reduced. For battery capacities above 70 kWh, Fig. 3.11(c) indicates a larger reduction in accumulated energy compared to the no-cooling case; however, the mean and maximum ramp rates shown in Fig. 3.11(a) and (b) are nearly eliminated. These results suggest that even low COP values can contribute effectively to ramp-

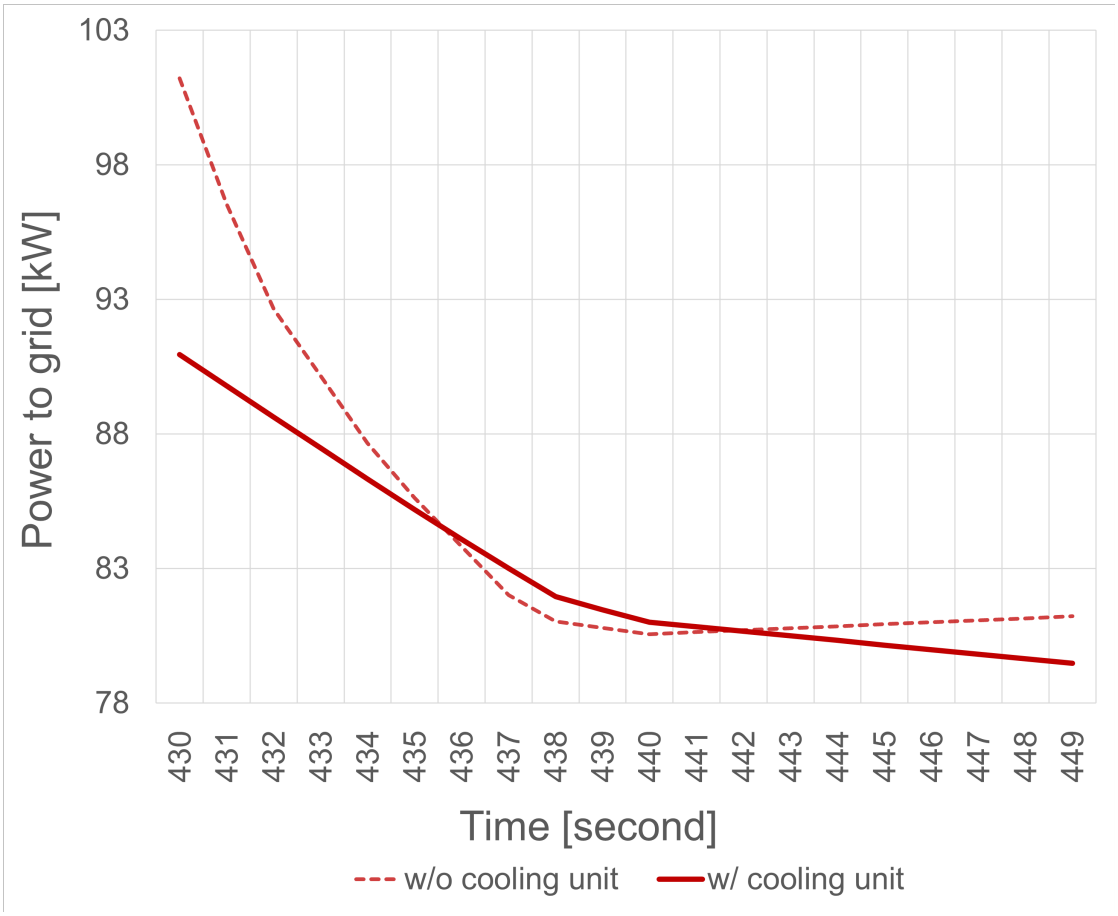
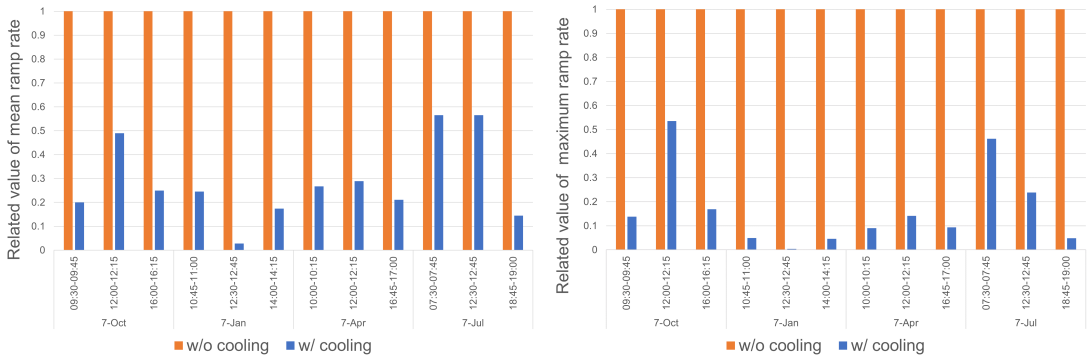


Figure 3.9: Power delivered to the grid between 430 and 450 seconds, with and without PV cooling.

rate suppression, despite reduced energy efficiency, demonstrating the robustness of the proposed approach against variations in cooling unit performance. Moreover, the ability to achieve significant ramp-rate mitigation with relatively small battery capacities highlights the potential for cost reduction and environmental benefits when PV cooling is appropriately integrated. Finally, a comparison of the battery capacity required to achieve equivalent ramp-rate performance reveals a substantial advantage of the proposed method. As indicated in Fig. 3.11(a) and (b), the mean and maximum ramp rates attained with a 20 kWh battery combined with cooling would require nearly 100 kWh of battery capacity in the absence of cooling, depending on the COP. This implies that the proposed method can reduce the required battery capacity by approximately 80%.



(a) (b)

Figure 3.10: Mean (a) and maximum (b) ramp rates for each season and time period, normalized to the no-cooling case.

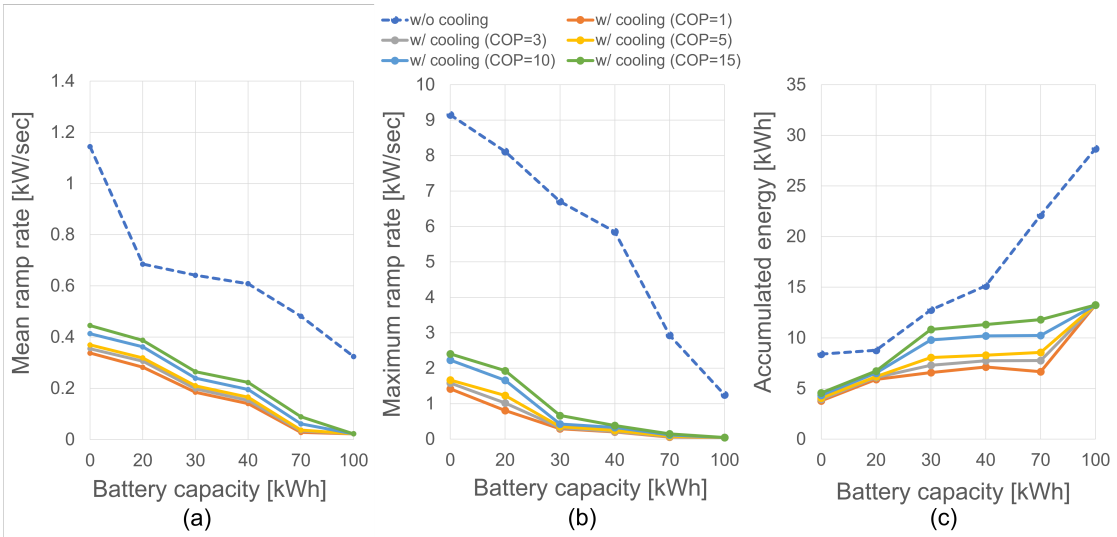


Figure 3.11: Mean (a) and maximum (b) ramp rates, and accumulated energy (c), for each battery capacity and COP.

3.6 Summary

This chapter has introduced a ramp rate control method for PV systems based on PV cooling. The proposed approach regulates power supplied to the grid by consuming surplus energy and improving PV generation efficiency through cooling, thereby avoiding reliance on large-capacity batteries or gas turbines, which are associated with high system costs and environmental impacts. Compared with conventional ramp rate control relying solely on batteries, the proposed method achieves a reduction of up to 76.2% in the maximum ramp rate during summer noon conditions. The effects of battery capacity and COP of the PV cooling unit on control performance were also examined. The results show that while PV cooling alone contributes to ramp rate mitigation, combining it with a small-capacity battery enables substantial ramp rate reduction with minimal energy loss. Finally, the assumptions, limitations, and potential mitigation strategies of the proposed method are discussed.

- **Integration with forecasting methods**: The ramp rate control method proposed in this chapter was developed under the assumption that solar irradiance and power demand can be perfectly predicted, which is an unrealistic condition for real-time operation. To address this limitation, future work should focus on integrating the proposed control method with a forecasting framework that can provide realistic and dynamic predictions of solar irradiance and power fluctuations. Such an integrated approach would enable more practical and adaptive ramp rate control. For this purpose, a framework incorporating the forecasting proposed in Chapter 2 is proposed and discussed in Chapter 3.
- **Expansion of test scenarios**: The current simulations are conducted using specific meteorological datasets. To further assess the robustness of the proposed approach, future studies will evaluate its performance across a broader range of geographic regions and weather conditions. In addition, small-scale experimental testbeds will be considered to demonstrate practical feasibility.
- **Cooling technology selection**: Practical deployment of PV cooling requires careful consideration of not only performance and reliability but also economic viability. Future work will investigate suitable cooling technologies by jointly considering cooling performance, integration complexity, operational efficiency, and maintenance cost.
- **Economic feasibility**: Although this study highlights the potential environmental and cost advantages over approaches relying on large-capacity batteries or gas turbines, a comprehensive economic evaluation is necessary prior to practical implementation. Future research will include detailed cost–benefit and life-cycle analyses to clarify the overall economic feasibility of the proposed method.
- **Convexification of the optimization model**: The current formulation is a nonlinear optimization problem, which yields a locally optimal solution, while globally optimal solutions may exist. Future work will explore convexification techniques

to reformulate the problem, which could guarantee optimality, reduce computational burden, and enhance suitability for real-time implementation on resource-constrained platforms.

- **Validation in residential applications**: Applying the proposed ramp rate control method to residential settings offers potential benefits such as improved self-consumption and local grid stability. However, practical challenges remain, including system sizing, regulatory constraints, diverse household load profiles, and limited installation space for PV and cooling equipment. Future studies will empirically evaluate the effectiveness of the proposed approach in residential environments and investigate adaptations to accommodate these constraints.

Chapter 4

Implementation of Forecast-Based Ramp Rate Control

As discussed in Chapter 3, the increasing integration of photovoltaic (PV) systems into power grids has intensified the challenge of output fluctuations caused by varying solar irradiance. Such rapid changes in PV output, known as ramp rates, can potentially destabilize the power system and hinder reliable grid operation. To address this issue, this chapter proposes an integrated framework that combines the high-resolution solar irradiance forecasting method—based on wavelet transform (WT) and long short-term memory (LSTM) networks—introduced in Chapter 2, with the ramp rate control strategy developed in Chapter 3[1]. Although energy management systems in general operate across multiple temporal horizons—from ultra-short-term control to day-ahead planning—the present dissertation focuses on the short-term layer of this hierarchy. Within this layer, the forecasting module predicts irradiance several tens of seconds ahead, and the control module uses these near-future predictions to determine pre-emptive adjustments of PV output. This short-term temporal hierarchy—forecast first, followed by optimization—forms the operational basis of the proposed framework. By utilizing the predicted irradiance to anticipate ramp rate violations and implementing optimization-based pre-adjustment of PV output, the proposed framework successfully reduces the number of ramp rate violations by up to 20%.

4.1 Introduction

The integration of PV systems into modern power grids has been accelerating worldwide due to the increasing demand for sustainable and renewable energy sources. However, the inherently intermittent nature of solar irradiance—driven by rapidly changing

[1]This chapter is a refined and reproduced version of the paper to be published in Proceedings of the 16th ACM International Conference on Future and Sustainable Energy Systems (e-Energy) [26].

weather conditions such as cloud movement—causes significant fluctuations in PV output. These rapid changes can place stress on the grid, leading to stability issues and challenges in power quality management.

To address this, ramp rate control has emerged as a critical solution. Ramp rate refers to the rate at which PV power output changes over time. Without adequate control, sudden increases or drops in generation can overload grid infrastructure and reduce the reliability of the power supply. Therefore, predicting and mitigating rapid PV output variations is essential for ensuring stable grid operations, particularly in microgrids and isolated systems.

A key to effective ramp rate control lies in accurate solar irradiance forecasting. By anticipating incoming fluctuations in irradiance, PV systems can be proactively managed—through techniques such as curtailment, energy storage, or PV module cooling—to smooth out power delivery. While several forecasting approaches have been proposed, recent studies have highlighted the potential of LSTM networks, a form of recurrent neural networks, for capturing temporal dependencies in weather data. In addition, the use of WT for time series decomposition has shown promise in improving forecasting accuracy by separating high-frequency noise from meaningful trends.

Despite this progress, prior studies either focus solely on forecasting without linking it to ramp rate control, or predict PV output directly, limiting interpretability and generalization across different installations and conditions. To bridge this gap, this chapter proposes an integrated framework that combines wavelet-based decomposition with LSTM-based forecasting to predict short-term solar irradiance, followed by model-predictive ramp rate control using a mathematical optimization framework. The main contributions of this work are as follows:

- The forecasting model is integrated into a real-time ramp rate control framework that applies correction via linear regression and utilizes PV cooling for output smoothing.
- The impact of forecast horizon and prediction error on control performance is quantified through simulation-based experiments using real-world meteorological data.
- The proposed method demonstrates reduced ramp rate violations and increased power delivery to the main grid compared to baseline methods.

The remainder of this chapter is structured as follows. Section 4.2 reviews related work in integrated forecasting and control approaches. Section 4.3 presents the proposed methodology. Section 4.4 describes the experimental setup and results. Finally, Section 4.5 concludes the paper and discusses future directions.

4.2 Related Works

While high-resolution solar forecasting has been combined with active PV power control in a few studies, truly integrated solutions remain rare. For instance, Hendrikx et

al. [111] highlight that accurate LSTM-based irradiance nowcasts enable grid operators to anticipate PV output fluctuations and adjust distribution or storage proactively. Logothetis et al. [112] demonstrated the potential of using LSTM forecasts to anticipate increases in irradiance. These demonstrate the potential of forecast-informed control, but without implementing a dedicated ramp-rate limiting strategy. Chen et al. [113] examined how forecasting parameters (horizon length, resolution, update frequency) affect a predictive curtailment algorithm's performance. Their results showed, for example, that shorter forecast horizons markedly improve ramp smoothing (up to 12% better smoothing rate), whereas more frequent forecast updates yield diminishing returns. However, neither of the above efforts implemented a full closed-loop control system. In other words, they are not feedback control systems where the controller's output affects the overall system state, and control parameters are updated based on that feedback.

Several researchers have attempted to integrate short-term solar predictions with active PV output control mechanisms. Ryu et al. [114] proposed a "predictive tracking" battery smoothing method that leverages deep-learning forecasts (including sky image nowcasts) to pre-charge or discharge a battery, thus limiting PV ramp rates with a smaller required storage capacity. Their simulation confirmed that using forecast-driven battery control can meet ramp-rate limits with significantly reduced battery size. Similarly, a recent study by Jiao et al. [115] introduced a predictive PV output curtailment scheme that uses a deep neural network forecast and an uncertainty estimator to throttle the inverter in advance of steep ramps. This approach, essentially a predictive active power curtailment strategy, adjusts the PV inverter's power set-point preemptively based on expected irradiance changes. In a related vein, Arévalo et al. [116] LSTM-based short-term prediction with real-time control of a hybrid energy storage system, achieving over a 74% reduction in PV/Wind power fluctuations compared to conventional smoothing methods (e.g. moving averages or simple ramp-rate limiters). These works demonstrate that coupling forecasts with active control (whether via battery, inverter throttling, or hybrid storage) can substantially mitigate ramp-rate volatility and reduce reliance on oversized buffers.

To the best of this author's knowledge, no prior study has proposed a framework that simultaneously (i) integrates forecasting into a closed-loop control architecture, where the controller's outputs actively influence system behavior and are used to update control parameters through feedback, and (ii) introduces a production-side control knob via PV panel cooling, thereby enabling ramp-rate regulation without relying on curtailment or oversized storage systems. This work addresses the above gap by designing and evaluating such a framework on real-world meteorological data, and by analyzing the effect of forecasting accuracy and horizon length on ramp rate violations and energy delivery to the main grid.

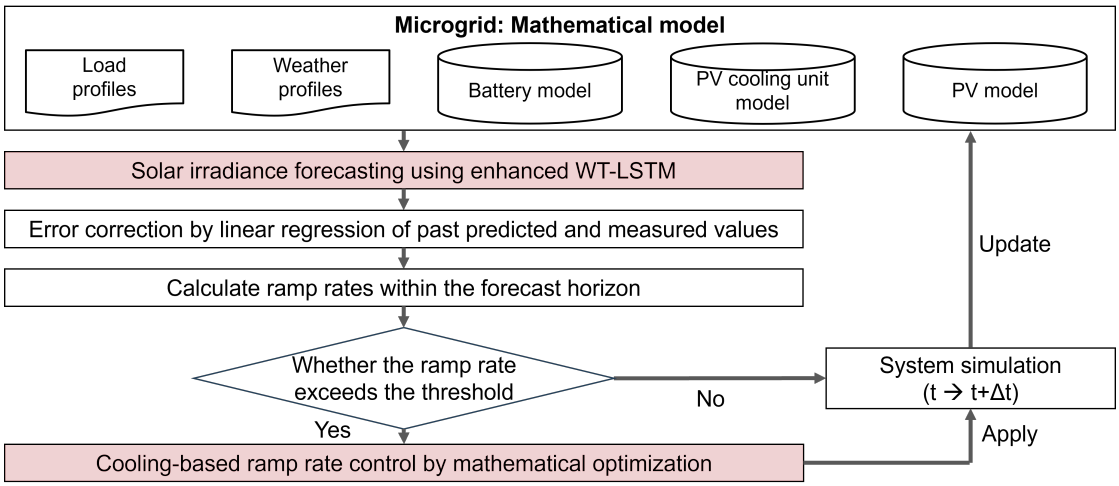


Figure 4.1: Workflow of the proposed framework.

4.3 Proactive Solar Power Control Through Integrated Forecasting

This section describes the proposed ramp rate control framework for PV systems, which integrates a solar irradiance forecasting model based on WT and LSTM networks. The solar irradiance forecasting method is based on WT and LSTM network proposed in Chapter 2, while the ramp control method is based on the PV cooling approach proposed in Chapter 3. This section first provides an overview of the proposed framework, then focuses on explaining how the prediction method in Chapter 2 and the ramp control method in Chapter 3 are integrated.

4.3.1 Overview of the Framework

The grid targeted in this study is shown in Fig. 3.1 in Chapter 3. The microgrid includes PV generation, a central controller, and optional auxiliary systems such as energy storage and PV panel cooling units. The microgrid is assumed to operate in grid-connected mode, where stable power injection is required to maintain grid reliability and comply with ramp rate limits.

Fig. 4.1 shows the complete workflow of the proposed ramp rate control framework. Of these, the historical irradiance data is first decomposed using WT to separate low-frequency trends from high-frequency variations. Each of the decomposed components, along with other features, are input into LSTM model to predict short-term irradiance values (e.g., 10 to 120 seconds ahead).

The predicted irradiance is then used to estimate the expected PV output and its ramp rate. If the forecasted ramp rate exceeds a predefined threshold (e.g., ±20 kW/s),

a predictive optimization model is triggered. This model calculates the optimal adjustment to the PV output to keep ramp rates within acceptable limits while minimizing energy loss or curtailment. In summary, the framework integrates:

- Data-driven time series decomposition,
- Neural network-based forecasting,
- Predictive control logic

This approach enables anticipatory ramp rate control, enhancing the stability and grid-friendliness of PV-rich microgrids.

In this study, solar irradiance is selected as the primary forecasting target because it is the dominant exogenous driver of PV power fluctuations and is directly governed by weather dynamics. Unlike PV power output, irradiance is independent of system-specific factors such as module temperature, inverter characteristics, or active control actions, including cooling-based regulation. Forecasting irradiance therefore provides more general and transferable information for proactive ramp rate control, particularly in systems where PV output is actively manipulated by control mechanisms. It should be noted that the proposed forecasting framework is not inherently limited to solar irradiance. With minimal modification, the same WT–LSTM-based approach can be applied to direct PV power forecasting, provided that sufficiently high-resolution historical PV power data are available. This flexibility allows the framework to be adapted to different control architectures and data availability conditions, depending on whether control decisions are driven by exogenous forecasts or directly by power output predictions.

4.3.2 Solar Irradiance Prediction and Error Correction

Accurate short-term solar irradiance forecasting is essential for proactive ramp rate control in PV systems. However, solar irradiance is inherently non-stationary and exhibits rapid fluctuations due to transient atmospheric conditions. To address this challenge, the hybrid approach of WT and LSTM proposed in Chapter 2 is employed. By leveraging the frequency-localization property of WT together with the temporal learning capability of LSTM, the proposed forecasting method aims to achieve high prediction accuracy.

The forecasting model takes the most recent T seconds of observations (e.g., $T = 60$ seconds) and predicts future irradiance values up to a horizon Δt (e.g., 10 to 120 seconds ahead). For each decomposed signal $X_i(t)$, the LSTM model generates a forecast $\hat{X}_i(t + \Delta t)$. These are then summed to reconstruct the final irradiance prediction:

$$\hat{G}(t+\Delta t) = \hat{A}_n(t+\Delta t) + \sum_{i=1}^{n} \hat{D}_i(t+\Delta t). \tag{4.1}$$

To mitigate prediction bias, a simple linear regression-based correction is applied by comparing recent forecasts with actual measurements. The input to each LSTM includes:

- Decomposed irradiance components,
- Meteorological features: temperature, humidity, wind speed/direction, cloud cover,
- Temporal features: time of day, day of year, solar altitude,
- Quality flags: cloud measurement confidence.

4.3.3 Ramp Rate Estimation, Optimization, and System Update

To mitigate the adverse effects of rapid PV output fluctuations on grid stability, this study incorporates a forecast-driven ramp rate control strategy. The control framework combines irradiance prediction, ramp rate estimation, optimization-based output adjustment, and system-level simulation within a microgrid environment.

Based on the short-term forecasted irradiance values $\hat{G}(t+\Delta t)$, the expected PV output is estimated using a PV model that considers conversion efficiency and potential cooling effects. The ramp rate $r(t)$ at time t is defined as:

$$r(t) = \frac{|S(t+\Delta t) - S(t)|}{\Delta t}, \tag{4.2}$$

where $S(t)$ denotes the power transferred between main grid and microgrid. If the absolute value of the ramp rate exceeds a predefined threshold (e.g., 20 kW/s), control actions are triggered.

When a ramp rate violation is predicted, the system adjusts the PV output using panel cooling units that runs on surplus power to control the power generation via the ramp rate control method proposed in Chapter 3. When there is surplus power, the cooling unit is activated to consume the surplus power and cool the panels at the same time. When there is not enough power, the cooling unit is turned off or turned down, and power is sent to the grid. Furthermore, at this time, the panels were cooled in advance, which prevents a reduction in power generation efficiency. The framework is solved as an optimization problem with load, forecasted solar irradiance, and temperature as inputs, the objective function as a function to minimize ramp rate and maximize power to the main grid, and battery and panel characteristics and energy balance in the grid as constraint equations. This allows for the scheduling of power to the main grid, panel cooling units, and battery operations. The simulation iteratively executes the following steps every second:

1. Irradiance Forecasting: Predict irradiance over the next Δt seconds using the wavelet-LSTM model.
2. Ramp Rate Estimation: Calculate expected ramp rate from the forecasted PV output.
3. Control Decision: If the ramp rate exceeds the threshold, trigger the optimization module.
4. Output Adjustment: Apply the optimized output and update the simulation state.
5. State Propagation: Advance the simulation by Δt and repeat.

4.4 Simulation Experiments

In this section, the proposed framework is validated with real measured data of summer days. This simulation evaluates the effectiveness of the proposed framework's ramp rate control for each prediction horizon. It is worth noting that the prediction accuracy for each prediction horizon has already been evaluated in Chapter 2.

4.4.1 Simulation Setup

High-resolution meteorological data collected in Oldenburg, Germany, is used. The dataset includes solar irradiance and auxiliary meteorological variables measured at 1-second intervals. Each input to the forecasting model uses the most recent 60 seconds of data as input to predict irradiance values over a specified forecast horizon (e.g., 10–120 seconds ahead). The ramp rate control threshold was set at 20 kW/s, i.e., ramp rate for 1 second was considered a ramp rate violation if the ramp rate exceeds 20 kW/s. If this violation is predicted in the proposed method, optimization-based adjustments are triggered. The evaluation period is July 7, 2015, 12:00-13:00. The experiment will compare the ideal control (Ideal) using measured solar radiation, i.e., control when the forecast error is zero, control based on forecasts (Prediction) in each forecast horizon (10/30/60/120 seconds), and no control (Baseline) methods. The evaluation metrics are the number of ramp rate violations (number of times ramp rate exceeds 20 kW/s) and the accumulated energy transmitted to the main grid. The reason that the accumulated energy transmitted to the main grid is included in the evaluation metrics is to monitor that the ramp rate is not being smoothed out by massive loss of power.

4.4.2 Simulation Results

Fig. 4.2 shows the number of ramp rate violations in each predicted range. The baselines are all the same value because no prediction is made. In Fig. 4.2, the number of ramp rate violations is reduced from the baseline at the prediction range of 30 and 60 seconds, especially at 30 seconds, from 15 to 12 violations, a 20% reduction. There is no change in the number of violations when the prediction range is 10 seconds, and the number of violations increases when the prediction range is 120 seconds. This is because there was not enough time for ramp rate control when the prediction range was 10 seconds, resulting in almost the same behavior as Baseline. It is also considered that a prediction range of 120 seconds did not allow for proper control due to the large prediction error. In this case, predictions are performed at a 1-second temporal resolution, and the accumulated forecasting errors combined with high-frequency variability can destabilize control decisions. As a result, overly frequent and fluctuating control inputs may be generated, leading to an increased number of ramp-rate violations. This highlights an important trade-off between forecast horizon length and control stability in second-level ramp-rate mitigation. Ideal was able to reduce the number of violations

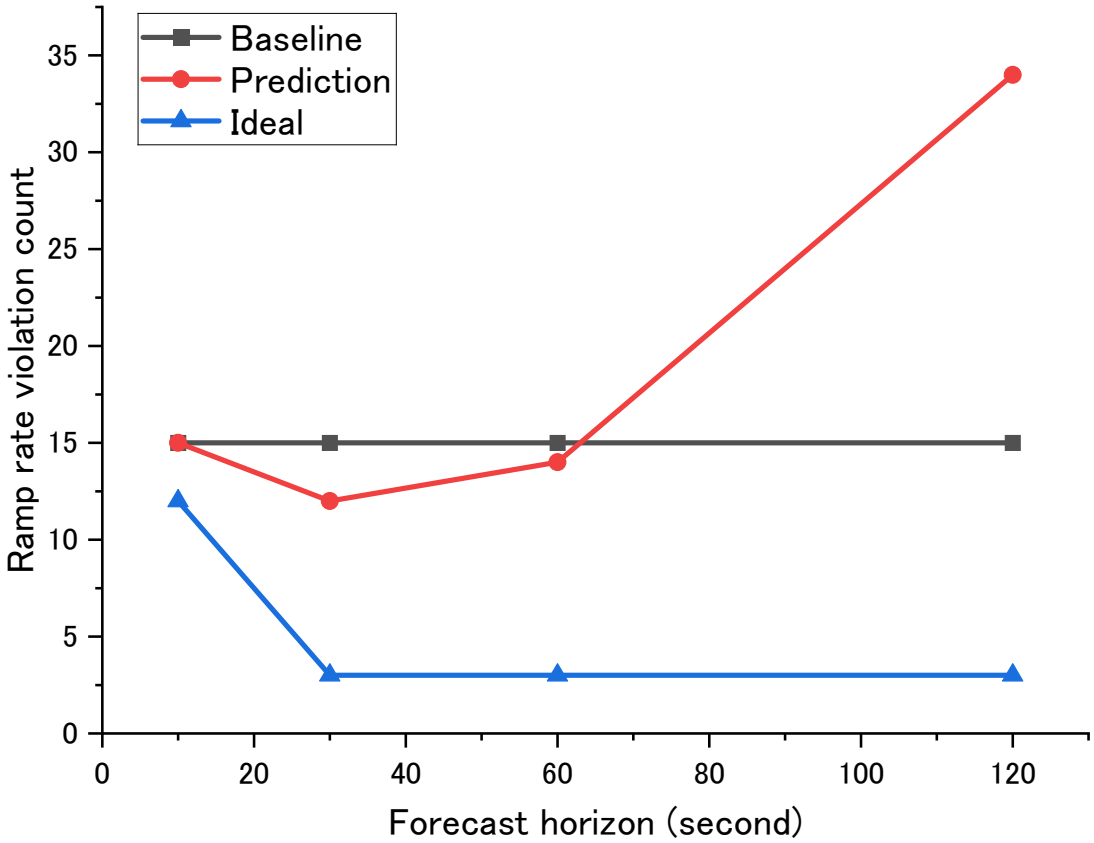


Figure 4.2: Number of ramp rate violations for baseline (no control), prediction-based control, and ideal prediction-based control at each forecast horizon.

by 80%, from 15 to 3, even with a prediction range of 30 seconds, suggesting the value of further improving the accuracy of solar radiation forecasts.

Fig. 4.3 shows the accumulated energy transmitted to the main grid for each of the methods shown in Fig. 4.2. It shows that for both Prediction-based Control (Prediction) and Ideal-based Control (Ideal), the amount of power increases as the forecast range increases. This may be due to the fact that ramp rate control can only be achieved by power consumption when the prediction range is short. In addition, the control based on the forecast is overall larger than the control based on the ideal forecast. This is thought to be because predicted solar radiation tended to be higher than measured solar radiation, so more power tended to be sent to the main grid for Prediction.

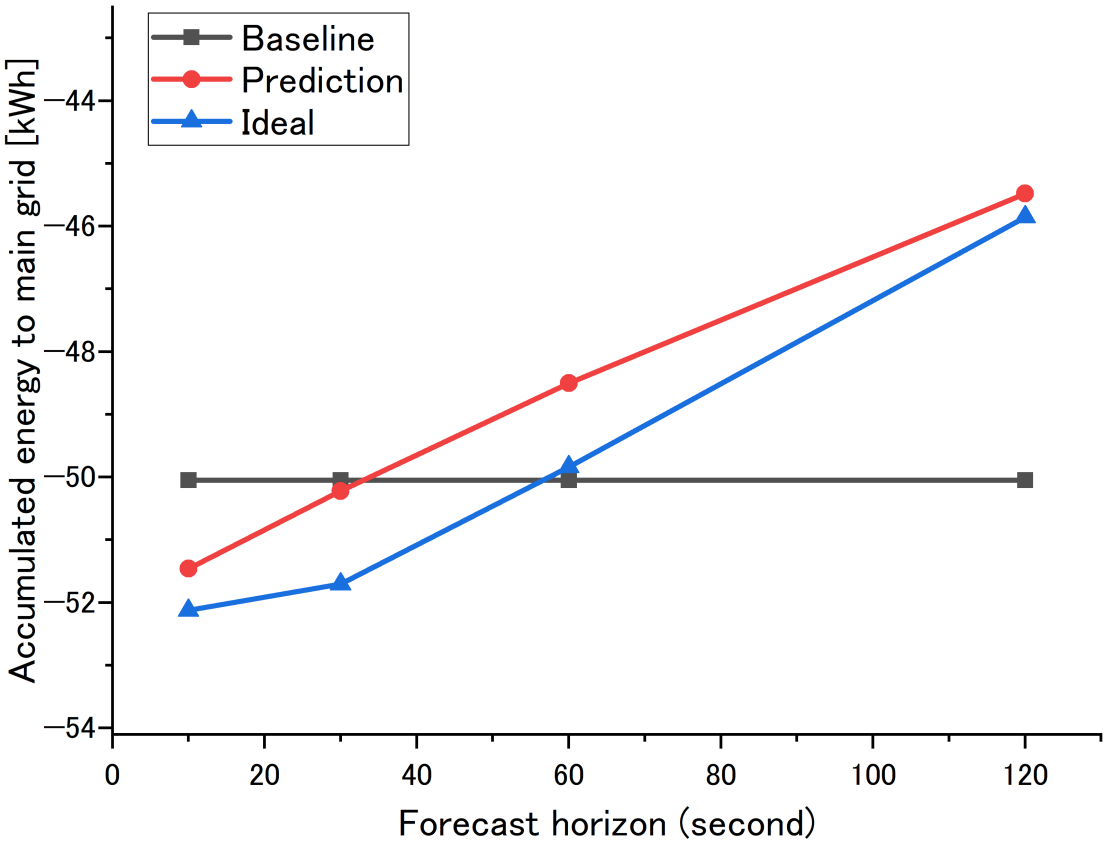


Figure 4.3: Accumulated energy transmitted to the main grid for baseline (no control), prediction-based control, and ideal prediction-based control at each forecast horizon.

4.5 Summary

This chapter proposed a ramp rate control framework for PV systems that integrates wavelet-transformed solar irradiance forecasting using LSTM proposed in Chapter 2 and optimization-based control logic within a microgrid environment proposed in Chapter 3. The proposed framework was designed to mitigate rapid fluctuations in PV output, which can stress power systems and reduce grid stability.

Experimental results showed that short-term prediction improved ramp rate control in ramp rate control with PV cooling. The 30- to 60-second prediction horizon was shown to significantly reduce ramp rate violations compared to the baseline (no control) scenario. In particular, the 30-second prediction window reduced the number of violations by up to 20%, demonstrating a balance between accuracy and control lead time. The 10-second prediction window was too short to allow for corrective action, and the 120-second window resulted in increased control errors due to cumulative prediction uncertainty. This highlights the importance of selecting an appropriate forecast horizon

for real-time applications.

While encouraging, the model in this chapter was trained and evaluated using meteorological data from a single location (Oldenburg, Germany). Extensive evaluation across a variety of climate zones and weather conditions is needed to confirm the universal applicability of this model. The cooling system was also modeled with basic assumptions regarding response time and thermal behavior. A more detailed coupled thermal and electrical model could improve control accuracy. Future work will explore the following points:

- Adaptive control strategies: Dynamically adjusting the forecast horizon or ramp rate thresholds based on environmental conditions and system constraints.
- Integration into multi-horizon EMS architectures: Integrating the proposed short-term PV forecasting–cooling control loop into a broader multi-horizon energy management system (EMS) architecture by combining it with the multi-time-scale wind-integrated EMS framework [117], enabling coordinated distributed energy resource operation across seconds-to-hours timescales.
- Hardware-in-the-loop experiments: Integrating the proposed system with real-time digital simulation or field-deployable controllers to validate the method in practice.
- Economic integration: Expanding the control scheme to account for electricity pricing and grid interaction costs, potentially enabling market-responsive PV control.

Chapter 5

Conclusion and Future Work

5.1 Conclusion

With the increasing penetration of rooftop photovoltaic (PV) systems in behind-the-meter (BTM) environments, the variability and unpredictability of solar generation are becoming critical challenges for stable and cost-effective power system operation. Traditionally, these fluctuations have been addressed predominantly on the front-of-the-meter (FTM) side through large-scale batteries, fuel-based generation, or power curtailment. However, such FTM-based balancing approaches impose significant economic costs, environmental burdens, and energy inefficiencies, revealing fundamental limitations in relying solely on centralized adjustment mechanisms. To address these challenges, this dissertation has investigated forecasting-driven and control-oriented methodologies that enable a portion of the system balancing effort to be shifted from the FTM side to the BTM side, thereby distributing the overall adjustment burden of the power system. In particular, the proposed approaches demonstrate that proactive ramp-rate control can be achieved within BTM systems by reducing reliance on large-capacity batteries and excessive power curtailment, which have traditionally constituted major limitations of FTM-based balancing. These results indicate that rapid PV output fluctuations can be mitigated locally and proactively, without depending exclusively on centralized resources. Specifically, this dissertation has addressed the three research questions defined in Chapter 1.

Answer to Question 1: How can accurate forecasting of the information necessary for EMS be achieved?

To support proactive energy management and enable effective control in BTM systems, accurate short-term forecasting of key variables—such as electricity demand, electricity prices, and solar irradiance—is essential. Since these variables exhibit strong volatility and non-stationary characteristics, traditional statistical and machine learning mod-

els often struggle to capture rapid fluctuations and long-term patterns simultaneously. Therefore, a forecasting methodology capable of addressing these time-varying properties is required.

Chapter 2 presents a forecasting method that combines wavelet transform and long short-term memory networks (WT-LSTM) to enhance prediction accuracy for non-stationary energy time series. The proposed method first decomposes raw signals into multi-resolution sub-components using WT, allowing long-term trends and short-term variations to be modeled separately by the LSTM predictor. In addition, explanatory variables and systematic feature selection are incorporated to improve the generality and interpretability of the forecasting model across different tasks. Finally, the method introduces a dynamic selection mechanism for the mother wavelet, in which the most suitable wavelet is periodically chosen based on recent prediction performance, thereby improving the decomposition process under changing time-series characteristics.

Comprehensive experiments were conducted for electricity demand, electricity prices, and solar irradiance. The results demonstrate that the proposed WT-LSTM model consistently outperforms conventional machine learning and baseline approaches. This improvement provides more reliable information for energy manegement system (EMS) decision-making, reducing prediction-related inefficiencies in subsequent control strategies.

In contrast to statistical forecasting models that express predictions as linear combinations of past values or features—an assumption that becomes increasingly unrealistic for complex and nonlinear energy time series—the proposed WT-LSTM approach explicitly incorporates nonlinear temporal dependencies through sequence learning. Moreover, unlike existing studies that combine WT with machine learning yet still rely on (1) limited explanatory variables, (2) ad hoc feature selection, and (3) static wavelet decomposition, the proposed method introduces systematic feature selection and dynamic mother wavelet adaptation. These contributions enable the forecasting model to better capture evolving time-series characteristics and provide more informative inputs for subsequent EMS control.

Answer to Question 2: How can PV ramp rates be effectively optimized without relying on large battery systems?

To mitigate rapid fluctuations in PV output, BTM systems typically rely on battery storage systems to smooth power trajectories. However, large-capacity batteries impose high initial investment, environmental impact, and non-negligible maintenance requirements, making them unsuitable as a standalone solution for high-frequency ramp rate control. Therefore, alternative methods that can regulate PV output without substantial storage deployment are desirable.

Chapter 3 focuses on a cooling-based ramp rate control strategy that exploits the temperature dependence of PV conversion efficiency. Instead of curtailing power or aggressively charging/discharging batteries, the method suppresses steep changes in PV

output by actively cooling PV modules only when rapid fluctuations are expected. Simulation studies using real-world irradiance data demonstrate that the proposed cooling-based method can reduce mean and maximum ramp rates by 43.5% and 76.2%, respectively, compared to conventional battery-driven strategies. Importantly, these improvements are achieved even with a cooling unit having a coefficient of performance below 10 and a minimal battery capacity of approximately 20 kWh. These results indicate that cooling-assisted regulation enables a stable and grid-friendly PV output with significantly reduced storage requirements and minimal curtailment loss. Existing methods for ramp rate control predominantly depend on large battery systems or energy curtailment, both of which can lead to undesirable cost increases or energy waste. In contrast, the cooling-based approach leverages inherent PV thermoelectric characteristics to achieve high-frequency output regulation with low operational cost and limited storage usage. This offers a practical and scalable alternative for enhancing PV integration in BTM environments.

Answer to Question 3: How can forecasting and optimization be integrated to achieve proactive and cost-effective BTM operation?

To enable BTM systems to act proactively against rapid variations in PV output, it is necessary to establish a framework that integrates forecasting and control in a way that informs real-time decisions. While forecasting models alone cannot improve system stability, and control mechanisms without future information remain reactive, a coordinated forecasting–control structure allows energy management systems to anticipate fluctuations and act in advance to minimize variability and operational inefficiencies.

Chapter 4 proposes an integrated forecasting–control strategy in which short-term predictions of solar irradiance are used as decision inputs to a sequential optimization process. The proposed approach combines forecast-guided PV regulation, cooling-based temperature control, and limited battery usage, enabling the system to selectively pre-adjust PV output before steep ramps occur. Simulation results demonstrate that using forecasts with a 30–60 second horizon enables proactive mitigation of ramp rate violations, reducing the number of violations by up to 20% compared to a no-control baseline. Moreover, the integration increases power delivery to the grid by enabling preemptive and efficient utilization of surplus PV energy that would otherwise be curtailed or dissipated as heat. State-of-the-art methods for ramp mitigation commonly rely on large battery systems or reactive control triggered only after violations occur, which can lead to unnecessary storage cycling or energy waste. In contrast, the proposed forecast-informed framework exploits cooling-based power regulation and minimal battery operation to achieve proactive stability improvements while reducing dependence on large storage capacity. Therefore, the integrated approach provides a practical, scalable, and computationally efficient path toward proactive and cost-effective BTM control under high rooftop PV penetration.

5.2 Future Work

The works presented in this dissertation will be able to extend in several directions.

Uncertainty-aware forecasting and control

To achieve more reliable and economically efficient operations, it is important to incorporate uncertainty into both forecasting and control decision-making. A promising direction for future work is to extend the deterministic point forecasting model into a probabilistic forecasting framework that characterizes prediction ranges and likelihood distributions. Furthermore, integrating such probabilistic outputs into optimization using stochastic or robust control formulations would enable risk-aware decision-making that accounts for fluctuations in solar generation and demand. Developing an uncertainty-aware forecasting–control paradigm will therefore enhance the practicality and resilience of BTM management under real-world environmental variability.

Adaptive and real-time learning

In Chapter 2, the proposed forecasting framework incorporates periodic adaptation through weekly re-selection of the mother wavelet based on recent prediction performance. This mechanism partially reflects changing time-series characteristics and improves decomposition quality over time. However, apart from periodic wavelet adaptation, the core LSTM parameters and feature-related configurations remain fixed after offline training. As a result, the forecasting model may still experience gradual degradation in performance when facing rapid environmental fluctuations, abrupt weather transitions, or evolving demand patterns that occur at a finer time scale than the weekly update cycle.

To maintain high prediction accuracy and stable control performance under more dynamic and unpredictable conditions, it is essential to extend this limited adaptation into a fully responsive learning process. A promising direction for future research is the development of online learning algorithms that update model parameters continuously or selectively as new observations become available, without requiring complete retraining. Such adaptive mechanisms would enable forecasting models to respond in real time to changing weather and demand trends, significantly improving their long-term usability in practical BTM systems.

Furthermore, incorporating real-time feedback from control decisions—such as cooling activation, ramp rate violations, or supply-to-grid transitions—into the learning process may enhance model relevance by linking prediction behavior with operational impact. By combining online learning and sequential control, BTM systems can evolve into self-adaptive management frameworks capable of sustaining reliable performance in dynamic real-world environments.

Extension of WT-LSTM to other renewable energy sources

The WT-LSTM forecasting framework developed in Chapter 2 was designed to address the challenges of non-stationary energy-related time series such as electricity price, electricity demand, and solar irradiance. These variables exhibit strong multi-scale temporal characteristics and abrupt fluctuations, making them well suited to a wavelet-based decomposition combined with LSTM-based sequential modeling.

However, many other renewable generation sources—particularly wind power and geothermal output—share similar non-stationary and multi-scale properties. Wind speed signals, for instance, contain both slowly varying meteorological trends and rapidly fluctuating turbulence components, while geothermal systems may exhibit variations linked to geological, thermal, and operational factors. These characteristics suggest that the WT-LSTM framework could potentially serve as a unified forecasting methodology for a broader class of renewable energy generation contexts.

At present, this generalization remains untested because the dissertation focuses primarily on solar irradiance and BTM-related variables. As a result, the applicability of WT-LSTM to wind or geothermal forecasting has not yet been validated, nor have domain-specific adjustments (e.g., modifying decomposition scales, integrating physical constraints, or incorporating additional explanatory variables) been explored.

To address these gaps, a promising direction for future work is a systematic investigation of WT-LSTM across multiple renewable energy domains. Such research would involve adapting the decomposition and learning modules to account for domain-specific characteristics, evaluating cross-domain performance, and identifying unified or hybrid model structures that can generalize across renewable resources.

Demonstrating multi-domain applicability would significantly broaden the impact of the WT-LSTM methodology and contribute to a more holistic forecasting foundation for future BTM and grid-interactive energy management systems.

Improvement of cooling models and exploration of economically viable cooling methods

The cooling-based ramp rate control strategy proposed in Chapter 3 regulates PV output by modulating module temperature and relies on simplified cooling performance assumptions characterized primarily by a coefficient of performance. While this abstraction is sufficient for demonstrating the viability of cooling-assisted ramp suppression, it does not capture the diverse characteristics of practical cooling systems such as startup delays, airflow distribution, nonuniform panel coverage, or degradation of cooling performance over time.

To enhance the practical applicability of cooling-assisted PV regulation, future research should focus on developing more detailed models of cooling technologies. Such cooling models should incorporate technology-specific characteristics of active and passive cooling systems, including evaporative cooling, liquid-based heat exchangers,

phase-change materials, hybrid passive–active approaches, and low-power fans. Additionally, the cooling model should capture non-linear dependencies between cooling effort, ambient weather conditions, and temporal fluctuations in irradiance to provide realistic estimates of energy consumption, ramp response, and control feasibility.

A refined cooling model will also enable more accurate evaluation of long-term cost effectiveness by considering installation complexity, operational energy cost, maintenance requirements, and potential degradation of cooling systems. Integrating these enhanced cooling models into EMS optimization will support the selection of the most appropriate cooling technology for different deployment scales (e.g., residential rooftops, commercial systems, or industrial PV plants) and facilitate practical, scalable implementation of cooling-based ramp rate control.

Scalability and multi-site deployment

The forecasting and control strategies developed in Chapter 2 through Chapter 4 were validated using data from specific meteorological conditions and a single-site BTM setup. These experiments demonstrate the potential of WT-LSTM–based forecasting and cooling-assisted ramp rate control for improving PV integration; however, site-specific irradiance patterns, weather variability, and installation environments may lead to different ramp characteristics and control requirements in practice. Therefore, verifying the generality of the proposed methods beyond a single test location is necessary for ensuring real-world applicability.

To evaluate robustness across diverse environmental and installation settings, future work should apply the proposed approach to multiple geographic locations and climate conditions, including areas with rapid irradiance transitions, high humidity, extreme seasonal variability, or different rooftop installation geometries. Additionally, expanding validation to networked systems—such as residential communities, commercial districts, or microgrids with multiple PV systems—would enable analysis of aggregated ramp behavior and potential benefits of cooperative control across distributed sites.

Such multi-site and multi-scale testing will allow assessment of scalability, computational requirements, and coordination strategies needed to manage multiple cooling-assisted PV systems simultaneously. These results will be instrumental in guiding future deployment strategies, including community-level EMS architectures and distributed ramp mitigation schemes that operate without excessive storage investment. Ultimately, expanding evaluation beyond a single site is a critical step toward enabling cooling-based ramp control as a broadly deployable solution for BTM PV integration.

Economic and market-responsive BTM management

The cooling-based ramp rate control and forecast-informed optimization discussed in Chapter 3 and Chapter 4 primarily address technical performance metrics such as ramp rate reduction, improved power delivery, and reduced dependence on large-capacity

battery systems. Although these results demonstrate operational benefits from an engineering perspective, the economic impacts of cooling-assisted PV control—such as installation cost, electricity savings, and cost recovery over time—have not yet been evaluated in detail. Furthermore, current formulations do not incorporate electricity pricing or market interactions, despite the fact that many BTM installations operate under tariff structures where energy export value varies by time and location.

To promote practical deployment, future research should conduct comprehensive economic evaluations that include life-cycle analyses of cooling technologies, maintenance requirements, and operational energy costs. Such evaluation would enable estimation of payback periods and identification of economically optimal system configurations for residential, commercial, and industrial deployments. Additionally, expanding the control framework to account for time-varying electricity prices and export tariffs could enable market-responsive PV regulation that maximizes revenue or minimizes operational cost while still maintaining ramp rate compliance.

Integrating economic objectives into BTM control will allow operators to jointly consider technical performance and economic profitability, potentially enabling cost-driven actuation of cooling resources, selective export strategies, and hybrid optimization between energy savings and stability enhancement. Incorporating such market-aware decision-making will be a key step toward transforming forecast-informed and cooling-assisted PV management into a financially viable solution for widespread adoption.

Integration into multi-horizon EMS architectures

Extending the proposed short-term forecasting–control loop toward a broader multi-horizon EMS architecture represents a promising direction for future research. In particular, an important opportunity lies in integrating the present method with existing multi-time-scale EMS frameworks, such as the wind-power-supported hierarchical EMS [117]. That study demonstrates how distributed energy resources (DERs) with different dynamical time constants (PV, wind, battery, HVAC, appliances) can be coordinated through layered optimization, where each layer operates at its own temporal resolution (seconds, minutes, hours).

By merging the methodological contributions of this dissertation with the multi-time-scale EMS architecture in the attached work, a more holistic behind-the-meter management framework could be realized—capable of coordinating DERs across seconds-to-hours horizons and supporting broader classes of renewable generation including PV and wind.

Hardware-in-the-loop and real-time deployment

The integrated forecasting–control approach developed in Chapter 4 demonstrated that forecast-informed PV regulation can proactively reduce ramp rate violations and in-

crease power delivery using a combination of cooling-based modulation and limited battery usage. However, all validations were conducted through numerical simulations, and the method has not yet been tested in real-time environments where factors such as sensor latency, controller delays, actuator dynamics, and communication constraints may affect performance. As a result, the practical feasibility of the proposed approach—especially the responsiveness of cooling devices and the stability of sequential control under hardware constraints—remains an open question.

To advance toward real-world implementation, future work should focus on hardware-in-the-loop experiments that emulate PV generation, irradiance fluctuations, and control actions using real-time digital simulation platforms. Such experiments would enable testing of the proposed algorithms under realistic operating conditions while capturing hardware-induced effects such as actuation delays, measurement noise, cooling activation limits, and intermittent communication. Furthermore, adopting embedded controllers such as microcomputers, programmable logic controllers, or field-programmable devices will help evaluate computational feasibility and responsiveness on restricted hardware platforms.

Real-time deployment studies would also facilitate co-design between control algorithms and cooling hardware to ensure reliable ramp mitigation, efficient energy use, and safe operation under rapidly changing irradiance. By bridging the gap between simulation and physical implementation, hardware-in-the-loop validation will be critical for transforming forecast-informed BTM control from a conceptual framework into a deployable technology capable of stabilizing PV systems in the field.

Bibliography

[1] AEMO, "Aggregated price and demand data," https://aemo.com.au/energy-systems/electricity/national-electricity-market-nem/data-nem/aggregated-data, [Online; accessed 25-Jan-2021].

[2] JEPX, "System price," http://www.jepx.org/, [Online; accessed 04-Feb-2021].

[3] Z. Chang, Y. Zhang, and W. Chen, "Electricity price prediction based on hybrid model of adam optimized LSTM neural network and wavelet transform," *Energy*, vol. 187, p. 115804, 2019.

[4] I. Dincer, "Renewable energy and sustainable development: A crucial review," *Renewable and Sustainable Energy Reviews*, vol. 4, no. 2, pp. 157–175, 2000.

[5] N. L. Panwar, S. C. Kaushik, and S. Kothari, "Role of renewable energy sources in environmental protection: A review," *Renewable and Sustainable Energy Reviews*, vol. 15, no. 3, pp. 1513–1524, 2011.

[6] Energy Institute and Our World in Data, "Statistical Review of World Energy (2025) – with major processing by Our World in Data," Dataset, 2025, original data from the Energy Institute, processed and presented by Our World in Data. [Online]. Available: https://ourworldindata.org/grapher/modern-renewable-energy-consumption

[7] N. Phuangpornpitak and S. Tia, "Opportunities and Challenges of Integrating Renewable Energy in Smart Grid System," *Energy Procedia*, vol. 34, pp. 282–290, 2013.

[8] S. R. Sinsel, R. L. Riemke, and V. H. Hoffmann, "Challenges and solution technologies for the integration of variable renewable energy sources — a review," *Renewable Energy*, vol. 145, pp. 2271–2285, 2020.

[9] X. Fang, S. Misra, G. Xue, and D. Yang, "Smart Grid — The New and Improved Power Grid: A Survey," *IEEE Communications Surveys & Tutorials*, vol. 14, no. 4, pp. 944–980, 2012.

[10] IEA, *Heat Pumps*. Paris, France: International Energy Agency (IEA), 2022.

[11] ——, *Global EV Outlook 2022*. Paris, France: International Energy Agency (IEA), 2022.

[12] ——, *World Energy Outlook 2022*. Paris, France: International Energy Agency (IEA), 2022.

[13] M. Shimomura, A. R. Keeley, K. Matsumoto, K. Tanaka, and S. Managi, "Unveiling and estimating behind-the-meter rooftop solar self-consumption using explainable AI," *npj Clean Energy*, vol. 1, no. 1, p. 11, 2025.

[14] O. Bamisile, C. Acen, D. Cai, Q. Huang, and I. Staffell, "The environmental factors affecting solar photovoltaic output," *Renewable and Sustainable Energy Reviews*, vol. 208, p. 115073, 2025. [Online]. Available: https://www.sciencedirect.com/science/article/pii/S1364032124007998

[15] International Energy Agency (IEA). (2022) Approximately 100 million households rely on rooftop solar PV by 2030. Paris, France. [Online; accessed 05-Dec-2025]. [Online]. Available: https://www.iea.org/reports/approximately-100-million-households-rely-on-rooftop-solar-pv-by-2030

[16] ——. (2023) Digital tools will help keep distributed solar PV growing strongly. Paris, France. [Online; accessed 05-Dec-2025]. [Online]. Available: https://www.iea.org/commentaries/digital-tools-will-help-keep-distributed-solar-pv-growing-strongly

[17] International Renewable Energy Agency (IRENA), "Behind-the-Meter Batteries: Market, Regulation and Economic Approaches," International Renewable Energy Agency (IRENA), Abu Dhabi, Tech. Rep., 2019, [Online; accessed 05-Dec-2025]. [Online]. Available: https://www.irena.org/-/media/Files/IRENA/Agency/Publication/2019/Sep/IRENA_BTM_Batteries_2019.pdf

[18] F. Mohammadi and M. Saif, "A comprehensive overview of electric vehicle batteries market," *e-Prime - Advances in Electrical Engineering, Electronics and Energy*, vol. 3, p. 100127, 2023. [Online]. Available: https://www.sciencedirect.com/science/article/pii/S2772671123000220

[19] National Renewable Energy Laboratory (NREL), "Behind-The-Meter Battery Energy Storage," National Renewable Energy Laboratory (NREL), Golden, CO, Tech. Rep. NREL/TP-7A40-79393, 2021, [Online; accessed 05-Dec-2025]. [Online]. Available: https://docs.nrel.gov/docs/fy21osti/79393.pdf

[20] X. Liu, W. Li, X. Guo, B. Su, S. Guo, Y. Jing, and X. Zhang, "Advancements in Energy-Storage Technologies: A Review of Current Developments and

Applications," *Sustainability*, vol. 17, no. 18, 2025. [Online]. Available: https://www.mdpi.com/2071-1050/17/18/8316

[21] D. Hall and N. Lutsey, "Effects of battery manufacturing on electric vehicle life-cycle greenhouse gas emissions," International Council on Clean Transportation (ICCT), Briefing, 2018, [Online; accessed 05-Dec-2025]. [Online]. Available: https://theicct.org/wp-content/uploads/2021/06/EV-life-cycle-GHG_ICCT-Briefing_09022018_vF.pdf

[22] R. Pereira, J. Figueiredo, R. Melicio, V. M. F. Mendes, J. Martins, and J. C. Quadrado, "Consumer energy management system with integration of smart meters," *Energy Reports*, vol. 1, pp. 22–29, 2015.

[23] K. Iwabuchi, K. Kato, D. Watari, I. Taniguchi, F. Catthoor, E. Shirazi, and T. Onoye, "Demand-Aware Electricity Price Prediction Based on LSTM and Wavelet Transform," in *Proceedings of the 38th European Photovoltaic Solar Energy Conference and Exhibition*, 2021, pp. 1668–1671.

[24] ——, "Flexible electricity price forecasting by switching mother wavelets based on wavelet transform and Long Short-Term Memory," *Energy and AI*, vol. 10, p. 100192, 2022. [Online]. Available: https://www.sciencedirect.com/science/article/pii/S2666546822000404

[25] K. Iwabuchi, D. Watari, D. Zhao, I. Taniguchi, and T. Onoye, "Flexible Electricity Demand Forecasting Based on mRMR Feature Selection and WT-LSTM," in *Proceedings of the 40th European Photovoltaic Solar Energy Conference and Exhibition*, 2023, pp. 020 491–001–020 491–004.

[26] K. Iwabuchi, D. Zhao, I. Taniguchi, F. Catthoor, and T. Onoye, "Ramp Rate Control for PV Systems Using Solar Irradiance Forecasting with Wavelet Transform and LSTM," in *Proceedings of the 16th ACM International Conference on Future and Sustainable Energy Systems*. New York, NY, USA: Association for Computing Machinery, 2025, p. 987–988. [Online]. Available: https://doi.org/10.1145/3679240.3734679

[27] Z. Zhao, C. Wang, M. Nokleby, and C. J. Miller, "Improving short-term electricity price forecasting using day-ahead LMP with ARIMA models," in *Proceedings of IEEE Power Energy Society General Meeting*, 2017, pp. 1–5.

[28] Z. Tan, J. Zhang, J. Wang, and J. Xu, "Day-ahead electricity price forecasting using wavelet transform combined with ARIMA and GARCH models," *Applied Energy*, vol. 87, no. 11, pp. 3606–3610, 2010.

[29] A. Mohsenian-Rad and A. Leon-Garcia, "Optimal residential load control with price prediction in real-time electricity pricing environments," *IEEE Transactions on Smart Grid*, vol. 1, no. 2, pp. 120–133, 2010.

[30] G. R. Newsham and B. J. Birt, "Building-level occupancy data to improve ARIMA-based electricity use forecasts," in *Proceedings of the 2nd ACM Workshop on Embedded Sensing Systems for Energy-Efficiency in Building*. New York, NY, USA: Association for Computing Machinery, 2010, p. 13–18. [Online]. Available: https://doi.org/10.1145/1878431.1878435

[31] K. Kandananond, "Electricity demand forecasting in buildings based on ARIMA and ARX models," in *Proceedings of the 8th International Conference on Informatics, Environment, Energy and Applications*, ser. IEEA '19. New York, NY, USA: Association for Computing Machinery, 2019, p. 268–271. [Online]. Available: https://doi.org/10.1145/3323716.3323763

[32] R. Lu, S. H. Hong, and M. Yu, "Demand response for home energy management using reinforcement learning and artificial neural network," *IEEE Transactions on Smart Grid*, vol. 10, no. 6, pp. 6629–6639, 2019.

[33] J. Lago, F. De Ridder, and B. De Schutter, "Forecasting spot electricity prices: Deep learning approaches and empirical comparison of traditional algorithms," *Applied Energy*, vol. 221, pp. 386–405, 2018.

[34] J. Xu and R. Baldick, "Day-Ahead Price Forecasting in ERCOT Market Using Neural Network Approaches," in *Proceedings of the Tenth ACM International Conference on Future Energy Systems*. New York, NY, USA: Association for Computing Machinery, 2019, p. 486–491. [Online]. Available: https://doi.org/10.1145/3307772.3331024

[35] L. Peng, S. Liu, R. Liu, and L. Wang, "Effective long short-term memory with differential evolution algorithm for electricity price prediction," *Energy*, vol. 162, pp. 1301–1314, 2018.

[36] J. Lago, G. Marcjasz, B. De Schutter, and R. Weron, "Forecasting day-ahead electricity prices: A review of state-of-the-art algorithms, best practices and an open-access benchmark," *Applied Energy*, vol. 293, p. 116983, 2021. [Online]. Available: https://www.sciencedirect.com/science/article/pii/S0306261921004529

[37] S. Zhou, L. Zhou, M. Mao, H.-M. Tai, and Y. Wan, "An Optimized Heterogeneous Structure LSTM Network for Electricity Price Forecasting," *IEEE Access*, vol. 7, pp. 108 161–108 173, 2019.

[38] H. Su, E. Zio, J. Zhang, M. Xu, X. Li, and Z. Zhang, "A hybrid hourly natural gas demand forecasting method based on the integration of wavelet transform and enhanced Deep-RNN model," *Energy*, vol. 178, pp. 585–597, 2019.

[39] Y. Liu, L. Guan, C. Hou, H. Han, Z. Liu, Y. Sun, and M. Zheng, "Wind power short-term prediction based on LSTM and discrete wavelet transform," *Applied Sciences*, vol. 9, no. 6, p. 1108, 2019.

[40] S. K. Aggarwal, L. M. Saini, and A. Kumar, "Electricity price forecasting in Ontario electricity market using wavelet transform in artificial neural network based model," *International Journal of Control, Automation, and Systems*, vol. 6, no. 5, pp. 639–650, 2008.

[41] N. Singh, S. Tiwari, S. Mohanty, and D. Yadav, "A Modified Cost Function Generalized Neuron for Electricity Price Forecasting in Deregulated Power Markets," in *Proceedings of the 6th International Conference on Computer and Communication Technology*, 2015, pp. 120–126.

[42] C. N. Babu and B. E. Reddy, "A moving-average filter based hybrid ARIMA-ANN model for forecasting time series data," *Applied Soft Computing*, vol. 23, pp. 27–38, 2014. [Online]. Available: http://www.sciencedirect.com/science/article/pii/S1568494614002555

[43] E. Ofori-Ntow Jnr, Y. Y. Ziggah, and S. Relvas, "Hybrid ensemble intelligent model based on wavelet transform, swarm intelligence and artificial neural network for electricity demand forecasting," *Sustainable Cities and Society*, vol. 66, p. 102679, 2021. [Online]. Available: https://www.sciencedirect.com/science/article/pii/S2210670720308945

[44] C. Li, M. Tang, G. Zhang, R. Wang, and C. Tian, "A hybrid short-term building electrical load forecasting model combining the periodic pattern, fuzzy system, and wavelet transform," *International journal of fuzzy systems*, vol. 22, no. 1, pp. 156–171, 2020.

[45] L. Saad Saoud, H. Al-Marzouqi, and R. Hussein, "Household Energy Consumption Prediction Using the Stationary Wavelet Transform and Transformers," *IEEE Access*, vol. 10, pp. 5171–5183, 2022.

[46] R. Barzegar, J. Adamowski, and A. A. Moghaddam, "Application of wavelet-artificial intelligence hybrid models for water quality prediction: A case study in Aji-Chay River, Iran," *Stochastic environmental research and risk assessment*, vol. 30, no. 7, pp. 1797–1819, 2016.

[47] I. Oksuz and U. Ugurlu, "Neural Network Based Model Comparison for Intraday Electricity Price Forecasting," *Energies*, vol. 12, no. 23, 2019. [Online]. Available: https://www.mdpi.com/1996-1073/12/23/4557

[48] M. Mitani, *From Fourier Transform to Wavelet Transform: Communication Mathematics for Reviewers and Learners [in Japanese]*. CQ Publishing Co., Ltd., 2008.

[49] M. Lang, H. Guo, J. E. Odegard, C. S. Burrus, and R. O. Wells, "Noise reduction using an undecimated discrete wavelet transform," *IEEE Signal Processing Letters*, vol. 3, no. 1, pp. 10–12, 1996.

[50] D. Zhang, "Wavelet transform," in *Proceedings of Fundamentals of Image Data Mining*. Springer, 2019, pp. 35–44.

[51] G. P. Nason and B. W. Silverman, "The discrete wavelet transform in S," *Journal of Computational and Graphical Statistics*, vol. 3, no. 2, pp. 163–191, 1994.

[52] M. Antonini, M. Barlaud, P. Mathieu, and I. Daubechies, "Image coding using wavelet transform," *IEEE Transactions on Image Processing*, vol. 1, no. 2, pp. 205–220, 1992.

[53] K. Greff, R. K. Srivastava, J. Koutník, B. R. Steunebrink, and J. Schmidhuber, "LSTM: A Search Space Odyssey," *IEEE Transactions on Neural Networks and Learning Systems*, vol. 28, no. 10, pp. 2222–2232, 2017.

[54] M. Sundermeyer, R. Schlüter, and H. Ney, "LSTM neural networks for language modeling," in *Proceedings of annual conference of the international speech communication association*, 2012, pp. 194–197.

[55] A. Graves, S. Fernández, and J. Schmidhuber, "Bidirectional LSTM networks for improved phoneme classification and recognition," in *Proceedings of International conference on artificial neural networks*, 2005, pp. 799–804.

[56] X. Shi, Z. Chen, H. Wang, D.-Y. Yeung, W.-K. Wong, and W.-c. Woo, "Convolutional LSTM network: A machine learning approach for precipitation nowcasting," *Advances in neural information processing systems*, vol. 28, 2015.

[57] V. Nourani, A. H. Baghanam, J. Adamowski, and O. Kisi, "Applications of hybrid wavelet–artificial intelligence models in hydrology: A review," *Journal of Hydrology*, vol. 514, pp. 358–377, 2014.

[58] P. D. Lund, J. Lindgren, J. Mikkola, and J. Salpakari, "Review of energy system flexibility measures to enable high levels of variable renewable electricity," *Renewable and Sustainable Energy Reviews*, vol. 45, pp. 785–807,

2015. [Online]. Available: https://www.sciencedirect.com/science/article/pii/S1364032115000672

[59] W. Huang, N. Zhang, C. Kang, M. Li, and M. Huo, "From demand response to integrated demand response: Review and prospect of research and application," *Protection and Control of Modern Power Systems*, vol. 4, no. 1, pp. 1–13, 2019.

[60] A. R. Jordehi, "Optimisation of demand response in electric power systems, a review," *Renewable and sustainable energy reviews*, vol. 103, pp. 308–319, 2019.

[61] F. Pallonetto, M. De Rosa, F. D'Ettorre, and D. P. Finn, "On the assessment and control optimisation of demand response programs in residential buildings," *Renewable and Sustainable Energy Reviews*, vol. 127, p. 109861, 2020.

[62] B. Liu, J. R. Lund, S. Liao, X. Jin, L. Liu, and C. Cheng, "Optimal power peak shaving using hydropower to complement wind and solar power uncertainty," *Energy Conversion and Management*, vol. 209, p. 112628, 2020.

[63] M. Uddin, M. Romlie, M. Abdullah, C. Tan, G. Shafiullah, and A. H. A. Bakar, "A novel peak shaving algorithm for islanded microgrid using battery energy storage system," *Energy*, vol. 196, p. 117084, 2020.

[64] X. Chen, L. Huang, J. Liu, D. Song, and S. Yang, "Peak shaving benefit assessment considering the joint operation of nuclear and battery energy storage power stations: Hainan case study," *Energy*, vol. 239, p. 121897, 2022.

[65] X. Zhao, W. Gao, F. Qian, and J. Ge, "Electricity cost comparison of dynamic pricing model based on load forecasting in home energy management system," *Energy*, vol. 229, p. 120538, 2021.

[66] M. Grzanić, J. M. Morales, S. Pineda, and T. Capuder, "Electricity cost-sharing in energy communities under dynamic pricing and uncertainty," *IEEE Access*, vol. 9, pp. 30 225–30 241, 2021.

[67] H. Taherian, M. R. Aghaebrahimi, L. Baringo, and S. R. Goldani, "Optimal dynamic pricing for an electricity retailer in the price-responsive environment of smart grid," *International Journal of Electrical Power & Energy Systems*, vol. 130, p. 107004, 2021.

[68] AEMO, "the national electricity market," https://www.aemo.com.au/-/media/files/electricity/nem/national-electricity-market-fact-sheet.pdf, [Online; accessed 04-Feb-2021].

[69] S. Voronin and J. Partanen, "Forecasting electricity price and demand using a hybrid approach based on wavelet transform, ARIMA and neural networks," *International Journal of Energy Research*, vol. 38, no. 5, pp. 626–637, 2014.

[70] A. J. Conejo, M. A. Plazas, R. Espinola, and A. B. Molina, "Day-ahead electricity price forecasting using the wavelet transform and ARIMA models," *IEEE Transactions on Power Systems*, vol. 20, no. 2, pp. 1035–1042, 2005.

[71] D. P. Kingma and J. Ba, "Adam: A Method for Stochastic Optimization," 2017. [Online]. Available: https://arxiv.org/abs/1412.6980

[72] J. Bergstra, R. Bardenet, Y. Bengio, and B. Kégl, "Algorithms for hyper-parameter optimization," *Advances in neural information processing systems*, vol. 24, 2011.

[73] Y. Ozaki, Y. Tanigaki, S. Watanabe, and M. Onishi, "Multiobjective tree-structured parzen estimator for computationally expensive optimization problems," in *Proceedings of the 2020 Genetic and Evolutionary Computation Conference*, 2020, pp. 533–541.

[74] P. Kumari and D. Toshniwal, "Deep learning models for solar irradiance forecasting: A comprehensive review," *Journal of Cleaner Production*, vol. 318, p. 128566, 2021. [Online]. Available: https://www.sciencedirect.com/science/article/pii/S0959652621027736

[75] K. Iwabuchi, D. Watari, D. Zhao, I. Taniguchi, F. Catthoor, and T. Onoye, "Enhancing grid stability in PV systems: A novel ramp rate control method utilizing PV cooling technology," *Applied Energy*, vol. 378, p. 124737, 2025. [Online]. Available: https://www.sciencedirect.com/science/article/pii/S0306261924021202

[76] W. Amorim, A. Cupertino, H. Pereira, and V. Mendes, "On sizing of battery energy storage systems for PV plants power smoothing," *Electric Power Systems Research*, vol. 229, p. 110114, 2024. [Online]. Available: https://www.sciencedirect.com/science/article/pii/S0378779624000038

[77] K. Abudu, U. Igie, O. Minervino, and R. Hamilton, "Gas turbine efficiency and ramp rate improvement through compressed air injection," *Proceedings of the Institution of Mechanical Engineers, Part A: Journal of Power and Energy*, vol. 235, no. 4, pp. 866–884, 2021.

[78] W. A. Omran, M. Kazerani, and M. M. A. Salama, "Investigation of Methods for Reduction of Power Fluctuations Generated From Large Grid-Connected Photovoltaic Systems," *IEEE Transactions on Energy Conversion*, vol. 26, no. 1, pp. 318–327, 2011.

[79] H. M. Ali, M. Mahmood, M. A. Bashir, M. Ali, and A. M. Siddiqui, "Outdoor testing of photovoltaic modules during summer in Taxila, Pakistan," *Thermal Science*, vol. 20, no. 1, pp. 165–173, 2016.

[80] H. M. Ali, "Recent advancements in PV cooling and efficiency enhancement integrating phase change materials based systems – A comprehensive review," *Solar Energy*, vol. 197, pp. 163–198, 2020. [Online]. Available: https://www.sciencedirect.com/science/article/pii/S0038092X19311752

[81] K. Lappalainen and S. Valkealahti, "Sizing of energy storage systems for ramp rate control of photovoltaic strings," *Renewable Energy*, vol. 196, pp. 1366–1375, 2022.

[82] J. Martins, S. Spataru, D. Sera, D.-I. Stroe, and A. Lashab, "Comparative Study of Ramp-Rate Control Algorithms for PV with Energy Storage Systems," *Energies*, vol. 12, no. 7, 2019. [Online]. Available: https://www.mdpi.com/1996-1073/12/7/1342

[83] H. Beltran, I. Tomás García, J. C. Alfonso-Gil, and E. Pérez, "Levelized Cost of Storage for Li-ion Batteries Used in PV Power Plants for Ramp-Rate Control," *IEEE Transactions on Energy Conversion*, vol. 34, no. 1, pp. 554–561, 2019.

[84] M. B. Abdelghany, A. Al-Durra, and F. Gao, "A Coordinated Optimal Operation of a Grid-Connected Wind-Solar Microgrid Incorporating Hybrid Energy Storage Management Systems," *IEEE Transactions on Sustainable Energy*, vol. 15, no. 1, pp. 39–51, 2024.

[85] A. Gonzalez-Moreno, J. Marcos, I. de la Parra, and L. Marroyo, "A PV ramp-rate control strategy to extend battery lifespan using forecasting," *Applied Energy*, vol. 323, p. 119546, 2022.

[86] A. Atif and M. Khalid, "Saviztky–Golay filtering for solar power smoothing and ramp rate reduction based on controlled battery energy storage," *IEEE Access*, vol. 8, pp. 33 806–33 817, 2020.

[87] E. Jiménez and M. Madrigal, "Mitigation of PV Power Fluctuations using Moving Average Control in an OpenDSS-Python Environment," in *Proceedings of IEEE International Autumn Meeting on Power, Electronics and Computing (ROPEC)*, vol. 4, 2020, pp. 1–6.

[88] D. Alvaro, R. Arranz, and J. A. Aguado, "Sizing and operation of hybrid energy storage systems to perform ramp-rate control in PV power plants," *International Journal of Electrical Power & Energy Systems*, vol. 107, pp. 589–596, 2019.

[89] P. Arévalo, D. Benavides, M. Tostado-Véliz, J. A. Aguado, and F. Jurado, "Smart monitoring method for photovoltaic systems and failure control based on power smoothing techniques," *Renewable Energy*, vol. 205, pp. 366–383, 2023.

[90] D. Benavides, P. Arévalo, M. Tostado-Véliz, D. Vera, A. Escamez, J. A. Aguado, and F. Jurado, "An experimental study of power smoothing methods to reduce renewable sources fluctuations using supercapacitors and lithium-ion batteries," *Batteries*, vol. 8, no. 11, p. 228, 2022.

[91] M. B. Abdelghany, A. Al-Durra, Z. Daming, and F. Gao, "Optimal multi-layer economical schedule for coordinated multiple mode operation of wind-solar microgrids with hybrid energy storage systems," *Journal of Power Sources*, vol. 591, p. 233844, 2024. [Online]. Available: https://www.sciencedirect.com/science/article/pii/S037877532301220X

[92] Y. S. Lim and J. H. Tang, "Experimental study on flicker emissions by photovoltaic systems on highly cloudy region: A case study in Malaysia," *Renewable Energy*, vol. 64, pp. 61–70, 2014. [Online]. Available: https://www.sciencedirect.com/science/article/pii/S0960148113005740

[93] S. Shivashankar, S. Mekhilef, H. Mokhlis, and M. Karimi, "Mitigating methods of power fluctuation of photovoltaic (PV) sources–A review," *Renewable and Sustainable Energy Reviews*, vol. 59, pp. 1170–1184, 2016.

[94] R. Tonkoski, L. A. Lopes, and T. H. El-Fouly, "Coordinated active power curtailment of grid connected PV inverters for overvoltage prevention," *IEEE Transactions on sustainable energy*, vol. 2, no. 2, pp. 139–147, 2010.

[95] S. Rostami, M. Afrand, A. Shahsavar, M. Sheikholeslami, R. Kalbasi, S. Aghakhani, M. S. Shadloo, and H. F. Oztop, "A review of melting and freezing processes of PCM/nano-PCM and their application in energy storage," *Energy*, vol. 211, p. 118698, 2020.

[96] L. Siahkamari, M. Rahimi, N. Azimi, and M. Banibayat, "Experimental investigation on using a novel phase change material (PCM) in micro structure photovoltaic cooling system," *International Communications in Heat and Mass Transfer*, vol. 100, pp. 60–66, 2019.

[97] N. Abdollahi and M. Rahimi, "Potential of water natural circulation coupled with nano-enhanced PCM for PV module cooling," *Renewable Energy*, vol. 147, pp. 302–309, 2020.

[98] R. Madurai Elavarasan, M. Nadarajah, R. Pugazhendhi, and S. Gangatharan, "An experimental investigation on coalescing the potentiality of PCM, fins and water to achieve sturdy cooling effect on PV panels," *Applied Energy*, vol. 356, p. 122371, 2024. [Online]. Available: https://www.sciencedirect.com/science/article/pii/S030626192301735X

[99] M. Mehrali, J. E. ten Elshof, M. Shahi, and A. Mahmoudi, "Simultaneous solar-thermal energy harvesting and storage via shape stabilized salt hydrate phase change material," *Chemical Engineering Journal*, vol. 405, p. 126624, 2021.

[100] A. K. Hamzat, A. Z. Sahin, M. I. Omisanya, and L. M. Alhems, "Advances in PV and PVT cooling technologies: A review," *Sustainable Energy Technologies and Assessments*, vol. 47, p. 101360, 2021. [Online]. Available: https://www.sciencedirect.com/science/article/pii/S2213138821003702

[101] F. Selimefendigil and C. Şirin, "Energy and exergy analysis of a hybrid photovoltaic/thermal-air collector modified with nano-enhanced latent heat thermal energy storage unit," *Journal of Energy Storage*, vol. 45, p. 103467, 2022.

[102] W. Wang, S. Aleid, Y. Shi, C. Zhang, R. Li, M. Wu, S. Zhuo, and P. Wang, "Integrated solar-driven PV cooling and seawater desalination with zero liquid discharge," *Joule*, vol. 5, no. 7, pp. 1873–1887, 2021.

[103] A. Mahdavi, M. Farhadi, M. Gorji-Bandpy, and A. Mahmoudi, "A comprehensive study on passive cooling of a PV device using PCM and various fin configurations: Pin, spring, and Y-shaped fins," *Applied Thermal Engineering*, vol. 252, p. 123519, 2024. [Online]. Available: https://www.sciencedirect.com/science/article/pii/S1359431124011876

[104] F. Bayrak, H. F. Oztop, and F. Selimefendigil, "Experimental study for the application of different cooling techniques in photovoltaic (PV) panels," *Energy Conversion and Management*, vol. 212, p. 112789, 2020.

[105] R. Li, Y. Shi, M. Wu, S. Hong, and P. Wang, "Photovoltaic panel cooling by atmospheric water sorption–evaporation cycle," *Nature Sustainability*, vol. 3, no. 8, pp. 636–643, 2020.

[106] P. Dwivedi, K. Sudhakar, A. Soni, E. Solomin, and I. Kirpichnikova, "Advanced cooling techniques of P.V. modules: A state of art," *Case Studies in Thermal Engineering*, vol. 21, p. 100674, 2020. [Online]. Available: https://www.sciencedirect.com/science/article/pii/S2214157X19305416

[107] D. Watari, I. Taniguchi, H. Goverde, P. Manganiello, E. Shirazi, F. Catthoor, and T. Onoye, "Multi-time scale energy management framework for smart PV systems mixing fast and slow dynamics," *Applied Energy*, vol. 289, p. 116671, 2021. [Online]. Available: https://www.sciencedirect.com/science/article/pii/S0306261921002002

[108] D. Zhao, D. Watari, Y. Ozawa, I. Taniguchi, T. Suzuki, Y. Shimoda, and T. Onoye, "A Thermal Comfort and Peak Power Demand Aware VRF Heating/Cooling

Management Framework: Simulation and On-site Experiment," *Journal of Information Processing*, vol. 30, pp. 476–485, 2022.

[109] V. Johnson, "Battery performance models in ADVISOR," *Journal of Power Sources*, vol. 110, no. 2, pp. 321–329, 2002. [Online]. Available: https://www.sciencedirect.com/science/article/pii/S0378775302001945

[110] D. Kurz and R. Nawrowski, "Thermal Time Constant of PV Roof Tiles Working under Different Conditions," *Applied Sciences*, vol. 9, no. 8, 2019. [Online]. Available: https://www.mdpi.com/2076-3417/9/8/1626

[111] N. Hendrikx, K. Barhmi, L. Visser, T. {de Bruin}, M. Pó, A. Salah, and W. {van Sark}, "All sky imaging-based short-term solar irradiance forecasting with Long Short-Term Memory networks," *Solar Energy*, vol. 272, 2024, publisher Copyright: © 2024 The Author(s).

[112] S.-A. Logothetis, V. Salamalikis, B. Nouri, J. Remund, L. F. Zarzalejo, Y. Xie, S. Wilbert, E. Ntavelis, J. Nou, N. Hendrikx, L. Visser, M. Sengupta, M. Pó, R. Chauvin, S. Grieu, N. Blum, W. v. Sark, and A. Kazantzidis, "Solar Irradiance Ramp Forecasting Based on All-Sky Imagers," *Energies*, vol. 15, no. 17, 2022. [Online]. Available: https://www.mdpi.com/1996-1073/15/17/6191

[113] X. Chen, Y. Du, E. Lim, L. Fang, and K. Yan, "Towards the applicability of solar nowcasting: A practice on predictive PV power ramp-rate control," *Renewable Energy*, vol. 195, pp. 147–166, 2022. [Online]. Available: https://www.sciencedirect.com/science/article/pii/S0960148122008266

[114] A. Ryu, H. Ishii, and Y. Hayashi, "Battery smoothing control for photovoltaic system using short-term forecast with total sky images," *Electric Power Systems Research*, vol. 190, p. 106645, 2021. [Online]. Available: https://www.sciencedirect.com/science/article/pii/S037877962030448X

[115] X. Jiao, X. Li, Z. Ge, Y. Yang, and W. Xiao, "A predictive power ramp rate control scheme with an updating Gaussian prediction confidence estimator for PV systems," *Solar Energy*, vol. 276, p. 112648, 2024. [Online]. Available: https://www.sciencedirect.com/science/article/pii/S0038092X24003438

[116] P. Arévalo, D. Benavides, J. A. Aguado, and F. Jurado, "Advanced wind/photovoltaic power smoothing using LSTM neural networks and machine learning," *Soft Computing*, pp. 1–19, 2025.

[117] S. Mitsunaga, D. Zhao, H. Nishikawa, I. Taniguchi, and T. Onoye, "Extending Multi-time Scale Energy Management System to Support Wind Power Generation," in *Proceedings of the 15th ACM International Conference*

on Future and Sustainable Energy Systems. New York, NY, USA: Association for Computing Machinery, 2024, p. 486–487. [Online]. Available: https://doi.org/10.1145/3632775.3661978